INFORMATION TO USERS

This manuscript has been reproduced from the microfilm master. UMI films the text directly from the original or copy submitted. Thus, some thesis and dissertation copies are in typewriter face, while others may be from any type of computer printer.

The quality of this reproduction is dependent upon the quality of the copy submitted. Broken or indistinct print, colored or poor quality illustrations and photographs, print bleedthrough, substandard margins, and improper alignment can adversely affect reproduction.

In the unlikely event that the author did not send UMI a complete manuscript and there are missing pages, these will be noted. Also, if unauthorized copyright material had to be removed, a note will indicate the deletion.

Oversize materials (e.g., maps, drawings, charts) are reproduced by sectioning the original, beginning at the upper left-hand corner and continuing from left to right in equal sections with small overlaps. Each original is also photographed in one exposure and is included in reduced form at the back of the book.

Photographs included in the original manuscript have been reproduced xerographically in this copy. Higher quality 6" x 9" black and white photographic prints are available for any photographs or illustrations appearing in this copy for an additional charge. Contact UMI directly to order.

UMI

A Bell & Howell Information Company
300 North Zeeb Road, Ann Arbor MI 48106-1346 USA
313/761-4700 800/521-0600

Sequence and functional analysis of the P97 swine cilium adhesin gene of *Mycoplasma hyopneumoniae*

by

Tsungda Hsu

A dissertation submitted to the graduate faculty

in partial fulfillment of the requirements for the degree of

DOCTOR OF PHILOSOPHY

Major: Microbiology

Major Professor: F. Chris Minion

Iowa State University

Ames, Iowa

1997

Graduate College
Iowa State University

This is to certify that the Doctoral dissertation of

Tsungda Hsu

has met the dissertation requirements of Iowa State University

Signature was redacted for privacy.

Major Professor

Signature was redacted for privacy.

For the Major Program

Signature was redacted for privacy.

For the Graduate College

TABLE OF CONTENTS

LIST OF FIGURES

LIST OF TABLES

LIST OF ABBREVIATIONS

A	adenine
AP	alkaline phosphatase
Ap	ampicillin
β-Gal	β-galactosidase
B.	*Bordetella*
bp	base pair
BSA	bovine serum albumin
C	cytosine
CHEF	contour-clamped homogeneous electric field
Cm	chloramphenicol
DNA	deoxyribonucleic acid
E.	*Escherichia*
ECM	extracellular matrix
EDTA	ethylenediamine tetraacetic acid
ELISA	enzyme-linked immunosorbent assay
EPP	enzootic pneumoniae of pigs
FHA	filamentous hemagglutinin
G	guanine
g	gram
Gal	galactose
Glc	glucose
HBSS	Hank's balance salt solution
HMW	high molecular weight
Ig	immunoglobulin
IPTG	isopropyl thio-β-D-galactopyranoside
kb	kilobase pair
kDa	kilodalton
Kn	kanamycin
LTA	lipoteichoic acid
M	molar
M.	*Mycoplasma*
Mab	monoclonal antibody
mg	milligram
µg	microgram
min	minute
ml	milliliter
µl	microliter
mm	millimeter
µM	micromolar
mM	millimolar
MPAA	microtiter plate adherence assay
MW	molecular weight

ng	nanogram
nm	nanometer
°C	degree Celsius
ORF	open reading frame
p	plasmid
PBS	phosphate buffered saline
PCR	polymerase chain reaction
pmol	picomole
PTX	pertussis toxin
r	recombinant
RBC	red blood cell
RFLP	restriction fragment length polymorphism
RGD	arginine-glycine-aspartic acid
S.	*Streptococcus*
SDS-PAGE	sodium dodecyl sulfate-polyacrylamide gel electrophoresis
T	thymine
Tc	tetracycline
Tn	transposon
U	units
g	g force
X-gal	5-bromo-4-chloro-3-indolyl-β-D-galactoside

ABSTRACT

Mycoplasma hyopneumoniae causes swine enzootic pneumonia, an important disease in the swine industry. Adherence of *M. hyopneumoniae* to the cilia of the tracheal epithelial cells is required to establish infection. Previous studies have identified a 97-kDa protein (P97) as the putative ciliary adhesin. To further characterize the P97 protein, the gene has been cloned, its DNA sequence analyzed, and the function of the P97 protein expressed in *Escherichia coli* studied. These results demonstrated that recombinant P97 has swine ciliary adherence activity. Further analysis revealed that the P97 gene was translated as a 124.9-kilodalton (kDa) protein and subjected to proteolytic cleavage at amino acid 195, resulting in a protein with a predicted molecular weight of 102 kDa. The translated P97 protein showed a high degree of hydrophilicity and contained no cysteine residues or acylation sites, confirming previous findings that P97 was not an integral membrane protein. Two repeat sequences, R1 and R2, were identified at the carboxy end of P97. The R1 sequence contained 15 repeats of AAKP(V/E) and was shown to function as the P97 ciliary binding motif. The adherence-blocking monoclonal antibody F1B6 antigenic epitope was also mapped to the 5′ end of the R1 sequence. Analysis of different *M. hyopneumoniae* isolates displaying variation in cilia binding activity, showed that the variation was not due to expression of P97, the number of R1 copies, or changes in the AAKP(V/E) repeat sequence. Thus, another mechanism must be functioning to control cilium binding activity in *M. hyopneumoniae*. The R2 sequence contained four repeats of NQGKK(S/A)EG(A/T)P and showed a high degree of homology to ribosome binding proteins. Analysis of the P97 contig region showed that the P97 gene was the first of a two gene operon, designated the P97 operon. The second open reading frame coded for a possible membrane protein with a predicted molecular weight of 102 kDa. It had no sequence homology with any known sequence. Hybridization studies showed that the P97 operon sequence existed as multiple copies in the *M. hyopneumoniae* chromosome. These findings support the hypothesis that P97 is involved in ciliary adherence of *M. hyopneumoniae*.

INTRODUCTION

Rationale and Hypothesis

Mycoplasma hyopneumoniae is the causative agent of porcine enzootic pneumonia, a significant and growing threat to the swine industry. In spite of years of work to develop effective vaccines against *M. hyopneumoniae*, no truly effective vaccine is available. This failure could be attributed to our lack of knowledge regarding the pathogenic mechanisms of mycoplasmas in general and to *M. hyopneumoniae* specifically. Little information is available concerning the adherence mechanisms and the specific *M. hyopneumoniae* proteins involved although previous studies by Ross and co-workers indicated that a surface protein called P97 plays an important role in the adherence of *M. hyopneumoniae* to swine cilia (264). The hypothesis addressed by this research was that P97 is a swine cilium binding protein. In order to address this hypothesis, a genetic approach was taken through cloning and analysis of the cloned product in *Escherichia coli*. The direct approach of obtaining mutants and using complementation to confirm the phenotype is not available in this system because of the inability to transform *M. hyopneumoniae*. The hypothesis was addressed by completing the following specific aims:

- to clone, sequence and analyze the P97 gene from *M. hyopneumoniae*;
- to map the cilia binding site of P97 to a specific DNA sequence; and
- to map the F1B6 monoclonal antibody (Mab) epitope in similar fashion.

Cloning and sequence analysis of the P97 gene would add significantly to our understanding of the mechanisms utilized by *M. hyopneumoniae* to adhere to swine tracheal epithelial cells and make progress in developing an effective vaccine for enzootic pneumonia. The approaches taken for the first goal involved screening a *M. hyopneumoniae* Lambda ZAP® II expression library using the cytadherence inhibiting Mab, F1B6. Screening of the expression library was enhanced by using an *E. coli* strain, ISM612, specifically developed for use with mycoplasmal genes (211). The resulting plasmid clones were subjected to Tn*1000* mutagenesis to locate the gene and to facilitate DNA sequencing. The Tn*1000* inserts were also used to map the cilia binding site and the Mab binding epitope of P97. Hybridization studies with P97 operon-specific probes were used to determine the copy number of P97 and its surrounding sequences in the *M. hyopneumoniae* chromosome. Additional studies were also performed by Contour-clamped Homogeneous Electric Field (CHEF) pulse-field gel electrophoresis to map the P97 gene to the published physical map of *M. hyopneumoniae*.

Dissertation Organization

This dissertation is organized in a standard format consisting of five chapters: an Introduction, Literature Review, Materials and Methods, Results, and Discussion. Following the discussion are the references which follow the convention of the American Society for Microbiology.

LITERATURE REVIEW

Bacterial Pathogenesis

Bacterial pathogenicity is a complex, multi-factorial property that enables the pathogens to infect mucosa surfaces, sometimes invade the tissue through these surfaces, spread and multiply, cause tissue damage, and interact with the host defense system. The molecular basis of these factors are the determinants of pathogenicity sometimes referred to as virulence factors (25, 47, 59, 95, 212-214). Successful infection requires the pathogen to express various virulence factors in a coordinated and timely manner in vivo. The pathogens first gain access to the mucosal surface through contact transmission or through aerosol droplet transmission. Pathogens then adhere to epithelial cells through the interaction of bacterial adhesins with host cell receptors. Some pathogens grow and multiply on the epithelial cell surface without tissue invasion. Tissue damage results upon release of bacterial toxins or as a consequence of an inflammatory response by the host. Invasive pathogens express virulence factors that induce phagocytosis by epithelial cells or prevent killing by phagocytes. Some pathogens invade through lymphoid tissue such as M-cells in Peyer's patches. Some pathogens pass between epithelial cells into the underlying submucosa. The subsequent growth of these bacteria often results in the death of host cells and in an inflammatory response. Damaged tissue allows the pathogens to enter the blood stream (sepsis) and spread to other organ tissues causing systematic infection. Certain bacteria express surface adhesins that bind to phagocytes and induce lectin-mediated phagocytosis. Concomitant expression of virulence factors allows the bacteria to resist the killing mechanisms of phagocytes after being ingested, resulting in growth inside the phagocytes. The intracellular growth of these pathogens protects them from the host immune defense system. Systemic infection often is the result of tissue tropism of the pathogens, which may be due to the expression of bacterial adhesin molecules that recognize specific receptor molecules on the surface of organ tissues. The invasion of tissues allows the pathogens to spread and multiply in immune privileged sites where the immune system does not function to full capacity such as in the brain. During infections, bacterial components called modulins are able to interact and modulate the host immune functions. Bacterial modulins stimulate the secretion of cytokines from a variety of host tissues. The combined effects of cytokine release are inflammatory responses, anti-inflammatory responses, or immune suppression depending upon the type of cytokines released. These bacterial components are considered a novel class of virulence factors (88).

Adherence as a Determinant of Pathogenesis

Buccal, respiratory, and urogenital tract epithelium are the major sites for pathogenic bacterial attachment and entry. These sites are normally covered with commensual flora which have reached a state of balance with host clearing mechanisms. These mechanisms include desquamation of epithelial cells, the respiratory mucocillary escalator, flushing of the urogenital tract by urine, and bowel movement (peristalsis). Normal flora function as an integral part of the host defense to help prevent infection. Normal flora compete with pathogens for available nutrients and attachment sites. In some instances, normal flora secrete antimicrobial bacteriocins that are harmful to pathogens. Therefore, tissue adherence is a prerequisite for colonization of pathogens, but there also needs to be a close association established with the epithelial cells where bacteria can grow and multiply.

Mammalian Epithelial Cell Surface: Extracellular Matrix

The surface structure of mammalian cells is complex. Bacteria bind to integral components of epithelial cell membranes or components of the extracellular matrix. Membrane glycolipids extend outward to the extracellular milieu with a complex carbohydrate structure. Glycoproteins also contain complex carbohydrate structures and function as a second class of receptor molecules. The normal function of these glycoconjugates in the host include cell-to-cell communication and hormone receptors (77, 165). These membrane glycoconjugates usually form a network through connections with cytoplasmic cytoskeletal components providing a conduit for the transduction of extracellular signals into the cell. These glycoconjugates also function as receptors for the binding of immune cells (165).

The surface of epithelial cells is normally covered with a layer of viscous components derived from the secreted products of the cell. This viscous layer is called mucus or extracellular matrix (ECM). It contains a variety of molecules including polysaccharides such as collagen, heparin sulfate, hyaluronic acid, and glycoproteins such as fibronectin and laminin (58). The ECM has been shown to be actively involved in mediating adherence of bacteria. Some extracellular matrix proteins were recently proposed as a unique class of molecules which mediate adherence of gram-positive bacteria to host tissue (167, 245).

When pathogens contact the epithelial surface, they first interact with the extracellular matrix. The mucus and its components may function as receptors for the bacteria to attach and multiply. In vivo multiplication of pathogens in the mucus layer may be a prerequisite for

subsequent adherence to epithelial cells. In some instances, the bacteria bind to mucus components and become restrained in the mucus layer and fail to adhere to underlining target cells due to the titration effects of available adhesins.

Bacterial Adherence

Because of the complexity of the surface structure of epithelial cells, it has become accepted that bacterial adhesion is a multi-phasic process involving multiple factors of bacterial and host origin. The first phase of bacterial adhesion involves nonspecific interaction between the surface components of bacterial and epithelial cells. In this phase, ionic interaction, hydrogen bonding, Van der Waal forces, and surface hydrophobicity may play important roles in determining the subsequent interaction. The second phase of bacterial adhesion involves specific reversible binding between surface components of bacterial and epithelial cells. As bacteria and epithelial cells are drawn closer together, specific and nonreversible binding occurs between bacterial adhesins and receptors on the surface of epithelial cells. The bacteria become firmly bound to the host epithelial cells. It is this adhesion that prevents clearance of the bacteria by the host's innate clearance mechanisms.

Pathogens, such as enterotoxigenic *Escherichia coli* (ETEC), enteropathogenic *E. coli* (EPEC) *Vibrio cholerae*, and *Campylobacter jejuni* adhere to host tissues but lack invasive mechanisms while pathogens such as enteroinvasive *E. coli* (EIEC), *Listeria monocytogenes*, and *Salmonella* spp. invade following cytadherence. The ability of bacteria to adhere to the host tissue is mediated by specialized bacterial surface components called adhesins. Receptor specificity was first recognized by Dugid and Gillies as the agglutination by some bacteria of red blood cells and its inhibition by mannose (mannose sensitive) (55). Not all hemagglutination activities of bacteria were sensitive to mannose; some were insensitive or mannose resistant. Bacterial adhesins are normally categorized according to their location, morphology, and receptor specificities. Bacterial adhesins can also be divided into two groups according to their association with fimbriae. The first group consists of fimbriated adhesins. These adhesins are protein molecules located either at the tip of the fimbriae or scattered throughout the whole fimbriae structure. The second group consists of adhesins not associated with fimbriae. These adhesins can be found scattering throughout the entire bacterial surface or concentrating at a specialized structure at one end of the bacteria as exemplified by the *Mycoplasma pneumoniae* P1 adhesin.

Classification of adhesins based on their binding specificity results in two classes. One class contains adhesins with carbohydrate binding specificities similar to plant lectins. The interaction between lectin-like adhesins and their receptors can be inhibited by polysaccharides

with similar structure. The other class of bacterial adhesins is defined by non lectin-like interactions. This class specificity is determined by the ability of the adhesin to recognize and bind to amino acid sequences in the receptor proteins or bind to other surface molecules such as sulfated glycolipids, etc.

Gram-positive bacteria posses lectin-like adhesins either as a component of fimbriae, as fibrial structures on the surface, or as non-fimbrial adhesins. Many gram-positive bacteria lack fimbriae and lectin-like adhesins, but nevertheless retain the ability to bind to host tissues through specific binding to ECM components. Bacterial surface components such as lipotechoic acid, peptidoglycan, and surface proteins can function as adhesins and bind to ECM components such as fibronectin and collagen. Selected bacterial adhesins that illustrate the scope of complexity from gram-negative and gram-positive bacteria as well as mycoplasmas will be reviewed in detail.

E. coli Type 1 Fimbriae

Most gram-negative bacteria posses fimbriae, surface extrusions consisting of protein subunits assembled into rod-shaped organelles about 7 - 11 nm in diameter and 0.5 to 10 μm long. The most common classification of bacterial adhesins is according to "type". Type 1 refers to fimbriae that are rigid and exhibit mannose-sensitive hemagglutination. Type 2 are morphologically related to type 1 but do not cause hemagglutination. Type 3 are flexible fimbriae with mannose-resistant hemagglutination common in the *Enterobacteriaceae*. Type 4 refers to fimbriae with the major subunit containing N-methylphenylalanine at the amino-terminal end. Type 5 are mannose-sensitive, but are thinner than type 1. As more and more fimbrial adhesins are identified, adhesins are discovered that cannot be classified according to any established scheme. The latest classification scheme was proposed by Orskov and Orskov (162). Most *E. coli* strains express more than one type of fimbriae with different receptor specificities at any particular time during infection (131).

Type 1 fimbriae are present in most *E. coli* strains. Studies have shown that type 1 fimbriae are associated with clinical isolates of acute urinary tract infection, chronic prostitis, pyelonephritis, sepsis, and meningitis of human and other animals (205). Identification of the type 1 fimbriae in clinical isolates was achieved by mannose-sensitive hemagglutination (234), serotyping (270), immunofluorescence (53), or hybridization with specific DNA probes (163, 210).

Epidemiology

Epidemiological studies failed to correlate the roles of type 1 fimbriae in bacterial infection in association with other types of fimbriae or virulence factors (50, 199, 235). However, studies using animal models infected with fimbriated *E. coli* have suggested a critical role of type 1 fimbriae in infection. Jayappa et al. (99) showed that anti-fimbriae serum protected newborn pigs from developing colibacillosis after challenge with *E. coli* expressing type 1 fimbriae. Another study using chickens experimentally infected with clinical isolates expressing either type 1 fimbriae or P fimbriae or both showed that type 1 fimbriae was involved in the early stages of development of colisepticemia by promoting the association of fimbriated bacteria with the trachea and air sacs (53). Nonetheless, conflicting results have been reported for the exact role of type 1 fimbriae in infection (171, 232).

Genetics

Genes coding for the assembly machinery of type 1 fimbriae have been cloned and characterized (131). The *fim* operon contains six genes that are major or minor components of type 1 fimbriae. Its organization is similar to operons coding for other types of fimbriae suggesting the presence of a common ancestor gene. Type 1 fimbriae is composed of 17 kilodalton (kDa) subunits, the product of *fimA*, assembled right-handed as a tubule with a diameter of 7 nm and length of 10 μm. There are about 1000 major subunit proteins per fimbriae. The FimA protein does not contain mannose-specific binding activity, however, but appears to play only a structural role. This was demonstrated in an experiment with recombinant *E. coli* strains that failed to produce type 1 fimbriae due to a *fimA* deletion. These strains retained binding ability to mannose-coated beads (109). FimC was suggested to play a role in the assembly of fimbriae since mutations in *fimC* abolished fimbrial synthesis (107). Its protein sequence was highly homologous to papD, a member of the periplasmic chaperone superfamily. The activity of PapD can complement FimC in vitro as well as in vivo (101). FimD is found in the outer membrane and appears to function as an anchor for the fimbriae structure (108). FimF and FimG are minor proteins with molecular weights of 16 and 14 kDa, respectively. Functional analysis of *fimF* and *fimG* mutants suggested that these two proteins are not associated with the fimbriae but are responsible for initiation and termination of fimbriae assembly (191). FimH, a 30-kDa minor protein, is the adhesin protein responsible for mannose-specific binding. It is located at the tip and the side of the fimbriae (117, 118).

Regulation

The promoter of the *fim* operon is located upstream of *fimA*. The expression of the operon is regulated by temperature and DNA superhelicity. Expression of the *fim* operon of type 1 fimbriae is controlled by the products of two regulatory genes located upstream (22, 106). FimB and FimE are basic proteins belonging to the integrase family that recognize and mediate inversion of an invertible 314 basepair (bp) segment containing a promoter upstream of FimA (56). The inversion of this segment results in an on/off phenotype of the promoter activity. The frequency of phase variation from off to on was measured at 10^{-3} per cell per generation, and was mediated by FimB, while phase switching from off to on was measured at 10^{-2} per cell per generation and was mediated by both FimB and FimE (140). Other factors affecting the regulation of phase variation of type 1 fimbriae included temperature, media (66), growth conditions (93, 201), presence of leucine-response regulatory protein (21), integration host factor (IHF), and H-NS nucleoid protein (51, 161).

Phase variants and various type 1 fimbriae mutants with modified phenotypes were used for studying the role of type 1 fimbriae in infection in tissue cultures and animal models. Alkan et al. demonstrated that phase variation occurred in vivo, and type 1 fimbriae conferred the advantage for the growth of *E. coli* in the peritoneal cavity, at least in early stages of infection in mice (2). Bloch et al. found that *fimA* mutations correlated with the loss of intestinal colonization in rats, while blood stream invasion was not affected (20). *E. coli* F-18, a human fecal isolate, produced type 1 fimbriae and colonized streptomycin-treated mouse large intestine (119, 141). *E. coli* strains carrying a plasmid over-expressing FimB proteins resulted in locking the phase in the "on" phenotype and became poor colonizers as compared to the parental strain (142).

Receptors

In general, glycoproteins and glycolipids at the surface of epithelial cells act as receptors for type 1 fimbrial adhesins. The sugar moieties on these glycoconjugates function as the binding site for the adhesins and determine the binding specificity. Type 1 fimbrial adhesins have been shown to mediate the agglutination of erythrocytes and yeast, the attachment of bacteria to buccal, respiratory, urogenital epithelial cells and leukocytes in a mannose-specific manner. Bacterial adherence to human colonic epithelial cells was inhibited by α-methyl mannoside (258). The bacteria bound to epithelial cells directly or were loosely associated with the cell surface. Attachment to guinea pig intestinal epithelial cells was inhibited by mannosides,

especially aromatic α-mannosides. 4-methylumbelliferyl α-mannoside and p-nitro-o-chlorophenyl α-mannoside inhibited adherence 1000 times stronger than did α-methyl mannoside (60).

Bacterial agglutination of yeast, erythrocytes, and human sperm also displayed a similar inhibition pattern (60, 149). Uropathogenic *E. coli* with type 1 fimbriae adhered to excised human ureter and bladder epithelia in a mannose-specific manner (64). Mannose-containing glycoproteins of tracheal epithelial cells have been suggested to be the receptor for type 1 fimbriae (38). A 65-kDa glycoprotein in a Triton X-100 fraction of guinea pig erythrocyte membranes was isolated and characterized as the receptor for type 1 fimbriae adhesin. Type 1 fimbriae inhibited the binding of fimbriated *E. coli* to purified glycoprotein receptors. This 65-kDa receptor bound to concanavalin A and type 1 fimbriae, and inhibited bacterial hemagglutination of guinea pig erythrocytes. The binding of receptors to adhesins was reduced when the glycoprotein was treated with sodium metaperiodate, endoglycosidase H, trypsin, and V8 protease (73). Leukocyte integrin CD11/CD18 complex has been demonstrated as a receptor for type 1 fimbriae which might result in lectinophagocytosis (68). Binding of type 1 fimbriae to leukocyte integrin was inhibited by methyl α-mannose and Mabs specific to CD11a, CD11b, or CD18 (69). Other leukocyte membrane glycoproteins have also been identified to function as receptors for type 1 fimbriae, though the consequence of these interactions is not fully understood (184, 197, 198). Integral membrane glycoproteins, extracellular glycoproteins, or glycoproteins loosely associated with the outer membrane of host cells can function as receptors for type 1 fimbriae. Laminin of the extracellular matrix acted as receptor molecules for type 1 fimbriae (120). A rabbit intestinal mucus glycoprotein was identified as a receptor for type 1 fimbriae, suggesting that the mucus layer constituted a site for bacteria to multiply prior to colonization of epithelial cells (206). A 118-kDa glycoprotein of rat intestinal mucin functioned as a receptor for type 1 fimbriae and acted as the intermediate link between bacteria and epithelial cells (193, 194). Secretory IgA has been proposed as a receptor for type 1 fimbriae. Secretory IgA and IgA myeloma proteins, especially those of IgA_2 subclass, contained carbohydrate moieties for type 1 fimbriae binding which resulted in agglutination of fimbriated bacteria regardless of the specificity of the antibody molecules (257).

Interaction with the immune system

Immunogenicity

Immunization of Peyer's patches of rats with *E. coli* carrying type 1 fimbriae was used to study antibody production and homing of secretory antibodies against fimbriae and bacterial

surface antigens. The primary immune response produced antibodies (IgA, IgG, IgM) to fimbriae in milk at a concentration 5 times higher than in bile (36). Repeated antigen stimulation resulted in the antibodies predominantly in the bile (37). In another study, aerosol immunization with fimbriated *E. coli* resulted in the detection of IgA in bile, but not in bronchoalveolar lavage. IgG were not detected in serum either (247). Similar results were also obtained in another study (155).

Modulation of the immune system

E. coli type 1 fimbriae binding to phagocytic cells via lectin-carbohydrate interactions often resulted in activation and degranulation of the phagocytes, and uptake and killing of the bacteria, a phenomenon called lectinophagocytosis (17, 23). Protein kinase C was believed to be involved in the activation of phagocytes (70). Preincubation of purified *E. coli* type 1 fimbriae with human neutrophils augmented subsequent activation by concanavalin A, opsonized zymozan, or type 1 fimbriae-coated latex particles (74). Fimbriated *E. coli* phase variants stimulated phagocyte oxidative metabolism more efficiently than non-fimbriated phase variants (75). Further more, type 1 fimbriated *E. coli* treated with specific Mab to form bundles of fimbriae on the cell surface activated neutrophils more effectively than did nonfimbriated *E. coli* or fimbriated *E. coli* without bundles (170). Differential degranulation was observed when neutrophils were activated with *E. coli* expressing type 1 fimbriae; a significant quantity of protease-myeloperoxidase and N-acetyl-β-D-glucosaminidase (the primary and tertiary granule marker, respectively) was released as compared to the release of vitamin B12-binding protein (the secondary granule marker)(215, 216). Purified FimH, the minor subunit of type 1 fimbriae responsible for the mannose-specific adherence, was a potent activator of human neutrophils and mast cells. This stimulation was suspected to play an important role in host defense against infection (134-136, 231).

Bordetella pertussis

Bordetella pertussis, the causative agent of whooping cough, has been the subject of intense study in order to better understand the mechanisms of bacteria adhesion to host epithelial cells. *B. pertussis* utilizes multiple mechanisms to adhere to tissue culture cells including the filamentous hemagglutinin (FHA), fimbriae (agglutinogens), pertactins, and pertussis toxin. Fimbriae and pertactin are cell surface proteins, pertussis toxin is secreted, and FHA is found to be a cell surface-associated secretory protein.

Filamentous hemagglutinin

The filamentous hemagglutinin mediates the adherence of *B. pertussis* to human respiratory tract epithelial cells and agglutination of red blood cells. Its structural gene, *fha*, has been cloned and sequenced (180). The filamentous hemagglutinin is synthesized intracellularly as a 367-kDa preprotein and subsequently processed into a mature 220-kDa protein. Processing and transportation to the cell surface is required for the adherence of *B. pertussis* to eucaryotic cells (4). The FHA contains multiple domains which have unique functions. Relman et al. found that an arginine–glycine–aspartic acid (RGD) domain in the FHA sequence might be involved in adherence since a *B. pertussis* mutant with a FHA gene devoid of the RGD domain lost the ability to bind to ciliated epithelial cells (180). Arico et al. demonstrated that this RGD domain mediated the binding of bacteria to Chinese hamster ovary (CHO) cells (4). Another study by Leininger et al. indicated that an RGD-containing peptide derived from the FHA sequence had no effect on the attachment of FHA to epithelial cells, prompting further studies to determine the function of the RGD domain in FHA molecules (125). The FHA interacted with macrophage galactose-containing glycoconjugates and the integrin CR3 (αMβ2, CD11β/CD18). The interaction between CR3 and FHA involved the RGD sequence according to Relman et al. (179). Ishibashi et al. demonstrated that the RGD domain promoted *B. pertussis* binding to monocytes, and this enhancement was blocked by antibodies directed against CR3 (96). Prasad et al. identified a carbohydrate recognition domain (CRD) located at the FHA amino acid sequence 1141 to 1279 that mediated the binding of FHA to lactosylceramide (174). In general, this region was believed to be critical for bacterial adherence to ciliated cells (129, 174). A third domain distinct from the RGD and CRD domains exhibited heparin-inhibitable lectin activity. Menozzi et al. proposed that this domain might be important to the interaction of *B. pertussis* with epithelial cells or the extracellular matrix (129, 145). Binding of *B. pertussis* to cultured epithelial cells was reduced by the sulfated polysaccharide heparin, dextran and purified FHA. Residual adherence activity of a *B. pertussis* mutant lacking FHA was not affected by the sulfated polysaccharides (145). The structure of FHA has also been determined. It formed monomeric rigid rods with a length of 50 nm and had the shape of a horseshoe nail, a globular head, a 35 nm long shaft and a small flexible tail (133). The structure contained two regions of tandem 19 residual pseudo-repeats that formed β-sheets separated by β-turns. Functional domains were also mapped to the FHA molecule. The RGD domain was assigned to the tail region, and the putative hemagglutination domain was assigned to the head (133).

Pertactin

Robert et al. demonstrated that a 69-kDa immunogenic surface protein of *B. pertussis*, P69 or pertactin (*prn*), played a role in mediating adherence to HEp2 cells. This was shown by a double mutant, *fha* and *prn*, that was significantly less adhesive than a *fha* single mutant. However, there was no discernible difference in the binding ability between a *prn* mutant and the wild type strain (183). The P69 protein has been purified and shown to attach to CHO cells (126). The attachment was inhibited by an RGD-containing peptide with homology to a region in the P69 protein. A mutant lacking P69 exhibited a reduced adherence to CHO and HEp2 cells. Leininger et al. first used the term pertactin to refer to the P69 protein (126). Over-expression of pertactin didn't seem to have an effect on the binding of *B. pertussis* to cultured cells (130). The structure of pertactin was determined by X-ray crystallographic studies (57). Pertactin appeared to contain a 16-stranded parallel β helix with a V-shaped cross-section. Several putative functional domains were also identified in the same study.

Pertussis toxin

Pertussis toxin (PTX) secreted from *B. pertussis* not only functioned as the major pathogenic determinant in damaging host epithelial cells through ADP-ribosyltransferase activity of the S1 subunit, but also mediated bacterial adhesion to ciliated epithelial cells and macrophages (237, 238). The binding domains of PTX were localized to the B oligomer. The subunits S2 and S3 of the B oligomer of PTX, but not S1 or S4 subunits, participated in the adherence of *B. pertussis* to human macrophages (241). The S2 subunit recognized ciliary lactosylceramides, and the S3 subunit recognized leukocyte gangliosides (196).

Fimbriae

B. pertussis produces several serotype-specific agglutinins. Serotype 2 and serotype 3 epitopes have been located on the fimbriae by use of type-specific Mabs in an immunoelectron microscopic study (9). Each type of agglutinin associated with fimbriae individually or simultaneously. These agglutinins constituted the major subunits of the fimbriae. A third serotype, X, was characterized as a silent fimbrial subunit gene. The genes coding for these agglutinins, *fim2*, *fim3*, and *fimX*, have been cloned and sequenced (127, 151, 168) Willems et al. identified three additional fimbrial genes in a gene cluster located directly downstream of the *fha* gene (249, 250). One of these genes, *fimB*, was homologous to chaperone-like fimbrial proteins. *fimC* was homologous to a class of outer membrane proteins involved in transportation and anchorage of fimbrial subunits. *FimD* was suggested to be the fimbrial adhesin based on high homology to MarK, a fimbrial adhesin from *Klebsiella pneumoniae*

(249). Interestingly, an in-frame deletion in *fimD* totally abolished FimD expression and also affected the expression of Fim2 and Fim3.

The role *B. pertussis* fimbriae play in pathogenesis is not well defined although it has been incorporated in different types of subcellular vaccines as an active component (102). Mooi et al. demonstrated that FHA played a more crucial role than fimbriae in the colonization of the mouse upper respiratory tract, while the persistence of *B. pertussis* in the lung was not affected by fimbriae expression (150). Funnell et al. showed that a *fim* negative mutant of *B. pertussis* adhered less well to the tracheal ring of *Papio snubis* than to Vero cells. The authors suggested that *B. pertussis* fimbriae might be important in the initial stages of colonization (65). Pertactin, FHA, and fimbriae mediated the binding of *B. pertussis* to monocytes. Mutant strains of *B. pertussis* lacking fimbriae bound less efficiently to monocytes (86). Fimbriae bound to monocytes through the surface interaction of FimD with Very Late Antigen-5 (VLA-5) (87). The interaction between FimD and VLA-5 also activated CR3 which resulted in an enhanced binding of *B. pertussis* to monocytes (87). Recently, Geuijen et al. demonstrated that fimbrial binding to sulfated sugars and HEp2 cells was mediated by the major subunit of fimbriae. The binding was not dependent on the minor fimbrial subunit. However, both FHA and fimbriae were required for this binding (72).

Streptococcus pyogenes

The lack of genetic systems has deterred the studies of adhesion mechanisms of gram-positive bacteria until recently. Nevertheless, a great deal of progress has been made (245). Surface components of some important Gram positive pathogens have been studied in detail for their possible roles in bacterial adhesion to host cells (166). These components include mucin (polysaccharide), capsule (usually hyaluronic acid), techoic acid (TA, polyribotol phosphate), lipoteichoic acid (LTA, poly glycerol phosphate), and surface proteins such as M protein and F protein. It is generally believed that multiple mechanisms are involved in adhesion of gram-positive bacteria to host tissues.

S. pyogenes colonizes pharyngeal epithelial cells and causes pharyngitis by releasing toxins which may result serious complications, and by causing host inflammatory responses. *S. pyogenes* binds to various host-derived proteins including albumin, fibronectin, α2-macroglobulin, immunoglobulin G, laminin, plasmin, collagen type IV, salivary glycoproteins, mucins, basement membrane proteins, and haptoglobin. Some of these proteins have been studied in detail and proven to be critical in *S. pyogenes* cytadherence, the remaining proteins merit more investigation.

Lipoteichoic acid

Lipoteichoic acid is the major adhesin of *S. pyogenes* mediating attachment to buccal, and pharyngeal, and phagocytic cells (28, 35, 239). Preparations of LTA inhibited the adherence of *S. pyogenes* to epithelial cells and was shown to protect against *S. pyogenes* challenge in a mouse study (39). Antibodies against the polyglycerol phosphate backbone of LTA also inhibited the cytadherence activity (15). Immunoelectron microscopic and ultrastructural studies of *S. pyogenes* established that LTA was located on the outer cell surface (192). In a study using protoplasted *S. pyogenes*, Mattingly et al. revealed that LTA of *S. pyogenes* was released into the environment. The released LTA became anchored in the bacterial membrane. The exposed hydrophobic domain (glycolipid) of LTA interacted with epithelial cell surface. Deacylated LTA preparations had no effect on this interaction (138).

The receptor for LTA has been identified as fibronectin deposited on the mucosal epithelial cell surface (13). Binding sites on fibronectin for LTA from *S. pyogenes* were located in a 28-kDa fragment of the N-terminal region. In contrast, LTA from *Staphylococcus aureus* reacted with the 28-kDa fragment, a 23-kDa fragment and other high molecular fragments, suggesting that different bacteria may interact with different fibronectin domains (13, 14, 209).

M protein

The M protein is secreted by *S. pyogenes* and becomes associated with the bacterial cell wall. It displays antiphagocytic activity by binding to serum factor H resulting in inactivation of the C3b complex (169). Other studies, however, suggested a role of M protein in adherence of *S. pyogenes* to epithelial cells. Expression of M protein correlated with the ability of *S. pyogenes* to adhere to epithelial cells after high in vitro passage of clinical isolates (221). Secretory IgA directed against M protein also blocked the adherence of *S. pyogenes* to nasal mucosal cells (121), but isogenic *S. pyogenes* strains lacking the ability to express M protein adhered to buccal, pharyngeal, or tonsillar epithelial cells. This suggested that M protein was not the primary adhesin although M protein promoted the aggregation of *S. pyogenes* to tonsillar epithelial cells (27, 35). In contrast, M protein-expressing strain of *S. pyogenes* bound to HEp-2 cells and mouse oral epithelial cells more effectively than did isogenic strains lacking M protein. The binding was inhibited by M protein treated with pepsin (33, 35, 243). The ligands on the HEp-2 cell surface were identified as two glycoproteins of 97 and 205 kDa which differed from fibronectin. These two glycoproteins were sensitive to trypsin, chymotrypsin, and heat (243). Binding of M protein to HEp-2 cells was inhibited by several fucose-containing oligosaccharides which might be present in these two glycoproteins (244). M protein mediated the binding of *S. pyogenes* to keratinocytes represent a possible role of M

protein in *S. pyogenes* skin infections (159). A C-repeat domain in M protein was found responsible for the adherence to the keratinocyte receptor, CD46 (160).

Other *S. pyogenes* surface proteins were found to be involved in bacterial adhesion. Protein F, a 74-kDa protein characterized by Hanski et al, binds to fibronectin (82). Its gene was cloned, and the recombinant protein F expressed in *E. coli* showed high affinity binding to fibronectin. Mutant *S. pyogenes* strain lacking protein F expression had a lower binding activity to respiratory epithelial cells. Interestingly, expression of protein F was environmentally regulated in response to atmospheric oxygen concentration (242). Its role in *S. pyogenes* pathogenesis was suggested (82, 83, 159). Sequence and functional analysis of the protein F gene revealed that there were two repeat domains, RD2 and UR, required for maximal fibronectin binding. Functional assays showed that these two domains bound to different parts of fibronectin (164).

Talay et al. also identified a 71-kDa fibronectin binding protein, Sfb, having a high degree of homology to Protein F. Sfb protein was also a putative adhesin for *S. pyogenes* binding to epithelial cells (230, 240). The Sfb gene was cloned, and recombinant protein made in *E. coli* bound to fibronectin and HEp-2 epithelial cells. A 37 amino acid sequence repeated 4 times was found to constitute the binding domain of the Sfb protein. Purified Sfb protein inhibited binding of fibronectin to *S. pyogenes* as well as the adherence of bacteria to epithelial cells. This repeat sequence had a high degree of homology to the 38 amino acid D3 repeat of the fibronectin binding protein of *S. aureus* (230). A two-step model for the adhesion of *S. pyogenes* to epithelial cells has been proposed in which the binding of LTA (anchored to the membrane LTA binding protein) to fibronectin preceded a secondary binding of another bacterial adhesin to a host receptor (85, 156, 208). A 54-kDa protein exhibited binding activity to fibronectin and fibrinogen was also cloned by Courtney et al. (34). This protein was suggested to participate in the adhesion of *S. pyogenes* to host cells.

Mycoplasmas

Mycoplasmas constitute a unique group of bacteria which are believed to have evolved from Gram positive bacteria. These bacteria lack the peptidoglycan cell wall and outer membranes that are characteristic to gram-positive and gram-negative bacteria, respectively. Mycoplasmas contain only a single membrane separating their cytoplasm from the extracellular environment. They are classified in the class *Mollicutes* with more than 100 recognized species. The class *Mollicutes* includes four orders: order *Mycoplasmatales* containing the family *Mycoplasmataceae* ; order *Entomoplasmatales* containing the families *Entomoplasmataceae* and *Spiroplasmataceae;* order *Acholeplasmatales* containing a single

family *Acholeplasmataceae*, and order *Anaeroplasmatales* containing a single family *Anaeroplasmataceae* (236). The class *Mollicutes* also includes several uncultivated or unclassified mycoplasma like organisms sometimes referred to as MLOs. The generic term mollicutes will be used throughout this dissertation to refer to all members of the class *Mollicutes* in a general way. The term mycoplasma will be used to refer only to the members of the family *Mycoplasmataceae*, genera *Mycoplasma* and *Ureaplasma*. The term acholeplasma will be used to refer to the members of the family *Acholeplasmatales*.

Mycoplasmas represent the smallest living organisms known. They are approximately 0.3 μm in diameter and can range up to nearly 100 μm in length for some spiroplasmas. Because of their small size and pleomorphic structure, mollicutes were once thought to be viruses because they can pass through filters. Mycoplasmas also have the smallest known genome ranging in size from 580 to 1,700 kb with a low G+C content ranging from 23 to 41%. Codon usage for most mycoplasmas, except the acholeplasmas, differ from that of other eubacteria. The codon UGA codes for tryptophan in mycoplasmas rather than functioning as a stop codon as in other organisms. The small genome of mycoplasmas suggests that there is limited coding capacity for protein synthesis. Therefore, they lack the biosynthetic capacity of other bacteria, requiring complex media with serum in vitro or are noncultivable. Most mollicutes are parasitic to human, animals, insects, or plants. Pathogenic mycoplasmas colonize respiratory and urogenital tracts of humans and animals where they form a close association with host epithelial cells. This close association is believed to allow mycoplasmas to extract nutrients directly from epithelial cells. Exchange of membrane components between mycoplasmas and host cell membranes has been documented (253). Surrounded by an amorphous layer of polysaccharide capsule, mycoplasmas lack any recognizable appendages such as flagella or fimbriae. However, some species of mycoplasmas including *M. pneumoniae*, *M. gallisepticum*, *M. pulmonis*, and *M. genitalium* exhibit a flask-shaped polarity of the cell body (176). Cytadherence and gliding motility have been demonstrated to be associated with the flask-shape organelle of mycoplasmas (24).

Mycoplasma pneumoniae

Since mycoplasmas lack cell walls, they have often been chosen as models to study membrane structure and function. Mycoplasmal membranes are made of a diverse group of lipids including neutral lipids, glycolipids, and phospholipids which are the most abundant. Unlike other eubacterial membranes, mycoplasmas contain sterols, in most instances cholesterol, as a major component of the membrane. Cholesterol is required for the normal growth of mycoplasmas which can be supplied exogenously or obtained from the in vivo

environment, possibly the host's cell membrane. To effectively derive cholesterols and other nutrients from the host, mycoplasmas need to adhere closely to epithelial cells.

P1

Most studies of mycoplasma cytadherence have been performed with *M. pneumoniae*, a human pathogen that causes atypical pneumonia (walking pneumonia) in children (>3 years) or young adults (10, 111, 176, 181). Powell et al. examined the attachment of radiolabeled *M. pneumoniae* to hamster tracheal ring organ cultures. Virulent *M. pneumoniae* was found to attach to the luminal surface of epithelial cells, while avirulent *M. pneumoniae* failed to interact with the epithelial cells (173). The pretreatment of tracheal rings with neuraminidase or sodium periodate significant reduced cytadherence. Electron microscopic studies by Wilson et al. revealed that *M. pneumoniae* adhered to non-ciliated epithelial cells of tracheal ring organ cultures using its differentiated tip structure sometimes referred to as the attachment organelle (252). This study also revealed that the attachment organelle had a dense central rod surrounded by a translucent space. Close association between *M. pneumoniae* and human RBCs was also demonstrated by scanning electron microscopy (175). *M. pneumoniae* attached to the RBC surface which resulted in an indentation at the site of attachment. The use of Mabs specific to the attachment organelle also confirmed its involvement in cytadherence. Adherence to erythrocytes in vitro could be inhibited by Mabs specific for the attachment organelle. Pretreating virulent *M. pneumoniae* with these Mabs significantly reduced the lung lesions in hamster (26).

The nature of the *M. pneumoniae* adhesin(s) has been studied by Razin et al. (177). Trypsin treatment of *M. pneumoniae* cells abolished the ability to attach to human RBCs suggesting a protein nature of the adhesins. Hu et al. identified a surface protein, P1, with an estimated molecular weight (MW) of 179 kDa as the major adhesin of *M. pneumoniae* (11, 90, 91). Monoclonal antibodies against P1 reacted with a region of the attachment organelle covered with peplomer-like particles and inhibited the attachment of *M. pneumoniae* to host cells (90). The P1 gene has been cloned using an oligonucleotide probe derived from the N-terminal amino acid sequence of purified P1 protein (227). Sequence analysis revealed that the gene contained a 4,881 bp open reading frame (ORF) encoding a protein with a predicted molecular weight (MW) of 176 kDa. Secondary processing of the 176-kDa protein by cleavage at the putative proteolytic recognition site resulted in a mature protein with a predicted MW of 169.8 kDa (227). Southern hybridization of *M. pneumoniae* genomic DNA using an internal P1 probe established that the P1 structural gene or gene sequence existed as multiple copies (225). Southern hybridization and restriction fragment length polymorphism (RFLP) analysis

of the P1 gene was used to the classify *M. pneumoniae* clinical isolates into two distinct groups (43, 226). Cross-hybridization between adhesin genes of *M. pneumoniae*, *M. genitalium*, and *M. gallisepticum* was observed under low stringency conditions indicating the existence of a family of adhesin-related genes among pathogenic mycoplasmas (40). The relationship of cytadhesins from different mycoplasmal species was also investigated by the cross-reactivity in immunoblot analysis (153). Infection with virulent strains of *M. pneumoniae* stimulated humoral responses in guinea pigs (97). Immunizing guinea pigs with purified *M. pneumoniae* P1 protein stimulated systemic and local humoral antibody responses along with the production of cytadherence inhibiting antibodies. In the same study, however, the immune response was not protective against subsequent challenge with *M. pneumoniae* and actually accentuated disease (98).

Little is known about the receptors for the P1 adhesin, but cytadherence studies of *M. pneumoniae* have produced some important results. Krivan et al. investigated the binding specificities of radiolabeled *M. pneumoniae* to various types of glycolipids and glycoproteins (115, 116, 182). *M. pneumoniae* bound strongly to sulfatide and sulfated glycolipids such as seminolipid and lactosylsulfatide all of which contain a terminal Gal ($3SO_4$)β1 linkage. Only metabolically active *M. pneumoniae* cells bound to sulfatide. Dextran sulfate inhibited binding of *M. pneumoniae* to purified sulfatides. Dextran sulfate also partially inhibited the binding of *M. pneumoniae* to cultured human colon adenocarcinoma cells (WiDr) (115). *M. pneumoniae* also bound to glycoproteins including laminin, fetuin, and human chorionic gonadotropin in a dose-dependent and saturable manner. Adhesion was energy dependent since no attachment occurred in media without glucose. The presence of a terminal neuraminic acid α2,3-β1,4-N-acetylglucosamine linkage was required for binding since soluble laminan, asparagine-linked sialyloligosaccharides from fetuin, and 3′-sialyllactose, but not 6′-sialyllactose, inhibited attachment of *M. pneumoniae* to laminin. Dextran sulfate and 3′-sialyllactose did not inhibit attachment to laminin and sulfatide, respectively, suggesting two distinct receptor specificities for the *M. pneumoniae* adhesion. Both 3′-sialyllactose and dextran sulfate partially inhibited binding of *M. pneumoniae* to WiDr cells; the combination of the two glycoconjugates inhibited binding by 90% (182).

The P1 operon contains the P1 gene flanked by two ORFs 4 and 6 with a coding capacity for 28-kDa and 130-kDa proteins, respectively (94). The latter protein is processed into two proteins of 40 and 90 kDa both of which are membrane-associated (122). Spontaneous mutants of *M. pneumoniae* lacking the 40- and 90-kDa proteins exhibited reduced adherence to host cells suggesting the participation of these two proteins in *M. pneumoniae* cytadherence. This was confirmed by nearest-neighbor analysis in which the homobivalent, thio-cleavable, and

nonmembrane-permeating cross-linking reagent 3,3′ dithiobis (sulfosuccinimidylpropionate) was used to treat *M. pneumoniae*. The resulting cross-linked protein complex was immunoprecipitated with antibody against P1, 40-kDa, or 90-kDa proteins. Immunoblot analysis indicated that P1, the 40- and 90-kDa proteins, and an unidentified 30-kDa protein were positioned at a maximal distance of 1.2 nm on the attachment organelle of *M. pneumoniae* (123). Southern hybridization and DNA sequence analysis has demonstrated that the ORF6 sequence existed as multiple copies in the *M. pneumoniae* genome (190).

P30

Another *M. pneumoniae* surface protein involved in cytadherent activity has been identified and characterized. P30 was first observed as a 32-kDa trypsin-resistant protein associated with hemadsorption activity. Hemadsorption negative strains of *M. pneumoniae* were avirulent and noncytadherent (113). Immunoelectron microscopic studies using colloidal gold-labeled antibody revealed that P30 proteins were clustered at the attachment tip (12). The P30 gene has been cloned and sequenced. It consists of an ORF of 825 nucleotides with a coding capacity for a protein of predicted MW of 29.7 kDa (42). Three types of proline-rich 6-amino-acid repeat sequences (PGMAPR, 7 repeats; PGMPPH, 3 repeats; PGFPPQ, 3 repeats) were identified at the carboxyl end of P30. These repeat sequences exhibited a significant degree of homology to the P1 adhesin protein. The importance of proline-rich repeat sequences of P30 in cytadherence was demonstrated by the identification of spontaneous hemadsorption negative mutants carrying a deletion in the P30 gene resulting in the expression of a 25-kDa protein lacking 8 of the 13 proline-rich 6-amino-acid repeat sequences (11, 12, 44, 113). Involvement of proteins other than the P1 and P30 adhesins in cytadherence of *M. pneumoniae* was also proposed by these studies.

HMW cytadherence accessory proteins

M. pneumoniae undergoes phase variation in its cytadherence phenotype with concomitant loss or reacquisition of several high molecular weight proteins. These proteins, HMW1 through HMW5, range in molecular weight from 140 to 340 kDa by SDS-PAGE gel analysis (11, 12, 113, 218). Peptide mapping and Triton-X114 partitioning demonstrated that HMW1 and HMW4 were structurally related membrane proteins associated with the detergent-insoluble cytoskeleton-like triton shell of the *M. pneumoniae* attachment organelle (219). Subsequent studies, however, showed that HMW4 was a modified product of HMW1 arising during sample preparation for gel electrophoresis (78). Immunogold labeling of Triton-extracted *M. pneumoniae* localized HMW3 to the triton shell of the attachment organelle, but HMW3 did not

appear to be membrane associated (220). HMW5 was identified as a very high molecular weight protein (>340 kDa in nonreducing gel) that was absent in the noncytadherent phase variant of *M. pneumoniae*. In nonreducing-reducing two dimensional gel electrophoresis, HMW5 dissociated into a single peptide of molecular weight at 190 kDa that co-migrated with HMW2 (218).

Cloning and physical mapping of cytadherence related genes revealed the existence of three distinct loci in the *M. pneumoniae* genome. The P1 operon has already been discussed. The second locus contained HMW2 as the second gene of a four gene operon (*crl* operon, cytadherence regulatory locus). The HMW2 gene was flanked by an upstream P65 gene and two downstream genes coding for P24 and P41 (111). The third locus, the *hmw* gene cluster, included genes coding for P30, HMW1, HMW3, and five unknown ORFs (48, 112, 157, 158). Sequence analysis of *hmw3* revealed an ORF with a coding capacity of molecular weight of 73.7 kDa. This was in disagreement with the 140 kDa size of HMW3 obtained by SDS-PAGE analysis. The authors suggested that it was due to the presence of an unusual distribution of charged residues, a high degree of hydrophilicity, and a high proline content in HMW3, the combined effects of which resulted in anomalous migration in SDS-PAGE gel electrophoresis (158).

Mycoplasma hyopneumoniae

M. hyopneumoniae, originally named *M. suipneumoniae*, causes Enzootic Pneumonia of Pigs (EPP), a chronic pneumonia characterized by a persistent and nonproductive cough (228). *M. hyopneumoniae* infection is a worldwide phenomenon and leads to a reduction in the weight gain/feed ratio which results in great economic loss (172, 185, 186). *M. hyopneumoniae* infects pigs older than 5 to 7 weeks with an incubation period of 10 days to 3 weeks or longer prior to the appearance of clinical signs, a sporadic nonproductive cough that persists for 6 weeks or longer. Gross lesions in the lung can be detected 7 to 10 days after infection. These lesions develop fully in 20 to 30 days and gradually resolve (186, 246). Other mycoplasma species isolated from swine include *M. hyorhinis*, *M. hyosynoviae*, and *M. flocculare*. The roles these mycoplasmas play in EPP are not clearly defined except that *M. hyosynoviae* is known to cause nonsuppurative arthritis without polyserositis in pigs (31).

Most studies of *M. hyopneumoniae* has been limited to diagnosis of EPP and detection of the infectious agent. Diagnostic techniques based on antibody production include complement fixation (152), hemagglutination (61, 260), enzyme-linked immunosorbent assays (ELISA) (49, 124), immunofluorescent assays (200), and indirect immunoperoxidase assays (52) have been developed and evaluated (16, 188). Specific DNA sequences identified in the *M.*

hyopneumoniae genome have been developed as diagnostic tools for identification purposes by DNA hybridization (1, 100, 217). DNA probes labeled with ^{35}S, ^{32}P, or ^{131}I have been used to detect 10 pg of mycoplasma DNA (equivalent to 10^4 organisms)(217). Recent developments in PCR techniques have greatly improved the detection and diagnosis of *M. hyopneumoniae* infections. Several PCR protocols based on specific *M. hyopneumoniae* genomic DNA sequences have been developed (5, 6, 84, 139).

Attempts to eradicate the disease or confine the spread of infection have been unsatisfactory, due to the difficulty in detecting the infection early and the lack of effective antimicrobial agents to treat the disease (54, 76). Administration of antimycoplasmal antibiotics in feed has been demonstrated to have some benefits in improving the weight gain and feed-conversion, but failed to eradicate or prevent the infection (32, 80, 81, 187). Higher cost incurred by the use of antibiotics with limited benefits has prompted the development of effective vaccines for swine mycoplasmal pneumonia.

M. hyopneumoniae infection stimulates both cell-mediated and humoral immune responses in natural infected and experimentally-challenged swine (114, 147, 262). Sheldrake showed that in experimentally-challenged animals, antibodies were detected 10 days after infection and continued to rise for another 50 days. In a field study by the same authors, 97.7% of animals sero-converted during the period from 86 to 144 days of life (202). Antibodies found in the lung were of the IgG class, whereas in the tracheal lamina propria, the majority of the antibodies were of the IgA class (147, 204). *M. hyopneumoniae* infection stimulates alveolar macrophage phagocytic functions, but suppresses the macrophage responses to secondary pathogens (29). Sodium azide-inactivated *M. hyopneumoniae* had immunosuppressive effects, reducing PHA-induced lymphocyte activation (105). Membrane preparations of *M. hyopneumoniae* had moderate nonspecific stimulatory effects on porcine lymphocytes (146). Dextran sulfate, however, appeared to enhance the immune response to immunization with *M. hyopneumoniae* (104). Co-incubation of peripheral blood neutrophils with *M. hyopneumoniae* resulted in an increased intracellular calcium concentration suggesting an altered signal transduction in neutrophils (46). *M. hyopneumoniae* infection also caused increased levels of IL-1, IL-6, TNFα, and prostaglandin E2 in bronchoalveolar lavage fluids which may be associated with the development of lung lesions (7, 8). Antisera to *M. hyopneumoniae* antigens have been used to identify mycoplasmal antigens potentially useful for effective vaccine development. Young et al. recognized five *M. hyopneumoniae* antigens of molecular weights 110, 64, 50, 41, and 36 kDa with hyperimmune sera (261). Some of these antigens cross-reacted with sera from animals immunized with *M. flocculare* and *M. hyorhinis*. Wise et al. identified four *M. hyopneumoniae* surface antigens including p65, p50, p44, and p41 (254).

The same authors also established that p65, p50, and p41 are hydrophobic membrane lipoproteins (103, 255). A species-specific 36-kDa immunodominant protein from *M. hyopneumoniae* was identified, and its gene has been cloned. Sequence analysis revealed that the gene coded for the lactate dehydrogenase of *M. hyopneumoniae* (79, 222). An ELISA assay based on lactate dehydrogenase of *M. hyopneumoniae* was developed for diagnostic purposes (62).

Several vaccines have been developed to help prevent *M. hyopneumoniae* infection (110, 128, 154, 189, 203). Ross et al. demonstrated that whole cell vaccines containing 10^9 CCUs were partially protective against the development of pneumonia, whereas freeze-thaw-saline solution extracts were inconsistent in protective activity, and in some instances, enhanced lesion development (189). *M. hyopneumoniae* membrane preparations were partially protective and enhanced elimination of *M. hyopneumoniae* from the respiratory tract of piglets (110). Formalin-treated *M. hyopneumoniae* vaccines appeared to reduce lung lesion scores when administered intraperitoneally (203).

Since bacterial adherence to epithelial cells is a prerequisite for pathogen colonization, interference with bacterial adherence by the immune response would most likely prevent infection. Therefore, studies to identify and characterize *M. hyopneumoniae* adhesins has become increasingly important to better understand adherent mechanisms and to assist in the development of more effective vaccines.

Electron microscopic studies of the respiratory tract of pigs experimentally-infected with *M. hyopneumoniae* have revealed gross lesions in the lung tissue, mild lesions in the trachea and bronchia with epithelial hyperplasia, and infiltration of the lamina propria by inflammatory cells. *M. hyopneumoniae* covered the tufts of cilia of ciliated epithelial cells in the mid trachea and bronchi during infection. Association of *M. hyopneumoniae* and cilia was predominantly at the top of the cilia. Eventually the infection resulted in loss of cilia and desquamation of epithelial cells (19, 143, 229). *M. hyopneumoniae* cytadherence has been studied in several in vitro systems including cultured swine tracheal rings (45, 251), lung fibroblasts (71), respiratory tract ciliated epithelial cells (267), and kidney cells and human lung fibroblasts (269). These studies reinforced the cytopathic effects observed in animals infected with *M. hyopneumoniae*.

Preincubation of *M. hyopneumoniae* with dextran sulfate, ammonium sulfate, magnesium sulfate, and methionine reduced attachment (267). Treatment of the mycoplasmas with periodate, trypsin, and formaldehyde reduced the adherence to cultured monolayer cells (269). Convalescent serum or lung lavage fluids from swine with pneumonia inhibited the attachment of *M. hyopneumoniae* to isolated ciliated epithelial cells (267, 269). These results suggested an

adhesin-receptor interaction mediating the adherence of *M. hyopneumoniae*. A microtiter plate adherence assay (MPAA) has been developed by Zhang et al. *M. hyopneumoniae* bound specifically to microtiter plates coated with purified swine tracheal cilia which contained the receptors for *M. hyopneumoniae* (266). The binding was dependent on the concentration of cilia and the number of mycoplasmas. Dextran sulfate, heparin, chondroitin sulfate, laminin, mucin, and fucoidan significantly inhibited the binding of mycoplasmas. Pretreatment of cilia with metaperiodate decreased binding suggesting the glycoconjugate nature of the receptors (266). Thin layer chromatography of lipid extracts from cilia over layered with radiolabeled *M. hyopneumoniae* led to the identification of three putative ciliary glycolipid receptors (La, Lb, and Lc) (263). These glycolipids appeared to be sulfated glycolipids as determined by laminin binding and staining with azure A. Binding of *M. hyopneumoniae* to these three lipids was blocked by dextran sulfate, heparin, chondroitin sulfate, mucin, and fucoidan. These glycolipids also blocked the adherence of *M. hyopneumoniae* to cilia and ciliated epithelial cells (263). A putative adhesin protein of *M. hyopneumoniae* was identified and characterized biochemically (264). Two Mabs, F2G5 and F1B6, were isolated which inhibited the adherence of *M. hyopneumoniae* to cilia. The Mabs reacted with multiple proteins in immunoblot analysis of *M. hyopneumoniae* antigen preparations. The dominant protein had a molecular weight of 97 kDa (designated as P97). Affinity chromatography with immobilized Mab F2G5 was used to partially purify the P97 protein. P97 protein bound to cilia and blocked the adherence of *M. hyopneumoniae* to cilia. Immunoelectron microscopy localized P97 to the surface of *M. hyopneumoniae*. These results suggested that P97 was a *M. hyopneumoniae* adhesin mediating the adherence of mycoplasma to cilia of swine tracheal ciliated epithelial cells (264).

MATERIALS AND METHODS

Bacterial Strains and Plasmids

Bacterial strains and plasmids included in this study are listed in Table 1. *E. coli* strains were grown in LB medium (195). λ was grown on *E. coli* using LB phage agar and soft agar overlays as described (195). All *M. hyopneumoniae* strains were a gift of Dr. R. F. Ross (Iowa State University). *M. hyopneumoniae* was grown in modified Friis medium (63). The medium contained (per liter) 15.625 ml solution A (160 g NaCl–8 g KCl–2 g $MgSO_4$ 7•H_2O–2 g $MgCl_2$ 6•H_2O–2.8 g $CaCl_2$ per liter), 15.625 ml solution B (3 g Na_2HPO_4 per liter), 5.125 g Brain Heart Infusion (Difco Laboratories, Detroit, Mich.), 5.435 g PPLO w/o CV (Difco), 1.125 ml phenol red (1% in 50% ethanol), 10 ml Cefobid (2.5 mg per ml in 50% ethanol), 37.5 ml fresh yeast extract, 206.25 ml acid-adjusted porcine serum (20% final concentration) and tissue culture grade water to bring the final volume to 1 liter. The medium was mixed and then passed sequentially through 3.0, 0.8, 0.45, and 0.2 μm cellulose nitrate membrane filters (Cat. No. 7188 004, Whatman Limited, Maidstone, UK) in Nalgene reusable filter holders (Cat. No. 300, Nalgene Nunc International, Milwaukee, Wis.). The final filtrate was sterilized by filtration through 0.2 μm Falcon 7111 bottle-top filters (Becton Dickinson & Company, Lincoln Park, NJ). Friis plates were prepared by mixing filter-sterilized 2X concentrated Friis medium with an equal volume of 2% molten sterile noble agar (Difco). All cultures were maintained at -70°C. Plasmids were stored at -20°C. *M. hyopneumoniae* specific primers (6) were used to confirm the *M. hyopneumoniae* strains.

Reagents and Buffers

Chemicals, porcine serum, ampicillin were purchased from Sigma Chemical Co. (St. Louis, Mo.). Restriction enzymes, T4 DNA ligase, DNA polymerase Klenow fragment, Taq DNA polymerase, calf intestinal alkaline phosphatase, and ribonuclease A were purchased from Promega Corporation (Madison, Wis.), GIBCO BRL (Gaithersburg, Md.), and New England Biolabs (Beverly, Ma.). Agarose was purchase from Bio-Rad Laboratories (Hercules, Calif.). Isopropyl thiogalactoside (IPTG) and X-gal were obtained from Gold Biotechnology, Inc. (St. Louis, Mo.). Alkaline phosphatase-conjugated, affinity-purified antibodies to mouse immunoglobulins was obtained from Organon Teknika Corp. (West Chester, Pa.). ^{32}P-Deoxyribonucleotides were purchased from ICN Biomedicals (Irvine, Calif.). Mab F1B6 and swine cilia were the gift of Dr. R.F. Ross (Iowa State University). Buffers used in this study are listed in Table 2.

Table 1. Bacterial strains and plasmids

Bacterial strain or plasmid	Genotype or phenotype*	Source
M. hyopneumoniae		
J	Avirulent nonadherent strain	R.F. Ross
232A	Virulent adherent strain	R.F. Ross
144L	Virulent field isolate	R.F. Ross
232A.H	High adherent clonal isolate of 232A, 232A91 P3	R.F. Ross
232A.M	Medium adherent clonal isolate of 232A, 232A20 P10	R.F. Ross
232A.L	Low adherent clonal isolate of 232A, 232A61 P3	R.F. Ross
E. coli		
DH5α	ϕ80d*lacZDM15 endl recA1 hsdR17 supE44-1 gyrA relA1* F⁻ Δ(*lacZYA argF*)U169	
LE392	F⁻ *hsd514*(rk⁻, mk⁻) *lacY supE44 supF58 galK2 galT22 trpR55 metB1* λ⁻	
XL1-Blue MRF′	Δ(*mcrA*) Δ(*mcrCB-hsdSMR-mrr*)*173 endA1 supE44 thi-1 recA1 gyrA96 relA1 lac* F′	Stratagene
SOLR	e14⁻(*mcrA*) Δ(*mcrCB-hsdSMR-mrr*)*171 sbcC recB recJ umuC*::Tn*5*(kan^r) *uvrC lac gyr96 relA1 thi-1 endA1* λ^R [F′*proAB lacI*^{Q}*ZD15*] Su⁻ (nonsuppressing)	Stratagene
BW22	F⁻ Kan^R	Gold Biotechnologies
DPWC	*supE43* Δ*recA* (*Sst1-EcoRI*) *srl*::Tn*10*(tet^S) F⁺	Gold Biotechnologies
ISM612	LE392 (pISM3001) Cm^r	(211)
Plasmid		
pMOB		Gold Biotechnologies
pMOB::Tn*1000*	pMOB with Tn*1000* insert	this study
pSK(-)		(3)
pKS(-)		(3)
pISM1136	pSK- with a 5.3 kb *M. hyopneumoniae* chromosomal fragment, pISM2136A+	this study
pISM1137	pSK- with a 5.3 kb *M. hyopneumoniae* chromosomal fragment, pISM2136A+	this study
pISM1138	pSK- with a 7.1 kb *M. hyopneumoniae* chromosomal fragment, pISM2136A+	this study
pISM1161	pSK- with 3.3 kb *Eco*RI fragment from P97 region	this study
pISM1165	pSK- with a 6.6 kb *M. hyopneumoniae* chromosomal fragment, pISM2136C+	this study
pISM1168	pSK- with a 5.5 kb *M. hyopneumoniae* chromosomal fragment, pISM2136C+	this study
pISM1169	pSK- with a 5.9 kb *M. hyopneumoniae* chromosomal fragment, pISM2136C+	this study

* pISM2136A, clone identified using the entire 615 bp insert of pISM2136; pISM2136C, clone identified using the 415 bp *SalI–PstI* fragment of pISM2136; plus, identified using the indicated probe.

Table 1. (continued).

pISM1170	pSK- with a 6.1 kb *M. hyopneumoniae* chromosomal fragment, pISM2136C+	this study
pISM1172	pSK- with a 6.5 kb *M. hyopneumoniae* chromosomal fragment, pISM2136C+	this study
pISM1174	pSK- with a 6.0 kb *M. hyopneumoniae* chromosomal fragment, pISM2136C+	this study
pISM1176	pSK- with a 7.7 kb *M. hyopneumoniae* chromosomal fragment, pISM2136C+	this study
pISM1210	pSK- with a 8.2 kb *M. hyopneumoniae* chromosomal fragment, pISM1161+	this study
pISM1212	pSK- with a 5.4 kb *M. hyopneumoniae* chromosomal fragment, pISM1161+	this study
pISM1213	pSK- with a 5.4 kb *M. hyopneumoniae* chromosomal fragment, pISM1161+	this study
pISM1214	pSK- with a 5.5 kb *M. hyopneumoniae* chromosomal fragment, pISM1161+	this study
pISM1217	pSK- with a 8.8 kb *M. hyopneumoniae* chromosomal fragment, pISM1161+	this study
pISM1228	4.2 kb *PstI/NciI* fragment from pISM2159 cloned into pKS-	this study
pISM1232	pSK- with 3.8 kb *Eco*RI fragment of *M. hyopneumoniae* chromosomal DNA containing second copy of P102	this study
pISM1233	pSK- with 4.2 kb *Eco*RI fragment of *M. hyopneumoniae* chromosomal DNA containing second copy of P102	this study
pISM2121	pSK- with a 7.2 kb fragment derived from pISM2139 and pISM2159	this study
pISM2136	pSK- with a 0.6 kb fragment of *M. hyopneumoniae* chromosomal DNA, Mab F1B6+	this study
pISM2139	pSK- with a 5.5 kb fragment of *M. hyopneumoniae* chromosomal DNA, Mab F1B6+	this study
pISM2155	pSK- with a 6.1 kb fragment of *M. hyopneumoniae* chromosomal DNA, Mab F1B6+	this study
pISM2167	pSK- with a 6.3 kb fragment of *M. hyopneumoniae* chromosomal DNA, Mab F1B6+	this study
pISM2168	pSK- with a 6.5 kb fragment of *M. hyopneumoniae* chromosomal DNA, Mab F1B6+	this study
pISM2169	pSK- with a 6.2 kb fragment of *M. hyopneumoniae* chromosomal DNA, Mab F1B6+	this study
pISM2170	pSK- with a 6.2 kb fragment of *M. hyopneumoniae* chromosomal DNA, Mab F1B6+	this study
pISM2171	pSK- with a 5.6 kb fragment of *M. hyopneumoniae* chromosomal DNA, Mab F1B6+	this study
pISM2172	pSK- with a 6.6 kb fragment of *M. hyopneumoniae* chromosomal DNA, Mab F1B6+	this study
pISM2173	pSK- with a 5.1 kb fragment of *M. hyopneumoniae* chromosomal DNA, Mab F1B6+	this study
pISM2159	pSK- with a 5.2 kb fragment of *M. hyopneumoniae* chromosomal DNA, Mab F1B6+	this study

Table 2. Buffers

Buffer	Component	Usage
PBS	10 mM Na_2HPO_4–150 mM NaCl, pH 7.4	
SM	5.8 g NaCl– 2 g $MgSO_4$•7H2O– 50 ml 1 M Tris•Cl (pH 7.5)–5 ml 2% gelatin	λ maintenance and dilution buffer
TS-Tween	0.01 M Tris–0.140 NaCl–0.01 % Tween 20	Immunoblot washing buffer
Electrode Buffer	25 mM Tris–192 mM glycine–20% methanol vol/vol; pH 8.3	Protein transfer buffer
TAE (50X)	242 g Tris–100 ml 0.5 M EDTA (pH 8.0)–57.1 ml glacial acetic acid	Electrophoresis
TE	10 mM Tris–1 mM EDTA, pH 8.0	DNA buffer
TNE	20 mM Tris–10 mM NaCl–1 mM EDTA, pH 8.0	Mycoplasmal DNA isolation (Basic protocol)
TNE	10 mM Tris–140 mM NaCl–1 mM EDTA, pH 8.0	Mycoplasmal DNA isolation (Alternative protocol)
SSC (10X)	1.5 M NaCl–150 mM sodium citrate, pH 7.0	DNA hybridization
Denhardt's reagent (50X)	5 g Ficoll–5 g polyvinylpyrrolidone–5 g bovine serum albumin per 500 ml	DNA hybridization
Denaturing buffer	0.5 N NaOH–1.5 M NaCl	DNA hybridization
Renaturation buffer	1.0 M Tris–1.5 M NaCl, pH 8.0	DNA hybridization
Prehyb/Hyb solution	5X SSC–5X Denhardt's reagent–0.1 g/ml denatured salmon sperm DNA–0.1% SDS	DNA hybridization
washing solution (2X)	2X SSC–0.1% SDS	DNA hybridization
washing solution (0.2X)	0.2X SSC–0.1% SDS	DNA hybridization
TES-1	20 mM Tris-HCl–10 mM EDTA–125mM sucrose, pH 7.2	Cilia isolation
AES	80 mM sodium Acetate–10 mM EDTA–125 mM sucrose, pH 6.8	Cilia isolation
$CaCl_2$ (10X)	200 mM $CaCl_2$	Cilia isolation
TES-2	50 mM Tris-HCl–10mM EDTA–10 % sucrose, pH 8.0	*E. coli* lysate preparation
Blocking buffer	1% gelatin in RPMI 1640	MPAA
Coating buffer	0.1M Sodium Carbonate, pH 9.3	MPAA

DNA Primers

Sequencing and PCR primers were designed using the Oligo Primer Analysis Software (National Biosciences, Inc., Plymouth, Minn.). DNA synthesis was performed in a DNA/RNA Synthesizer (Model 399, Applied Biosystems, Perkin-Elmer Corporation, Morwalk, Conn.) at the DNA Instrumentation Facility, Iowa State University. Table 3 lists the PCR and sequencing primers used in this study.

Table 3. Primers

Primer	Sequence (5′–3′)	Specificity
PCR Primers		
TH120	AAGGTAAAAGAGAAGAAGTAG	P97 first repeat
TH121	TTGTAAGTGAAAAGCCAGTAT	
TH122	AGCGAGTATGAAGAACAAGAA	P97 second repeat
TH123	TTTTTACCTAAGTCAGGAAGG	
Mhp3	AAGTTCATTCGCGCTAGCCC	*M. hyopneumoniae*
Mhp4	GCTCCTACTCCATATTGCCC	
TH127	TATTCGCTTTTTGTATTTTCA	pISM2136 sequence position No. 550 - 569
TH128	GCAGCTAAAACTAGTAAGTTTGAA	pISM2136 sequence position No. 30 - 53
Sequencing primers		
G186	ATATAAACAACGAATTATCTCC	Tn*1000* 3′ end
G188	TAAGTTATACCATAAACG	Tn*1000* 5′ end
TH125	GCGGCTGCTAAACTAAGACTA	pISM1232-specific
Universal	TGTAAAACGACGGCCAGT	Bluescript plasmid
T3	ATTAACCCTCACTAAAG	
Reverse	CAGGAAACAGCTATGACC	
T7	AATACGACTCACTATAG	

DNA Preparation

M. hyopneumoniae chromosomal DNA was prepared as follows. Fifty to 500 ml of *M. hyopneumoniae* culture was serially amplified in Friis medium to early stationary phase (color of the medium changed to orange and cloudiness of culture became apparent). The culture was centrifuged at 8,000 x *g* for 15 minutes to collect the bacterial cell pellet. The milky-white appearance of the pellet indicated that the culture was healthy which was critical for the isolation of high quality chromosomal DNA. The pellet was washed once with phosphate buffered saline (PBS, Table 2), centrifuged, and suspended in 7.5 ml of TNE buffer (Table 2). Cells were lysed by adding an equal volume of TNE buffer plus 1% sodium dodecyl sulfate (SDS) and 200 mg per ml proteinase K final concentration (Fisher). The mixture was incubated in a water bath at 50°C overnight. The lysate was extracted with an equal volume of phenol:chloroform: isoamyl alcohol mixture (24:24:1) overnight in a 250 ml polypropylene centrifuge tube rotated slowly at 4°C. The upper layer containing the DNA sample was decanted into a 40 ml oakridge tube and centrifuged at 12,000 x *g* for 15 minutes to separate

the phases and remove protein contaminants. The clear supernatant fraction was pipetted into a new tube and precipitated with 0.1 vol of 3M sodium acetate (pH 4.8) and 2 vol of 100% ethanol in a large petri dish. The DNA precipitated as threads which were collected using a sterile pasteur pipette with a sealed tip. The DNA was rinsed with 70% ethanol, air-dried, and dissolved in 2 ml of TE buffer after incubation for at least two days at 4°C. The extraction procedure was repeated once more beginning with proteinase K and SDS treatment, and the extracted DNA was dissolved in 50 to 250 µl of TE at 4°C.

Plasmid DNA was isolated from *E. coli* according to the method of Birnboim (18). This DNA was of adequate purity for general purposes such as restriction digestion, labeling, and cloning. For DNA sequencing, plasmid DNAs were prepared using a QIAGEN plasmid purification kit (QIAGEN Inc., Chatsworth, Calif.) per manufacturer's instructions. DNA precipitated with isopropanol was centrifuged in eppendorf tubes in a microfuge. Air-dried pellets were dissolved in sterile H_2O or Tris buffer (10 mM Tris-HCl; pH 8.0). All agarose gel electrophoresis was conducted using 0.4 to 1.5% agarose in 1X TAE buffer (Table 2).

Library Construction

The construction of the *M. hyopneumoniae* chromosomal DNA genomic library in Lambda ZAP® II using *Tsp*509 I partially digested DNA has been described (148). Briefly, *M. hyopneumoniae* chromosomal DNA was partially digested with restriction enzyme *Tsp*509 I (New England Biolabs, Inc., Beverly, Maine), and 5 to 10 kb fragments were isolated from agarose gels using glassmilk (BIO 101, La Jolla, Calif.). The fragments were ligated into *Eco*RI-digested Lambda ZAP® II DNA (Stratagene), and the recombinant phage were packaged using the Packagene Lambda DNA packaging system (Promega, Madison, Wis.). The recombinant phage were grown on *E. coli* LE392, and single plaques were picked, individually amplified and stored in 96-well microtiter plates as described previously (148). The remaining recombinant phages were amplified using standard techniques (195).

Screening of *M. hyopneumoniae* Genomic Libraries

Screening of the *M. hyopneumoniae* genomic library was performed as follows. In the primary screening, an amplified Lambda ZAP® II library was grown as single plaques on *E. coli* LE392 or XL-1 Blue at a concentration of 500-1,000 plaques per 85 mm plate. Plaques were lifted onto nitrocellulose membranes taking care to precool the plates prior to overlaying the membranes and carefully marking the plates and membranes prior to removal from the plate. The membranes were then treated with denaturation buffer (Table 2) followed by treatment with renaturation buffer (Table 2). The membranes were baked in a 80°C oven for

1.5 to 2 hour to fix the DNA to the membranes. Prehybridization and hybridization were conducted as described for the DNA hybridization experiments. Putative positive plaques were picked using sterile pasteur pipettes by stabbing the pipette into the center of the plaque and dispensing the agar into 1 ml of SM (Table 2). The phage were eluted overnight at 4°C. Secondary screening was performed by growing the eluted phage at a concentration of 20-100 plaques per plate and repeating the plaque lift and hybridization procedure described above. Positive plaques were used for M13 phage growth and subsequent excision of cloned genomic DNA inserts into Bluescript plasmids as described (207).

Plasmid Constructions

DNA cloning was performed according to established methods (195). Plasmid pISM2121 was constructed by joining the *Pst*I-*Bam*HI fragment from pISM2139 with the *Bam*HI-*Pst*I fragment from pISM2159 and cloning into plasmid pMOB (223). The *Pst*I site was within the vector's multiple cloning site. This provided a single continuous 7.4 kb chromosomal DNA fragment from *M. hyopneumoniae* which was then analyzed for P97 gene expression using Tn*1000* mutagenesis, immunoblot analysis and cilia binding assays. Plasmid pISM2159 was excised from a recombinant Lambda ZAP® II clone by M13 rescue (207). It carries a 5.2 kb insert of *M. hyopneumoniae* genomic DNA in the pSK- vector (Stratagene). Plasmid pISM1228 was constructed by cloning the *Nci*I - *Pst*I fragment from pISM2159 into *Pst*I - *Sma*I digested pKS- vector DNA. Following digestion with *Nci*I, the site was filled-in using the Klenow fragment of DNA polymerase (5 mM dCTP, 5 mM dGTP and 0.1 U of Klenow, 30 minutes at 30°C), and then the Klenow fragment was inactivated by treatment at 70°C for 15 minutes. The DNA was then precipitated with ethanol and subsequently digested with *Pst*I. The *Nci*I-*Pst*I fragments were purified from agarose gels (QIAEX Gel Extraction Kit, QIAGEN, Inc. Chatsworth, Calif.) and ligated to agarose purified *Sma*I-*Pst*I digested pKS- II vector DNA. The structure of the resulting recombinant plasmid was confirmed by restriction digestion. This cloning strategy maintained the reading frame and direction of β-galactosidase promoter activity as found in the original plasmid, but deleted all but two base pairs downstream of the P97 structural gene.

Transformation of *E. coli*

Transformation of plasmid DNA into *E. coli* was performed by electroporation using an Electro Cell Manipulator (Model ECM 600, BTX, San Diego, Calif.). The parameters of electroporation included 2 consecutive pulses at 8 kV and 129 Ohms in a 0.2 cm electroporation cuvette. The time constant was maintained at about 5.5 msec. *E.* coli was

prepared for electroporation in the following way. *E. coli* stock cultures were inoculated into 3 to 5 ml of LB broth supplemented with the proper antibiotics followed by overnight growth under vigorous shaking. A 1:1000 dilution of the cultures were made into 200 to 500 ml of 2X LB broth without antibiotics. The growth of the cultures was monitored by optical density at 600 nm until the density reached approximately 1.0. From this point, the cells were maintained at 4°C on ice water. The cultures were centrifuged at 9,000 x *g* at 4°C, and cell pellets were washed twice with an equal volume of pre-chilled distilled water followed by a final wash in 20 ml of pre-chilled 10% glycerol in water. The pellets were suspended in 3 to 5 ml of 10% glycerol and dispensed in 50 µl aliquots in 0.5 ml eppendorf tubes. The aliquots of cells were snap-frozen in a dry ice-ethanol bath prior to storage at -70°C. *E. coli* competent cells thus prepared and stored at -70°C have a transformation frequency of approximately 2 - 5 x 10^7 transformants per µg of plasmid DNA for 3 to 6 months. For *E. coli* ISM612, superbroth (32 g of tryptone (Difco)–20 g yeast extract (Difco)–5 g glucose per liter) was used for growth instead of LB broth. The transformation frequency for ISM612 was significantly (10 - 100 times) lower than for other *E. coli* strains used in this study.

Forty microliter of *E. coli* competent cells was used in each transformation with 5–50 ng plasmid DNA. The cell mixtures were diluted into 1 to 1.5 ml of SOC media (20 g Tryptone (Difco)–5 g yeast extract (Difco)–2.03 g $MgCl_2 \cdot 6H_20$–2.46 g $MgSO_4 \cdot 7H_20$ –3.6 g glucose per liter) and then incubated at 37°C for 30 minutes prior to plating the transformation mixture on selective media.

Tn*1000* Mutagenesis

Tn*1000* mutagenesis was performed by conjugal mating in the following way. Briefly, plasmids to be mutagenized were first transformed into *E. coli* DPWC. The resulting strains which carried both F and the recombinant plasmid were used as donor strains for conjugation with kanamycin resistant recipient *E. coli* BW22. One hundred microliters of overnight donor and recipient cultures were mixed and diluted into 2 mls of LB and grown for 3 hours at 37°C (shaking). Different amounts of the mating mixtures (1-100 µl) were then plated onto 2X LB agar supplemented with 100 µg per ml ampicillin and 50 µg per ml kanamycin. The resulting ampicillin and kanamycin resistant colonies contained recombinant plasmids with Tn*1000* randomly inserted. The location of the Tn*1000* inserts were determined by restriction digestion of the isolated plasmid with *Sal*I and *Eco*RV.

DNA Sequencing and Polymerase Chain Reaction

DNA sequencing was performed by the Iowa State University DNA facility using cycle sequencing protocols and an automated DNA Sequencer (Model 373 or 377, Applied Biosystems, The Perkin-Elmer Corporation, Norwalk, Conn.). DNA sequence analysis was performed with MacVector software (Eastern Kodak Company, Rochester, N.Y.).

All polymerase chain reaction (PCR) amplifications were performed using a TwinBlock System (model EZ cycler, Ericomp Inc., San Diego, Calif.). The annealing temperature was determined by Oligo primer analysis software (National Biosciences, Inc., Plymouth, Minn.). The basic PCR reaction mixture contained 2 mM $MgCl_2$, 25 pmol each primer, 1-50 ng template DNA, 0.25 U Tag DNA polymerase in 50 µl 1X manufacturer's reaction buffer. PCR products were analyzed by agarose electrophoresis.

Clamped Homogeneous Electrical Field Electrophoresis

Preparation of intact *M. hyopneumoniae* genomic DNA and restriction digestion were performed according to the method described by Mahairas and Minion (132). *M. hyopneumoniae* cells were pelleted by centrifugation and resuspended in 50 µl of TNE buffer (Table 2). The tube was equilibrated to 37°C and then an equal volume of 2% low-temperature melting agarose (Seaplaque, FMC Corp., Rocklane, Maine) in TNE was added. The suspension was placed in a plug mold and allowed to harden. The plugs were then transferred to 12 x 75 mm snap cap tubes at which time 100 µl of lysis buffer (2 mg per ml protease K, 1% Sarkosyl, 0.5 M EDTA, and 10 mM Tris-HCl; pH 9.5) was added. The tube was then incubated at 50°C for 12 hours, and then dialyzed against 1 ml volumes of TE at least four times for 1 h. Dialyzed agarose blocks were stored in TE buffer at 4°C. The concentration of cells was determined empirically by assessing the DNA isolated from different dilutions of cells by CHEF.

DNA digestions were performed in 1 ml of 1X digestion buffer containing 30 - 40 U of each enzyme at 37°C for 12 hours. Prior to electrophoresis, the blocks were equilibrated in 0.5X Tris-Borate electrophoresis buffer (45 mM Tris base, 45 mM boric acid, 1 mM EDTA) for at least 1 hour. Electrophoresis was performed according to the manufacturer's instructions with a Bio-Rad CHEF-DR II pulse field electrophoresis system, Pulsewave 760 switcher, and a Model 200/2.0 power supply. Digested DNA was electrophoresed in a 5-10 mm thick, 1.5% agarose gel using lambda DNA as size markers (CHEF DNA size standards, Cat. No. 170-3635, Bio-Rad Laboratories, Hercules, CA.). The electrophoresis was carried out at 200 V for 20 hours at 14°C with ramping from 2 to 14 seconds. Transfer of the DNA to nylon membranes was performed according to protocol described elsewhere in this thesis.

Radiolabeling

Oligonucleotides were end labeled as described (195). The labeling solution contained 50 pmole of oligonucleotide, 150 mCi γ ^{32}P-ATP, and 20 U T4 kinase in 50 µl of 1X Taq polymerase buffer (New England Biolabs). Labeling mixtures were incubated at 37°C for 30 minutes. Labeled oligonucleotides were purified from unincorporated ^{32}P-ATP using the Mermaid kit (BIO 101, Inc., La Jolla, Calif.).

DNA probes were labeled with α ^{32}P-dCTP using the Multiprime DNA labeling system (Amersham International plc., Amersham, UK) according to the manufacturer's instructions. Unincorporated α ^{32}P-dCTP was separated from radiolabeled probes by passing labeling reaction mixtures through MicroSpin S-300 HR columns (Pharmacia Biotech Inc., Piscataway, N.J.).

Hybridization

DNA digested with restriction enzymes was electrophoresed in agarose gels (0.4% to 1.0%) to separate the fragments. Agarose gels were treated with 0.25 N HCl for 10 minutes, rinsed with distilled H_2O, and the DNA was denatured by incubating the gels in denaturing buffer (Table 2) for 30 minutes to 1 hour. The DNA was renatured by directly transferring the gel into renaturation buffer (Table 2) and incubating for 30 minutes to 1 hour. The DNA was then transferred to nylon membranes (Biodyne Plus, Pall Corporation, New York, N.Y.) by capillary transfer overnight with 10X SSC buffer.

The DNA was fixed to the nylon membranes by baking in a vacuum oven for 1 to 1.5 hours at 80°C. Membranes were prehybridized in Prehyb/Hyb solution (Table 2) at 65°C for at least 1 hour. Hybridization was then carried out overnight with ^{32}P radiolabeled probe at 65°C in Prehyb/Hyb solution. After hybridization, the Prehyb/Hyb solution was discarded or stored at -70°C for further use. The membranes were washed with 2X washing solution (Table 2) twice at 25°C, and 0.2X washing solution twice at 65°C unless indicated otherwise. Autoradiography was performed with membranes placed on wet (with 2X washing solution) 3M filter paper wrapped in saran wrap to prevent non-reversible cross-linking of probes to the membranes and exposed to X-ray film (BioMax MR Film, Eastern Kodak Company, Rochester, N.Y.).

Immunoblot Analysis

Immunoblotting was performed according to Towbin (233). Proteins resolved by SDS-PAGE were transferred to nitrocellulose membranes (Midwest Scientific, St. Louis, Mo.). A Transphor Electrophoresis Unit (TE series, Hoefer Scientific Instrument, Piscataway, N.J.)

was used with Electrode buffer (Table 2), and transfer was conducted for at least 2 hours at 1 mA or overnight at 0.5 mA at 4°C. After electroblotting, membranes were blocked with TS-Tween buffer (0.01 M Tris–0.140 NaCl–0.01 % Tween 20) plus 5% powdered milk for 1 hour and washed 3 times with TS-Tween for 15 minutes each. The blots were incubated with Mab F1B6 (diluted 1:1000 in TS-Tween buffer) overnight at room temperature. Membranes were washed as described above. Alkaline phosphate conjugate diluted in TS-Tween was incubated with the membranes for 2 hours. After washing, the blots were developed with AP substrate (Naphthol 0.03 g–Fast red 0.06 g in 2 mM Tris•HCl; pH 7.4). The reaction was halted by rinsing membranes with a large amount of H_2O and air dried.

Adherence Assay

Ten to 20 ml of log to stationary phase *M. hyopneumoniae* culture was centrifuged at 8,000 x *g* for 15 minutes. The cells were washed by suspending them in 1 ml of PBS, transferring to an eppendorf tube, and centrifuging in a microfuge at full speed for 1 minute. The pellet was resuspended in 100 µl of PBS. Thirty to 40 ml of overnight *E. coli* ISM612 cultures were induced with 2.5 mM isopropyl thiogalactopyranside (IPTG) for 5 to 6 hours. The *E. coli* pellets were resuspended in 5 ml of TES-2 buffer (Table 2) and centrifuged again. The final *E. coli* pellets were suspended in 2 ml of TES-2 buffer. Cells were lysed by sonication in a 13 ml centrifuge tube (Cat. No. 62.515.006, Sarstedt, Inc., Newton, NC) with a sonicator (Cell disrupter, model W225R, Heat systems-ultrasonics, Inc., Plainview, N.Y.) set at 70 % maximum output and 50% duty cycle using a microtip probe. Each cell suspension was kept on wet ice and received 20 pulses with a 20 second break between pulses. Lysates were collected after centrifugation at 12,000 x *g* for 20 minutes. Protein concentration was determined by standard Bio-Rad protein assay (Bio-Rad Laboratories, Richmond, CA) using 5 to 20 µl of sample. Bovine serum albumin was used to determine the standard curve.

Swine cilia were prepared in the following way. Swine trachea were aseptically removed from pigs and immersed in HBSS (Cat. No. 14185, Life Technology Inc., Gaithersburg, Md.). The epithelium was scraped from trachea using a laboratory spatula into 25 ml TES-1 buffer (Table 2) in a conical centrifuge tube. This cell suspension was then centrifuged at 288 x *g* for 10 minutes. The pellet was washed with TES-1 buffer and centrifuged once more, resuspended in 6 ml of AES buffer (Table 2), mixed, and 6 ml of 20 mM $CaCl_2$ was added. The mixture was vortexed vigorously for 10 minutes prior to passage through an 18G needle once and a 22G needle twice. The mixture was brought to 40 ml with TES-1 buffer and centrifuged at 472 x *g* for 5 minutes twice to remove cell debris. The supernatant was

transferred to a clean centrifuge tube followed by a 20 minute centrifugation step at 20,000 x *g*. The pellet containing the cilia was washed with PBS prior to centrifugation again. The final pellet was resuspended in 1 ml of PBS, aliquoted and stored at -70°C.

For coating microtiter plates, cilia were removed from the -70°C freezer and diluted with PBS to 1 mg protein per ml. One fourth volume of a 5 mg per ml SDS solution was added to the cilia suspension and the tube was incubated at 37°C for 45 minutes. The cilia preparation was then diluted with coating buffer in which the cilia final concentration was 10 mg per ml. Immulon 4 microtiter plates (Dynatech Industries, Inc., McLean, Va.) were coated with solubilized cilia at 1 mg per well overnight at room temperature. The plate was either used for a MPAA assay immediately or was stored at -70°C freezer until use. Incubation at 37°C was sometimes used to shorten the time required to coat the plate.

For most MPAA assays, cilia-coated Immulon 4 plates were taken from -70°C freezer and thawed at 25°C. The plate was washed 4 times with PBS and blocked with blocking buffer (1% gelatin (Sigma) in RPMI 1640) for 2 hours at 37°C. Without washing the plate, antigen in 100 µl blocking buffer was added to each well. The plate was incubated at 37°C for 1 hour. After 4 washes with PBS, 100 µl of primary antibody F1B6 diluted 1:100 in blocking buffer was added to each well and incubation was continued for 90 minutes at 37 °C. This was followed by 4 washes with PBS and incubation for 1 hour at 37°C with alkaline phosphate-labeled goat anti-mouse immunoglobulins conjugate (Cappel, Cat. No. 59294, Organon Teknika Corp., West Chester, Pa.) diluted to 1:200 in blocking buffer. After 4 washes with PBS, 100 ml of alkaline phosphate substrate (Sigma 104) was added to each well. The plate was developed at 37°C, and the absorbance was read in a Microplate Autoreader (Model EL310, BIO-TEK Instruments Inc., Winooski, Vt.) at an optical density of 405 nm. Negative controls included wells with negative control antigens or wells with blocking buffer. All experiments were performed in triplicate with freshly prepared antigens and experiments were repeated at least twice.

The MPAA inhibition assay was performed with three inhibitors, heparin, fucoidan, and mucin. Each of these materials have been shown to inhibit binding of *M. hyopneumoniae* to cilia (266). To examine the ability of these chemicals to inhibit the binding of recombinant P97 in *E. coli* lysates to cilia, inhibitors and antigens dissolved in blocking buffer were added to eppendorf tubes containing antigens and then immediately added to microtiter plates without any further incubation. The assay was then completed according to the protocol described above. Control wells contained no inhibitor.

RESULTS

Analysis of Mab F1B6-Reactive Lambda ZAP® II Clones

A total of 1,920 individually picked clones from the *M. hyopneumoniae* genomic library in Lambda ZAP® II had been screened previously in this laboratory with Mab F1B6. Four positive clones were identified and rescued into pSK- by excision from Lambda ZAP® II. The resulting plasmids, pISM2136, pISM2139, pISM2155 and pISM2159, were isolated and restriction mapped. According to the restriction map, the inserts of plasmids pISM2139, pISM2155, and pISM2159 appeared to overlap a single region of the *M. hyopneumoniae* chromosome (Figure 1). Therefore, it appeared that this region was likely to contain the P97 adhesin gene. This hypothesis was supported by subsequent isolation of additional clones from the amplified *M. hyopneumoniae* genomic library using Mab F1B6 (Figure 1). To increase the opportunity of successfully deriving the complete P97 gene sequence, the plasmid pISM2121 was constructed by ligating inserts from pISM2139 and pISM2159 at the *Bam*HI site and cloning the combined fragment into pMOB, a vector designed to facilitate Tn*1000* mutagenesis (Materials and Methods). Interestingly, of the four Mab reactive clones, pISM2136 contained an insert of 600 bp in length and contained a single *Sal*I site, a restriction site (GTCGAC) rarely observed in mycoplasma DNA because of the high A+T content. The presence of the *Sal*I site suggested that the cloned fragment in pISM2136 was derived from the same chromosomal region of P97 which also contained a *Sal*I site (Figure 1), but DNA sequence analysis of both pISM2136 and pISM2121 failed to identify the source of the pISM2136 fragment.

Immunoblot Analysis

To locate the P97 gene in pISM2121, Tn*1000* mutagenesis was performed as described in Materials and Methods. pISM2121::Tn*1000* plasmids were isolated and restriction mapped to determine the site of the Tn*1000* insertion. A series of pISM2121::Tn*1000* plasmids with transposon inserts spanning the entire pISM2121 insert were examined for P97 expression by immunoblot analysis with Mab F1B6 (Figure 2). Each of these plasmids was transformed into *E. coli* ISM612, a strain constructed to enhance the expression of mycoplasma genes by suppressing opal stop codons (211). Each of the ISM612 (pISM2121: Tn*1000*) derivatives were cultivated under IPTG induction, and whole cell proteins were prepared and separated in 10% SDS-PAGE gels. The proteins were transferred to nitrocellulose membranes and analyzed for the expression of Mab F1B6-reactive antigens. The results of one experiment are shown in Figure 2. Tn*1000* insertions (1-3, 1-15, 26-14, and 1-14) within a 2.0 kb region of pISM2121

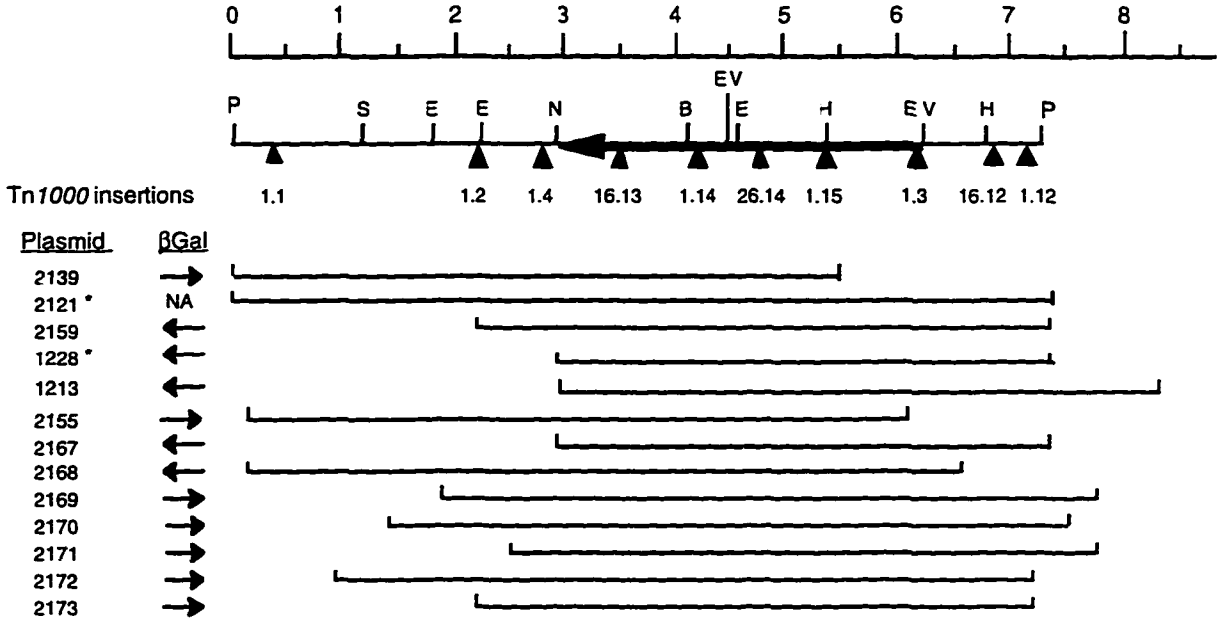

Figure 1. Restriction map of the P97 region of the *M. hyopneumoniae* chromosome and overlapping fragments from cloned sequences. The location and direction of transcription of P97 is shown by the large arrow. Selected recombinant clones (designated as plasmid numbers) expressing the P97 epitope are mapped to the chromosomal region. The small arrows (βGal) indicate the direction of transcription in each plasmid due to *lac* promoter activity from vector sequences. Plasmids pISM2121 and pISM1228 constructed from clones pISM2139 and pISM2159 are marked with asterisks. Also shown (▲) are selected Tn*1000* insertion sites in pISM2121 used in immunoblot analysis to identify the P97 coding region. Sizes of the cloned fragments are given in kilobases. B = *Bam*HI; E = *Eco*RI; EV = EcoRV; H = *Hin*dIII; N = *Nci*I; P = *Pst*I; S = *Sal*I. NA = not applicable. The *Pst*I site is part of the cloning vector's multiple cloning site.

abolished the production of Mab F1B6-reactive antigens, while inserts outside this region failed to abolish antigen production (Figure 2). It was concluded that the P97 coding sequence was located in the region between inserts 1.14 and 1.3 (Figure 1). Interestingly, our results indicated that *E. coli* produced a major antigen of approximately 126 kDa which was significantly larger in size than the 97 kDa protein observed in *M. hyopneumoniae*. This suggested that the coding region was larger than expected or that *E. coli* was improperly initiating transcription of the structural gene. Also, *E. coli* ISM612 (pISM2121::Tn*1000* 16-13) produced a dominant protein with a reduced size of approximately 98 kDa (Figure 2, lane 7).

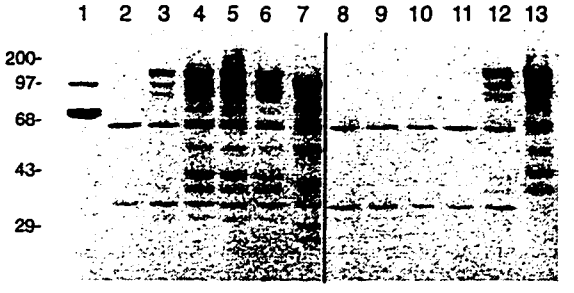

Figure 2. Western blot analysis of selected Tn*1000* insertions in pISM2121. Protein antigens were prepared from IPTG-induced cultures as described in the Materials and Methods, separated on a 10% SDS-PAGE mini-gel, and blotted to nitrocellulose. The blots were developed with Mab F1B6 as described. Lane 1 contained *M. hyopneumoniae* antigen, and the remaining lanes contained protein preparations from IPTG-induced ISM612 with pSK- (lane 2); pISM2121 (lane 3); pISM2121 derivatives containing Tn*1000* insert 1.1 (lane 4); 1.2 (lane 5); 1.4 (lane 6); 16.13 (lane 7); 1.14 (lane 8); 26.14 (lane 9); 1.15 (lane 10); 1.3 (lane 11); 16.12 (lane 12); and 1.12 (lane 13). Apparent molecular masses, in kilodaltons, are indicated on the left. The blot was digitized using a Cohu model 4900 high performance charge-coupled device camera (Cohu, Inc., San Diego, Calif.) and a Macintosh IIci equipped with a Scion Corporation (Frederick, Md.) video board. The resulting TIFF file was cropped and assembled in Adobe Photoshop and labeled in Aldus FreeHand.

Construction of pISM2159::Tn*1000* Insertion Mutants

Since plasmid pISM2159 seemed to include the entire P97 gene sequence (Figure 1), it was chosen to sequence. Plasmid pISM2159 was mutagenized with Tn*1000*, and pISM2159:: Tn*1000* plasmids were isolated and restriction-mapped to determine the location of each insert (Figure 3). A series of pISM2159::Tn*1000* plasmids representing Tn*1000* inserts distributed

throughout the pISM2159 insert sequence was analyzed by immunoblot with Mab F1B6 as described above, and a similar result to Figure 2 was obtained (data not shown). The Tn*1000* series was then used to derive the DNA sequence of pISM2159 using Tn*1000* -specific sequencing primers.

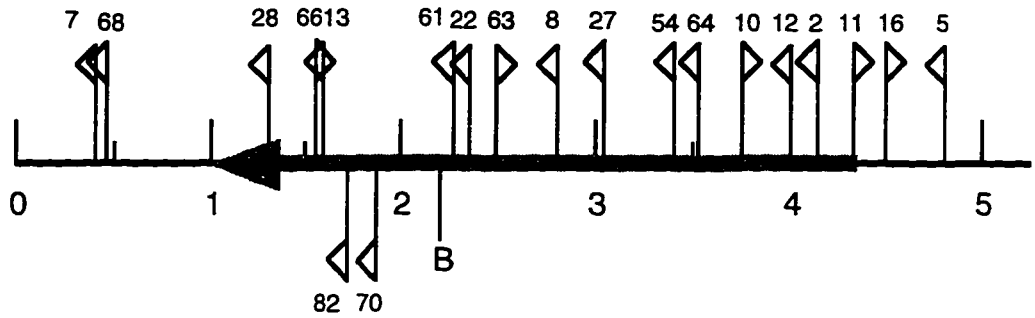

Figure 3. The location of Tn*1000* insertions within the cloned insert of plasmid pISM2159. Each flag represents one individual pISM2159::Tn*1000* isolate. The orientation of each transposon correlates with the direction of the flag which is pointing towards the 3′ end of the transposon. The scale is shown in kilobases. The numbers are insert designations. The arrow indicates the position and direction of transcription of P97. B, *Bam*HI restriction site.

Sequence analysis of P97 Gene and Translated Protein Product

The DNA sequence of pISM2159 was analyzed with MacVector software. A 3,324 base pair (bp) open reading frame (ORF) was identified with a coding capacity for a protein with a predicted molecule weight of 124.9 kDa. This has been designated the structural gene for P97 (Figure 4). The translated protein had a predicted pI of 8.71. A putative promoter region was identified 145 bp upstream of this ORF P97 structural gene. The -10 sequence (TATAAT) and -35 sequence (TTGCAA) was separated by a stretch of 17 adenine residues including the two within the -35 sequence. A putative Shine-Dalgarno sequence (GAGGT) was identified 7 bp upstream of the ATG start site. No termination signal could be identified immediately downstream of the P97 structural gene, but an uninterrupted ORF was identified which could constitute a second gene of an operon.

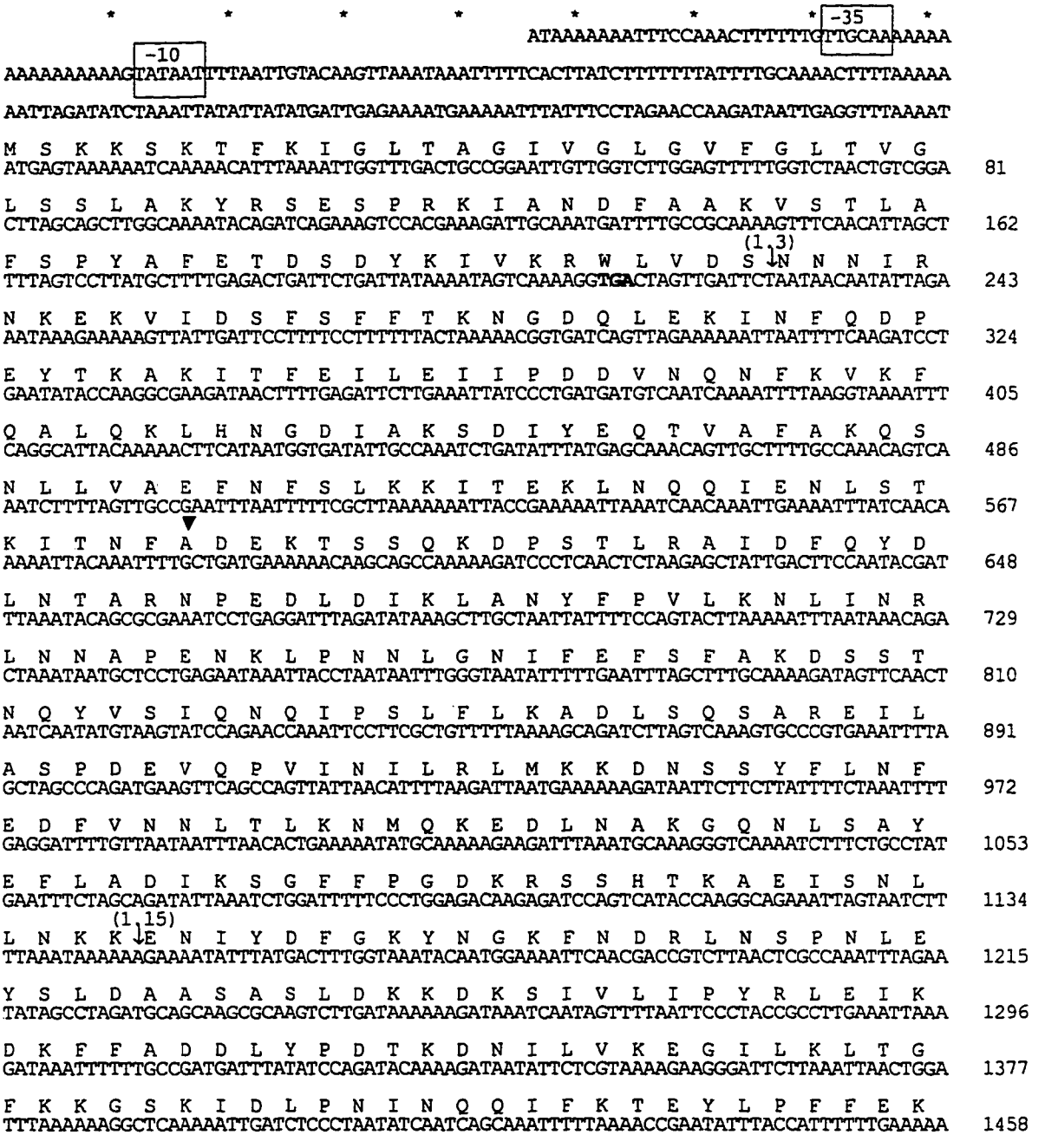

Figure 4. Nucleotide and amino acid sequence of P97 of *M. hyopneumoniae* strain 232A. The putative -35 and -10 sequences are boxed. The repeating motifs are indicated by a single underline for the AAKP(V/E) motif or double underline for the NQGKK(S/A)EG(A/T)P motif. Plus (+) indicates the beginning of each repeating motif. Base numbering begins with the start codon of P97. The posttranslational cleavage site is indicated by (▼). Arrows pointing downward indicate Tn*1000* insertion site; the insertion number is given above the arrow. UGA codons are boldface.

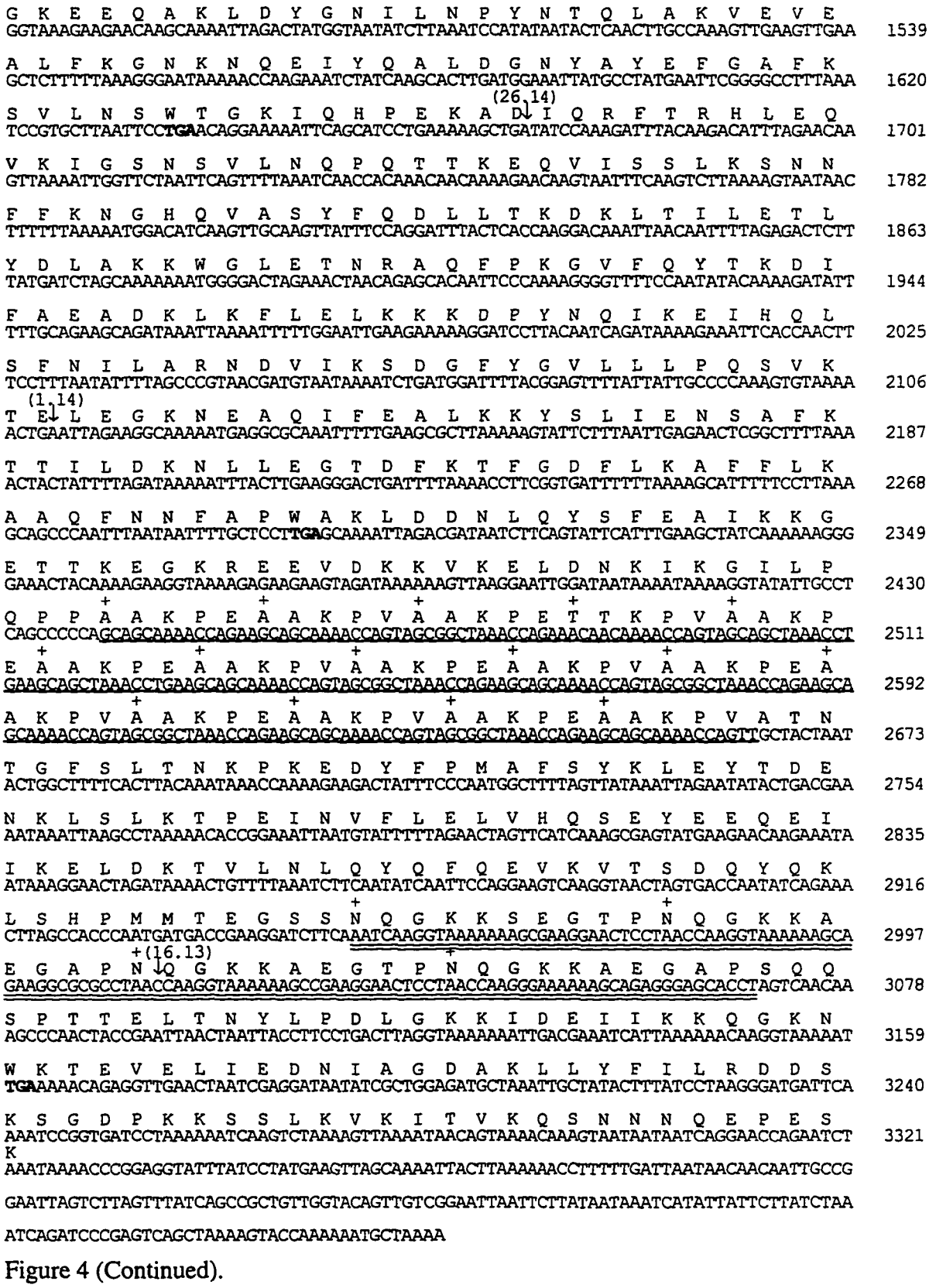

Figure 4 (Continued).

The P97 structural gene was translated using a mycoplasma translation table. The amino acid sequence of the predicted P97 protein has been included in Figure 4. The protein displayed high hydrophilicity throughout the entire protein that is predicted to be rich in helix structure (Figure 5). Two putative overlapping transmembrane helices comprising 17 amino acids (numbers 13 to 29) and 20 amino acids (numbers 12 to 31) were identified at the amino terminus using TMpred software (89) located at URL: http://ulrec3.unil.ch/software/tmpred_ form.html. The two helices have opposite orientations relative to the membrane, In-Out and Out-In. A protein kinase ATP-binding region signature was also identified at the amino terminus of the protein overlapping the transmembrane domain by the use of MOTIF software at URL: http://www. genome.ad.jp/ sit/motif.html. The amino acid composition is shown in Table 4. Most notably, the protein contains no cysteine residues. There was no identifiable lipoprotein acylation site, such as has been observed in other mycoplasma membrane proteins (248, 259). Four UGA codons were found in the P97 DNA sequence at positions 214, 1636, 2296, and 3160. Expression of proteins terminated at these codons would result in production of proteins with predicted MWs at 7.8, 62.0, 87.5, and 118.7 kDa assuming that translation begins at the normal ATG start codon. Two proline-rich repeated sequences, R1 and R2, were identified near the carboxy terminus. R1 comprises 15 repeats of the 5 amino acid consensus sequence of AAKP(V/E), and R2 consists of 4 repeats of the 10 amino acid consensus sequence of NQGKK(S/A)EG(A/T)P. The amino terminal amino acid sequence of P97 has been obtained (264). This sequence, ADXKTDSDKDPSTLRAIDEQ, aligned to the predicted amino acid sequence of P97 beginning at position 195, indicating that P97 in *M. hyopneumoniae* was produced as a 124.9-kDa precursor and then processed to 102.9 kDa by proteolytic cleavage at that position.

Table 4. Amino acid composition of the translated P97 sequence.

		No.	Percent			No.	Percent
Non-polar:	A	89	8.03	Polar:	G	49	4.42
	V	46	4.15		S	71	6.41
	L	105	9.48		T	55	4.96
	I	64	5.78		C	0	0
	P	55	4.96		Y	36	3.25
	M	6	0.54		N	84	7.58
	F	65	5.87		Q	57	5.14
	W	5	0.45				
Basic:				Acidic:			
	K	146	13.18		D	65	5.87
	R	18	1.62		E	84	7.58
	H	8	1.72				

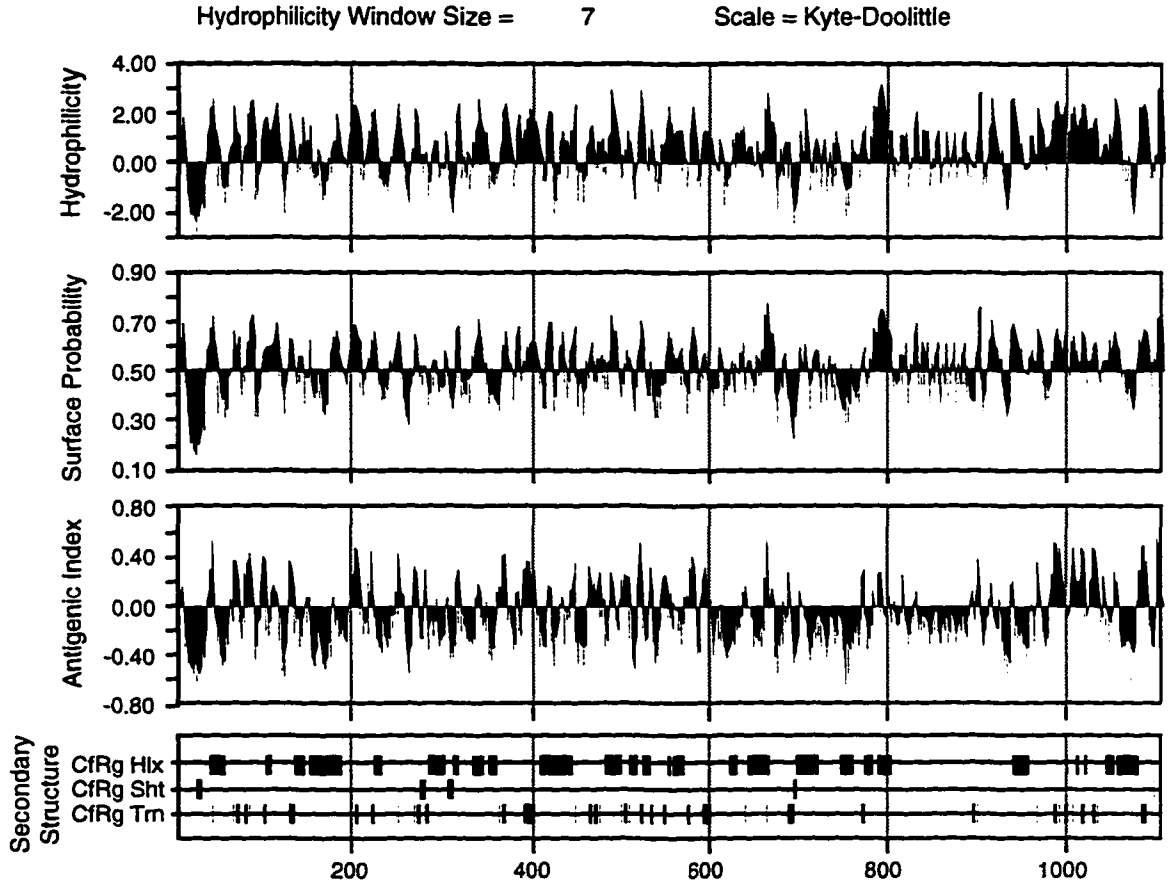

Figure 5. Predicted hydrophilicity and structural properties of the translated sequence of P97. The scale at the bottom of the figure indicates the amino acid residue number. The type of analyses are indicated on the left. Positive numbers indicate high probability for hydrophilic regions, surface exposure and antigenicity. Shown in the bottom panel are the regions of secondary structure that agree using the Chou-Fasman (Cf) (30) and Robson-Garnier (Rg) (67) methods. Hlx, α-helix; Sht, β-sheet; Trn, turn.

Functional Analysis of P97 Protein Expressed in *E. coli*

Previous studies had suggested a role for P97 in the binding of *M. hyopneumoniae* to swine cilia (264). Immunoblot analysis of ISM612 clones containing pISM2121 or pISM2159 indicated that proteins related to P97 were being expressed, but additional studies were needed to confirm the role of P97 in ciliary adherence. To demonstrate that pISM2121 coded for a swine ciliary adhesin, MPAA analysis was performed. This was accomplished by transforming pISM2121 and pISM2121::Tn*1000* derivatives into *E. coli* ISM612, preparing lysates and examining the lysates for cilia binding activity in the MPAA assay. Figure 6 shows the results

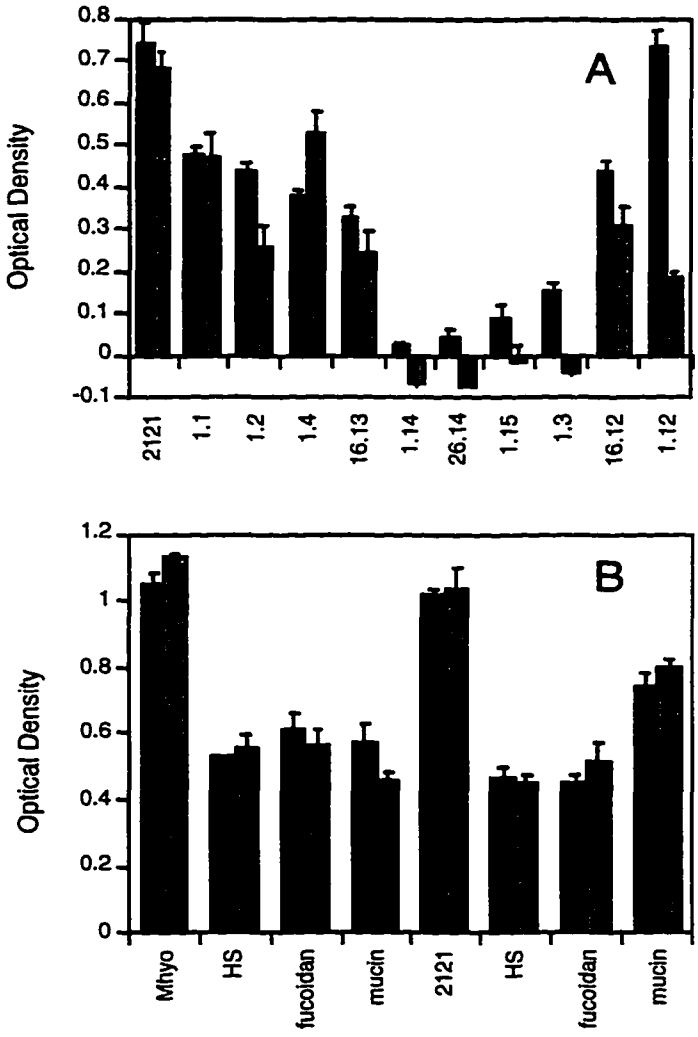

Figure 6. Binding of *M. hyopneumoniae* and recombinant P97 preparations to swine cilia. A: Data represent the means of triplicate wells from two experiments (solid and shaded bars). The *E. coli* strains are indicated as 2121 (the positive control) or by the number of the Tn*1000* insert. Not shown are the values for *M. hyopneumoniae* antigen which were greater than 2.0 in both experiments. B: Data are from two representative experiments (solid and shaded bars) with *M. hyopneumoniae* (first four sets of bars) or *E. coli* (pISM2121) preparations (second four sets of bars), with or without an inhibitor. Values in both panels are given in mean optical density units ± standard deviation of triplicate wells. Zero values indicate 0 or lower values after background (pMOB::Tn*1000*) subtraction. Mhyo, *M. hyopneumoniae* antigen; HS, heparin sulfate; 2121, *E. coli* lysate containing recombinant P97 produced by plasmid pISM2121.

of these assays. Lysates containing control plasmids, pMOB or pMOB::Tn*1000* failed to show binding activity. *M. hyopneumoniae* antigen or *E. coli* lysates from strains containing pISM2121 bound to cilia and gave positive optical density responses (Figure 7). To map the ciliary binding activity and correlate it with the immunoreactivity on immunoblots, Tn*1000* inserts in pISM2121 were also examined. Tn*1000* insertions outside the P97 ORF retained cilia binding activity and were immunoblot positive whereas Tn*1000* inserts within the P97 ORF abolished cilia binding activity and immunoreactivity (Figure 2). Interestingly, insertion pISM2121::Tn*1000* 16-13, previously shown to produce a dominant Mab F1B6-reactive protein with reduced size, retained cilia binding activity (Figure 6).

Previous studies by Zhang et al. demonstrated that *M. hyopneumoniae* adherence to cilia was inhibited by heparin, fucoidan, and mucin (266). These polysaccharide inhibitors were also examined for their ability to inhibit ciliary binding of ISM612 (pISM2121) lysate as compared to that of *M. hyopneumoniae* whole cells. Heparin, fucoidan, and mucin inhibited the ciliary binding of *E. coli* ISM612 (pISM2121) lysate and *M. hyopneumoniae* whole cell antigens in a similar manner (Figure 6).

In order to rule out the possibility that sequences downstream of the P97 gene were involved in cilia binding, these sequences were removed by cloning the *Nci*I - *Pst*I fragment from pISM2159 into *Pst*I - *Sma*I digested pKS as described in the Materials and Methods. The resulting plasmid, pISM1228, was transformed into ISM612 and lysates prepared for immunoblot and MPAA assays. Figure 7 shows the results of these studies. Lysates from ISM612 containing pISM2121, pISM2159 and pISM1228 gave similar immunoblot banding patterns (Figure 7, panel A). This was also true for the ciliary binding activities (Panel B). These results demonstrate that the P97 gene, but not downstream sequences, were producing the ciliary binding activity.

Construction of the P97 Operon Restriction Map

Since other mycoplasmal adhesins are within multigene operons, it was important to determine if this was also true for *M. hyopneumoniae*. The first step was to obtain as many clones as possible containing P97 gene sequences. This was accomplished by screening the *M. hyopneumoniae* genomic Lambda ZAP® II library with a radiolabeled probe derived from the 3.3 kb *Eco*RI fragment of pISM1161 spanning the upstream region and the 5′ end of the P97 gene. Five recombinant phage were subsequently identified and the DNA inserts rescued into pSK- plasmids. These plasmids were isolated and restriction mapped (Figure 8). The alignment of some of these plasmids were confirmed by Southern analysis with the same probe

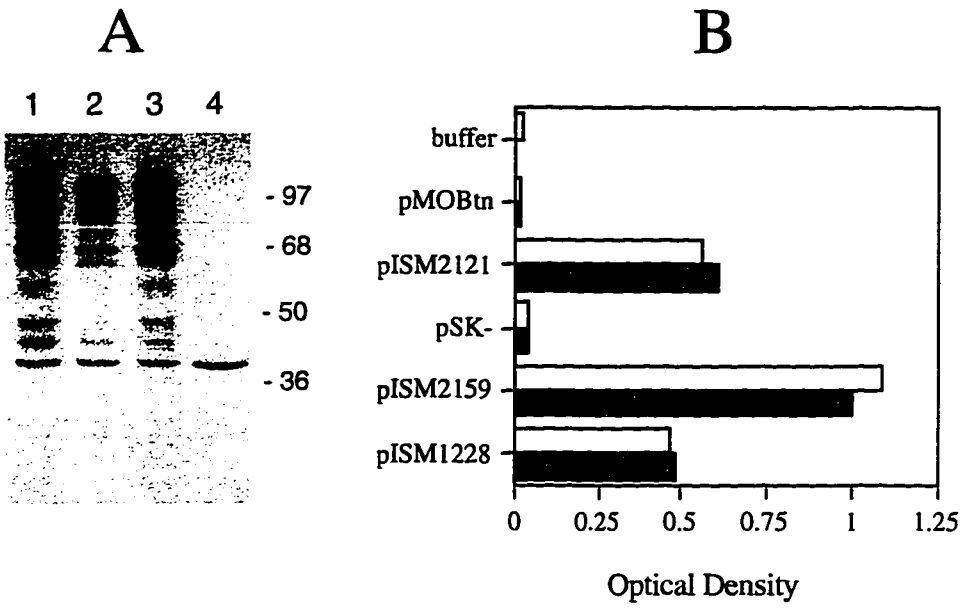

Figure 7. Immunoblot and cilia binding analysis of *E. coli* lysates from strains containing pISM2121, pISM2159 and pISM1228. A. Immunoblot analysis with Mab F1B6. Lanes contain lysates from ISM612 with plasmids pISM2121 (lane 1); pISM2159 (lane 2); pISM1228 (lane 3); or pMOB::Tn*1000* (lane 4). Molecular masses are given in kDa on the right. B. Optical density of cilia binding assay. Data represent the means of triplicate wells of two identical experiments (white and shaded bars). pMOBtn, pMOB::Tn*1000*.

(data not shown). These plasmids overlapped a 16 kb region (designated as the P97 contig) including the two largest plasmids, pISM1210 and pISM1217 corresponding to the up and downstream regions of the P97 gene, respectively.

Sequence and Structure Analysis of the P97 Operon

Tn*1000* mutagenesis was performed on plasmids pISM1210 and pISM1217 to facilitate DNA sequencing of this region as described in Material and Methods. The location of each Tn*1000* insert was restriction mapped, and a series of Tn*1000* inserts were chosen to use as template DNAs for sequencing reactions based upon their location in the operon and their usefulness in adding to the DNA sequence information upstream and downstream of the P97 sequence already obtained. A total of 9,455 bp of DNA sequence was subsequently obtained including the sequence of the P97 gene. The remaining portion of this sequence is shown in Figure 9 except for the P97 gene sequence which is given in Figure 4.

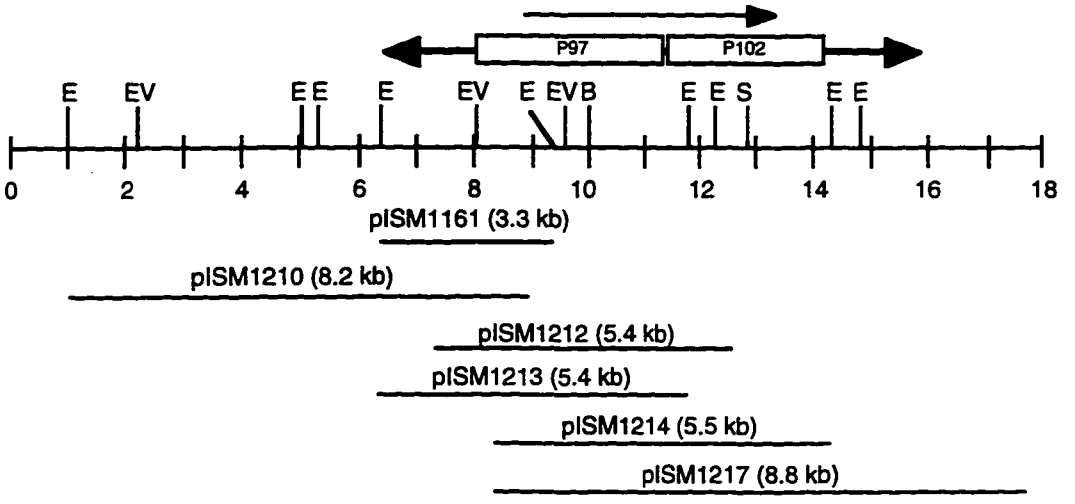

Figure 8. Restriction map of the P97 contig and overlapping clones obtained by DNA hybridization with the cloned fragment from pISM1161. The restriction maps of the five clones from the *M. hyopneumoniae* library obtained by DNA hybridization are shown along with their insert size in parentheses. Also shown are the positions of the P97 and P102 structural genes, the direction of their transcription (arrow), and the region of DNA sequence analysis (double headed arrow). The sizes are given in kilobases. Restriction sites: B, *Bam*HI; E, *Eco*RI; EV, *Eco*RV; S, *Sal*I.

A total of 6 ORFs were identified in this 9,455 bp sequence using MacVector software (Figure 10). P97 appeared to be first gene of a two gene operon, the P97 operon. The second structural gene in the P97 operon, initiated 20 bp downstream of the P97 structural gene, and was preceded by a putative Shine Dalgarno sequence (GGAGGT) 10 bp upstream of the ATG start codon (Figure 9). The ORF was 2,712 bp in length with a coding capacity for a 102.3-kDa protein. This protein was designated as P102, had a calculated pI of 9.28, and lacked cysteine (Table 5). The protein was highly hydrophilic with a putative 25 amino acid membrane-spanning domain at its amino terminus (amino acids 10 to 34). Searching the database for homology with P102 revealed no significant match to any known sequence, including adhesin genes from other eubacteria. The protein predictions for P102 are shown in Figure 11. The P97 operon is flanked upstream and downstream, respectively, by ORF 1 and ORF 5 which are transcribed in the reverse direction to P97. The ORF 1 translated sequence is highly homologous to the ribosomal protein S10 from other eubacteria. ORF 5 codes for a 26.3-kDa protein whose sequence is homologous to proteins of unknown function from other bacteria. ORF 6 has a high homology to *alaS* which codes for alanyl-tRNA synthase.

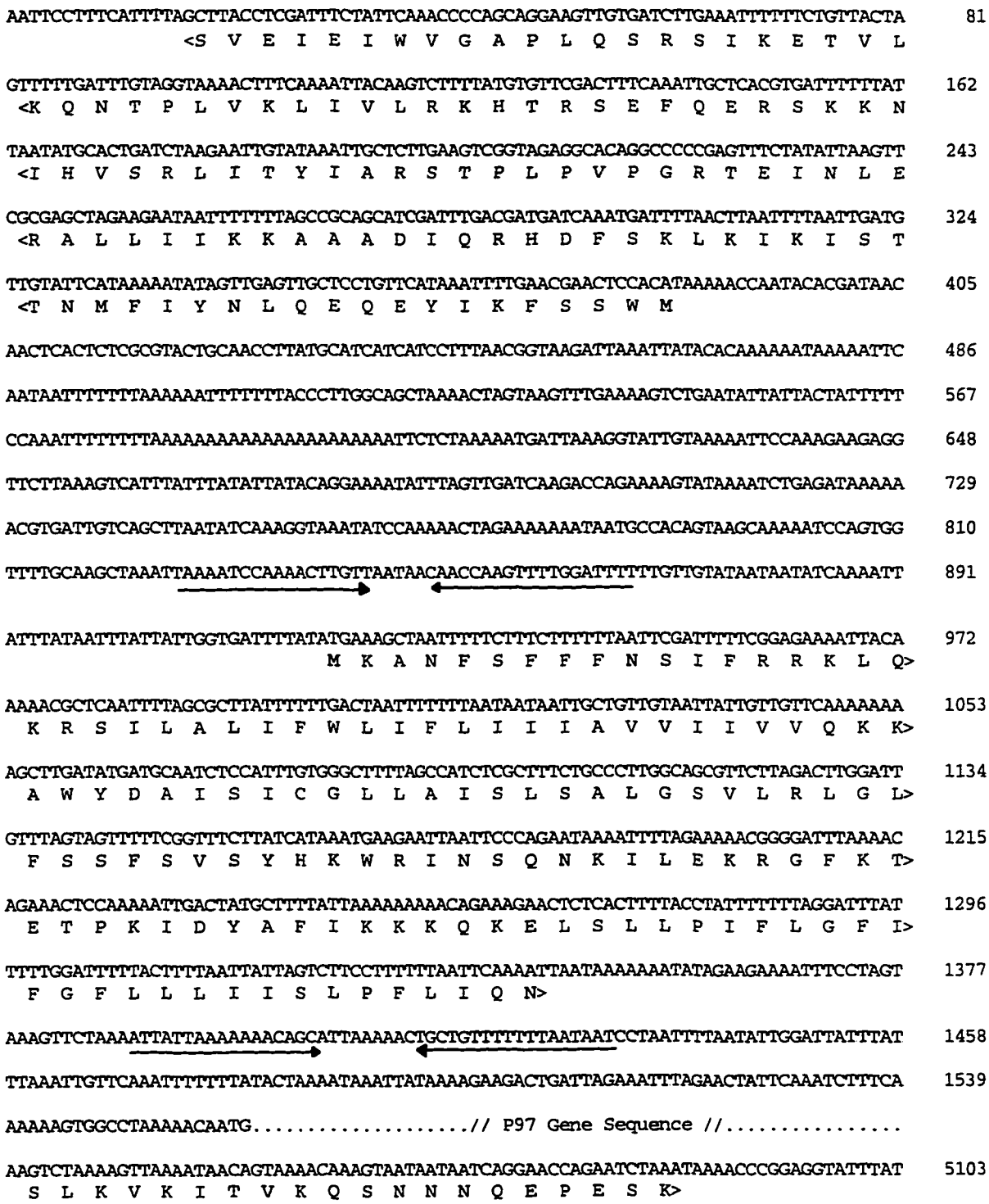

Figure 9. Sequence of the P97 operon and adjoining sequences. Most of the P97 structural gene sequence has been deleted to conserve space with truncation beginning at the first base of Figure 4. The direction of transcription for each ORF is given by < or >. The arrows indicate stem loop structures which flank ORF 2. The last ORF is not a complete sequence.

```
CCTATGAAGTTAGCAAAATTACTTAAAAAACCTTTTTGATTAATAACAACAATTGCCGGAATTAGTCTTAGTTTATCAGCC  5184
   M  K  L  A  K  L  L  K  K  P  F  W  L  I  T  T  I  A  G  I  S  L  S  L  S  A>

GCTGTTGGTACAGTTGTCGGAATTAATTCTTATAATAAATCATATTATTCTTATCTAAATCAGATCCCGAGTCAGCTAAAA  5265
 A  V  G  T  V  V  G  I  N  S  Y  N  K  S  Y  Y  S  Y  L  N  Q  I  P  S  Q  L  K>

GTAGCAAAAAATGCTAAAATTAGTCAGGAAAAATTTGATTCAATTGTTTTAAATCTTAAAATTAAAGATAATTTTAAAAAA  5346
 V  A  K  N  A  K  I  S  Q  E  K  F  D  S  I  V  L  N  L  K  I  K  D  N  F  K  K>

TGATCGGCAAAAACAGTTTTAACTGCTGCCAAAAGTGATCTTTATCGTTATAATCTTGTTTCTGCTTTTGATTTAAGTGAA  5427
 W  S  A  K  T  V  L  T  A  A  K  S  D  L  Y  R  Y  N  L  V  S  A  F  D  L  S  E>

CTAATAAACAATGATTATTTAGTAAGTTTTGATCTTGAAAATGCAGTAGTTGATCAAAATTCAATTAAAAATGTTGTTATT  5508
 L  I  N  N  D  Y  L  V  S  F  D  L  E  N  A  V  V  D  Q  N  S  I  K  N  V  V  I>

TATGCAAAATCTGATAAGGATCAAATAACTTATTCAAAACAAATTGTACTTAAAGGCTTTGGAAATACAGAACAAGCTAGA  5589
 Y  A  K  S  D  K  D  Q  I  T  Y  S  K  Q  I  V  L  K  G  F  G  N  T  E  Q  A  R>

ACTAATTTTGATTTTAGTCAAATTGATTCAAGCAAGTCTTTTGTTGATCTTTCAAGAGCAAATCTAACTTTGATGGAATTC  5670
 T  N  F  D  F  S  Q  I  D  S  S  K  S  F  V  D  L  S  R  A  N  L  T  L  M  E  F>

CAAATTTTGCTTGCCCAAAATTTTGAAAATGAAAGAGGAAGTAATTGATTTTCACGACTTGAAAGAGCTTTGGTTGCATCA  5751
 Q  I  L  L  A  Q  N  F  E  N  E  R  G  S  N  W  F  S  R  L  E  R  A  L  V  A  S>

AAAGCGAGTCTTTCACTTTATAATTCCTTAGGAGAACCCGTATTTTTAGGCCCAGATTATCAATTAGACCCAGTTTTGGAC  5832
 K  A  S  L  S  L  Y  N  S  L  G  E  P  V  F  L  G  P  D  Y  Q  L  D  P  V  L  D>

CGAAAAAAATTATTAACTTTGTTAAATAAAGATGGAAAATTAGTTCTTGGACTTAATTTAGTGCAAATTTCAACTAAAAAA  5913
 R  K  K  L  L  T  L  L  N  K  D  G  K  L  V  L  G  L  N  L  V  Q  I  S  T  K  K>

ACTATGAATTTAAATCTTGAAGTTCGCGGCGCGATTTCAAATCAGGAAATTTCTAAAATTCTAAAATCCTGACTTGAAACA  5994
 T  M  N  L  N  L  E  V  R  G  A  I  S  N  Q  E  I  S  K  I  L  K  S  W  L  E  T>

AATCTTCAAGGCAAATTAAAAACCAAAGATGATTTGCAAATGGCACTAGTAAAAGATAAAATTAGCCTCTCTGATTATTGA  6075
 N  L  Q  G  K  L  K  T  K  D  D  L  Q  M  A  L  V  K  D  K  I  S  L  S  D  Y  W>

TATGGATCTCCGAATTCAAAAGTAAATACATCCCAAATTTTAACAAAAAGTAAAGAATTTAAAGATCTTTTTGATTTAAGT  6156
 Y  G  S  P  N  S  K  V  N  T  S  Q  I  L  T  K  S  K  E  F  K  D  L  F  D  L  S>

GAGACAAATTTTTTTCTTAATACCAAAATCGGAACTGTCTATTTAAGTATTATTCCCAAACTTTTAGATCCAAGTCAGATT  6237
 E  T  N  F  F  L  N  T  K  I  G  T  V  Y  L  S  I  I  P  K  L  L  D  P  S  Q  I>

TCTGTTGTTGATAAGAAAAAACTAGTTGAAAATCAAAAAATTCGCTTTGAAATTACTGCTTCTTTAAAACGAAAAGCTATT  6318
 S  V  V  D  K  K  K  L  V  E  N  Q  K  I  R  F  E  I  T  A  S  L  K  R  K  A  I>

GATAAAAAATTTATCATCCAGGATCTTCCAGTTTTTGTTGATCTAAAAGTTGATTTTAATAAATACCAAGCCGCTGTTGCC  6399
 D  K  K  F  I  I  Q  D  L  P  V  F  V  D  L  K  V  D  F  N  K  Y  Q  A  A  V  A>

CAAATGTTTGGAACGATAAAAGCAGTTAAAGAATTTTCAATGCCTGAAGATCAAGATGCAAAAACTTTATCCTCAAATGAA  6480
 Q  M  F  G  T  I  K  A  V  K  E  F  S  M  P  E  D  Q  D  A  K  T  L  S  S  N  E>

ATAAAACAGCGAGTTGATCGACTTTTTGAACTAGCAAAAACAGTGACTAATTTGGAAAATCCAAGTGAAGAAGTTCTTAAA  6561
 I  K  Q  R  V  D  R  L  F  E  L  A  K  T  V  T  N  L  E  N  P  S  E  E  V  L  K>

AGCATTTATTTATTAAATACGGGAAAATATTTAGTCGACCAAGACCAGGAAAAAGTAAAACAAGAGCTAAAAACCGTGATT  6642
 S  I  Y  L  L  N  T  G  K  Y  L  V  D  Q  D  Q  E  K  V  K  Q  E  L  K  T  V  I>

GAGGGCTTAAAATCAAAGGCAAATACTCAAAAAACAGAAAAAAATAGCCCCACACAACCGAAAAAACCAGAGGTTTCACTA  6723
 E  G  L  K  S  K  A  N  T  Q  K  T  E  K  N  S  P  T  Q  P  K  K  P  E  V  S  L>
```

Figure 9. (Continued)

```
GCTAAAACAACAGAAAATTCAGCAAAAACAGTCAAGGTAAGCACTTTTGCAGAAGAAGCTAAGGGTCAAAGTCAAAGTCAG   6804
 A  K  T  T  E  N  S  A  K  T  V  K  V  S  T  F  A  E  E  A  K  G  Q  S  Q  S  Q>

CAAACACAACCAGTTTCCACTTCATCGCCTCAAACTAGTCAAAATTCACTTCCTAATTCCACAAGCAGCTCAAATTCTGTA   6885
 Q  T  Q  P  V  S  T  S  S  P  Q  T  S  Q  N  S  L  P  N  S  T  S  S  S  N  S  V>

TTAGAAAATGAAAAATTTGGGACAAGCATTTGAACAGCTTTTAATTTCGCTAATATTTATAATCTTGAAAATACAAAAAGC   6966
 L  E  N  E  K  F  G  T  S  I  W  T  A  F  N  F  A  N  I  Y  N  L  E  N  T  K  S>

GAATATGAGATCTCAACTTTAGGAAATAAGCTATTTTTTGATTTTAAATTAGTTGATAAAACTAATCAAAATCTAATTTTG   7047
 E  Y  E  I  S  T  L  G  N  K  L  F  F  D  F  K  L  V  D  K  T  N  Q  N  L  I  L>

GCTCAGTCCAAAATTAGTCTTAATAATATTATTAATTCTAATAAATCTGCCTATGATATAATTAAGAAATTCAATCCCGAT   7128
 A  Q  S  K  I  S  L  N  N  I  I  N  S  N  K  S  A  Y  D  I  I  K  K  F  N  P  D>

GTGTTTTTAGATGGAACAATTAATTATCAAAATCAAGGAAAAGATAAAAAAGAATTTATCCTAAAAGATTTAAGTGATAAT   7209
 V  F  L  D  G  T  I  N  Y  Q  N  Q  G  K  D  K  K  E  F  I  L  K  D  L  S  D  N>

AAATTAATATTTAAATCAGAAGATGCAATTCAAACTGATCAAGGTTTAGAGCTAAAGAAACCTTTGAAATTACAGTCAAAA   7290
 K  L  I  F  K  S  E  D  A  I  Q  T  D  Q  G  L  E  L  K  K  P  L  K  L  Q  S  K>

TCGTCTAATCCAGAAAAAGAAATATCAACTTCTTTATATACCGGAGCAATTTATTTAGTTTTTGATGCAAAAAATATTTCC   7371
 S  S  N  P  E  K  E  I  S  T  S  L  Y  T  G  A  I  Y  L  V  F  D  A  K  N  I  S>

GATGGTAATTGGATTAATCTTTTAGCCGATAGAAAAGGAAAAGGGCTTGTAATTAAAGTTCAAAATTCAAATAATAATGTA   7452
 D  G  N  W  I  N  L  L  A  D  R  K  G  K  G  L  V  I  K  V  Q  N  S  N  N  N  V>

CCTAAAACCAAAGAAATTGTTGAGAATGGTACCTATTTATATGAAATTCTTGCTGGCAAGGATTCGATTAAGGTAAATTCT   7533
 P  K  T  K  E  I  V  E  N  G  T  Y  L  Y  E  I  L  A  G  K  D  S  I  K  V  N  S>

TATTTTTTTCCAACAAAGTACCCAAAACGTGTAAAACGTCTTAAATTCGAGATTAACCCTAAAGACACCTTGCCAAATTTC   7614
 Y  F  F  P  T  K  Y  P  K  R  V  K  R  L  K  F  E  I  N  P  K  D  T  L  P  N  F>

TTTACTTTAGAATGATTTCATCTTGATTGGTATCAAATCGGCCCAGGCGAACAAAATAAAAAACCACAACAAAACGCTAAA   7695
 F  T  L  E  W  F  H  L  D  W  Y  Q  I  G  P  G  E  Q  N  K  K  P  Q  Q  N  A  K>

AAAGAACCTACAATTATATTAAAAACGCTGGCAATATTTAATGATAAATCATTTGCAGAGAAAGGAAGTTTAACAAAAAGA   7776
 K  E  P  T  I  I  L  K  T  L  A  I  F  N  D  K  S  F  A  E  K  G  S  L  T  K  R>

AGTGAATTAATTAACGGGTTGATTAGAAACTATGTTAAAAAGTAACGATCAAATTTTTGTTAAAAAACAGAATTTAGTAAA   7857
 S  E  L  I  N  G  L  I  R  N  Y  V  K  K>

AGATTTTTTATTTAAATTATAAAAAGCAAACCCTAATTAAAAGTGGAAAAAATTAGGAAAAAGAAGCTATTTTTACTTTTT   8019

TTTGATTATTTTATAATTTTTTGATAATATTGGTGATATATTATTAAATCTATTTTTTCGTTGAAAAAGGATGTTTAATAA   8100

TGCAAATTTTTATAAAAATTTGCATTTCTAGCCAAAATTAATCTTTTATACATTTGTTAAAAGAAAAATTGCGGCTGTCT   8181
                                        <D  K  I  C  K  T  L  L  F  I  A  A  T  E

CAGATCTAAGAATTCTTTTCCCGAGTGTGATACTTTGAAACCCTAATTTTTCTGCTTGTTGGATTTCAACATCATCAAACC   8262
 <S  R  L  I  R  K  G  L  T  I  S  Q  F  G  L  K  E  A  Q  Q  I  E  V  D  D  F  G

CACCTTCAGGCCCAATAATTATAATTGTATTTTGGGGGTTATCAGGGATATTTATATTGTTTTTTGCTCTTTCAAAACTGA   8343
 <G  E  P  G  I  I  I  I  T  N  Q  P  N  D  P  I  N  I  N  N  K  A  R  E  F  S  I

TTAATTTTACTGGAAAATTTTTGGCTTGTTCTAAAAGATCCTTATAATTTATAGGTAAATTTATTTTTGGAATCAAATTGC   8424
 <L  K  V  P  F  N  K  A  Q  E  L  L  D  K  Y  N  I  P  L  N  I  K  P  I  L  N  R

GGAAACTTTGTTGGGCACTATGAAGACAAATTTGTTCTCATCTTTTGAGTTTTTTTTCAAGATCCCCGCTTAGTTTTTGGG   8505
 <F  S  Q  Q  A  S  H  L  C  I  Q  E  W  R  K  L  K  K  E  L  D  G  S  L  K  Q  S
```

Figure 9. (Continued)

```
AAACATTTTTACTATAAAAAGGTCAAATTTCATTAACCCCAATTTCAACAGCTTTCTGGATTGCAAATTCAAATGATTTTG   8586
 <V  N  K  S  Y  F  P  W  I  E  N  V  G  I  E  V  A  K  Q  I  A  F  E  F  S  K  T

TCTTCAAAATTGCAAGTGCGAGAACAACTTTGTTTTTTGGTTCGTTATTCCCCTTAATTTTTTCAATTATTTCTGCTTTGT   8667
 <K  L  I  A  L  A  L  V  V  K  N  K  P  E  N  N  G  K  I  K  E  I  I  E  A  K  N

TTGAATTAGGGACTAATCTCACAAGGTAGAATTCATTTTGATAAACACAAATAAAATTTTCATTTTTAATTCTTACAGTTT   8748
 <S  N  P  V  L  R  V  L  Y  F  E  N  Q  Y  V  C  I  F  N  E  N  K  I  R  V  T  K

TAATATGATTTAAGGTTAGATTTGTTAAGATAAAGAAATTTTCTTGTTTTTCATTGACAAAAAAGCGATACATAATAAAAA   8829
 <I  H  N  L  T  L  N  T  L  I  F  F  N  E  Q  K  E  N  V  F  F  R  Y  M

TTTTAAAGGAAAATTGATAAACTATTTAAAAAATAGTTTAAAATTATTAAAAAAGAAGGAAAAACTATGGAAAAATTATCA   8910
                                                                    M  E  K  L  S>

GCAAACGAAATAAGACAACTTTGAATTGATTTTTTTCGCGAAAAAAATCATTTTTTTATCGAATCAAAACCACTTGTTCCC   8991
 A  N  E  I  R  Q  L  W  I  D  F  F  R  E  K  N  H  F  F  I  E  S  K  P  L  V  P>

CAAAATGATGACTCACTTCTTTGAATAAATTCAGGAGTTGCCACTTTAAAAGATTATTTTACCGGCAAAAAAATTCCCCCA   9072
 Q  N  D  D  S  L  L  W  I  N  S  G  V  A  T  L  K  D  Y  F  T  G  K  K  I  P  P>

TCAAAACGACTTGTAAACTCCCAAAAAGCCTTAAGAACAAATGACATTGAAAATGTTGGTCTAACCTCGCGCCATCACACC   9153
 S  K  R  L  V  N  S  Q  K  A  L  R  T  N  D  I  E  N  V  G  L  T  S  R  H  H  T>

TTATTTGAAATGCTTGGGAATTTTTCAATTGGTGACTATTTTAAAACAGAAGCAATTGACTATGCTTATGAATTTTTAACT   9234
 L  F  E  M  L  G  N  F  S  I  G  D  Y  F  K  T  E  A  I  D  Y  A  Y  E  F  L  T>

AAAAAGTTAAAATTAGATCCCAAAAATTTGTTTATTACTTATTATGATGGTGATGATATAACTTTTGAAAAATGAAAAAGT   9315
 K  K  L  K  L  D  P  K  N  L  F  I  T  Y  Y  D  G  D  D  I  T  F  E  K  W  K  S>

TTGGGATTTTCTAATGAAAAATTAATAAAAGGCAGCAAAAAAACAAATTTTTGGGATTTAGGTCAGGGGCCTTGTGGTCCT   9396
 L  G  F  S  N  E  K  L  I  K  G  S  K  K  T  N  F  W  D  L  G  Q  G  P  C  G  P>

TGTAGTGAAATTTATTTTGACCGCGGGCCAAAATTTGATAGTCGAGGGAGCGAACTAA
 C  S  E  I  Y  F  D  R  G  P  K  F  D  S  R  G  S  E  L>
```

Figure 9. (Continued)

Table 5. Amino acid composition of the translated P102 sequence.

		No.	Percent			No.	Percent
Non-polar	A	45	4.98	Polar:	G	33	3.65
	V	52	5.75		S	86	9.51
	L	103	11.39		T	54	5.97
	I	62	6.86		C	0	0
	P	28	3.10		Y	29	3.21
	M	6	0.66		N	74	8.19
	F	44	4.87		Q	47	5.20
	W	9	1.00				
Basic:				Acidic:			
	K	114	12.61		D	50	5.53
	R	17	1.88		E	50	5.53
	H	1	0.11				

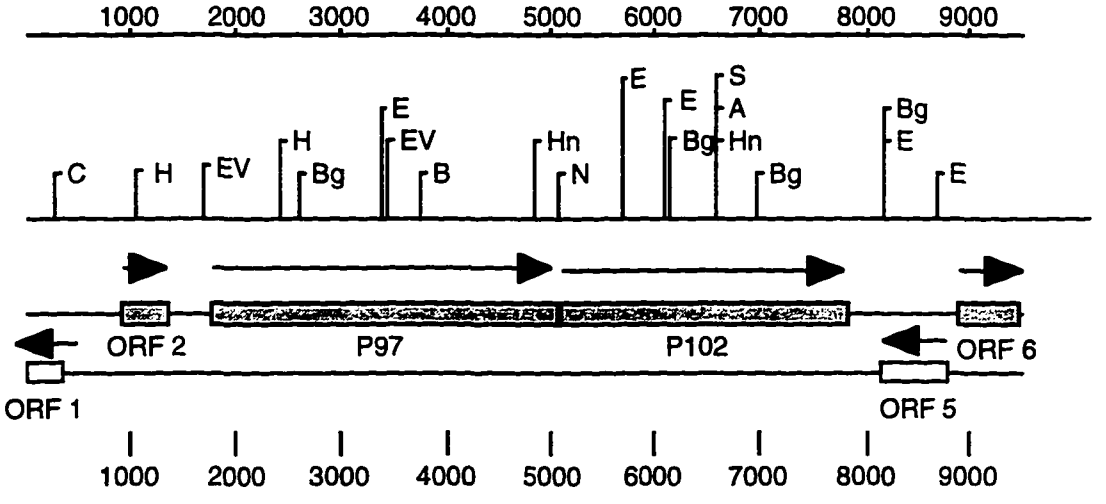

Figure 10. Analysis of the P97 contig for ORFs and direction of transcription. Bars indicate ORFs identified using MacVector software and a mycoplasma codon table. The ORF or gene designation is given below each bar. Shaded bars indicate transcription of left to right, white bars indicate transcription right to left. Sizes are given in kilobases. P97, ORF 3; P102, ORF 4. Restriction enzymes: A, *Acc*I; B, *Bam*HI; Bg, *Bgl*II; C, *Cla*I; E, *Eco*RI; EV, *Eco*RV; H, *Hin*dIII; Hn, *Hin*cII; S, *Sal*I.

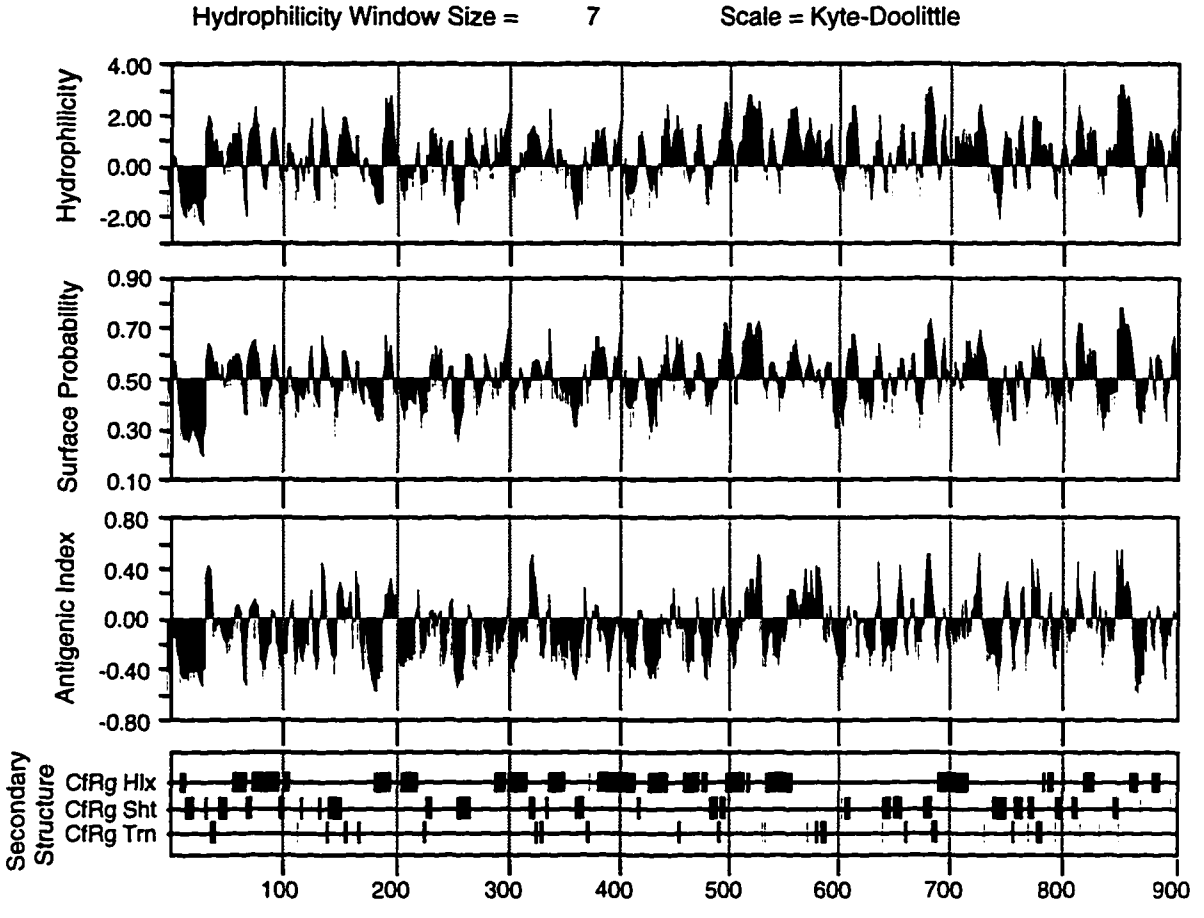

Figure 11. Predicted hydrophilicity and structural properties of the translated sequence of P102. The scale at the bottom of the figure indicates the amino acid residue number. The type of analyses and regions of secondary structure are as described in Figure 5.

In the approximately 1 kb region between ORF1 and P97 is ORF2 which is transcribed in the same direction as P97. ORF2 is 426 bp long and has a capacity coding for a 16.4-kDa protein with a pI of 10.52. The sequence of ORF2 displays no significant homology to known sequences. 340 bp upstream of ORF 2 is a 21 bp polyadenine sequence of unknown function. Two stem-loop structures were also identified flanking the ORF 2. The first stem loop, which is located 60 bp upstream of ORF 2, consists of 16 bp stem and a loop of 11 nucleotides. The second stem loop, which is located 40 bp downstream of ORF 2, consists of an 18 bp stem and a loop of 8 nucleotides (data not shown). An 133 bp sequence located 140 bp upstream of ORF 2 was found to be highly homologous to a sequence in the P102 gene (80% identity). One explanation for the 600 bp cloned fragment in plasmid pISM2136 is a recombination event between these two sequences with a deletion of the intervening sequences (Figure 12).

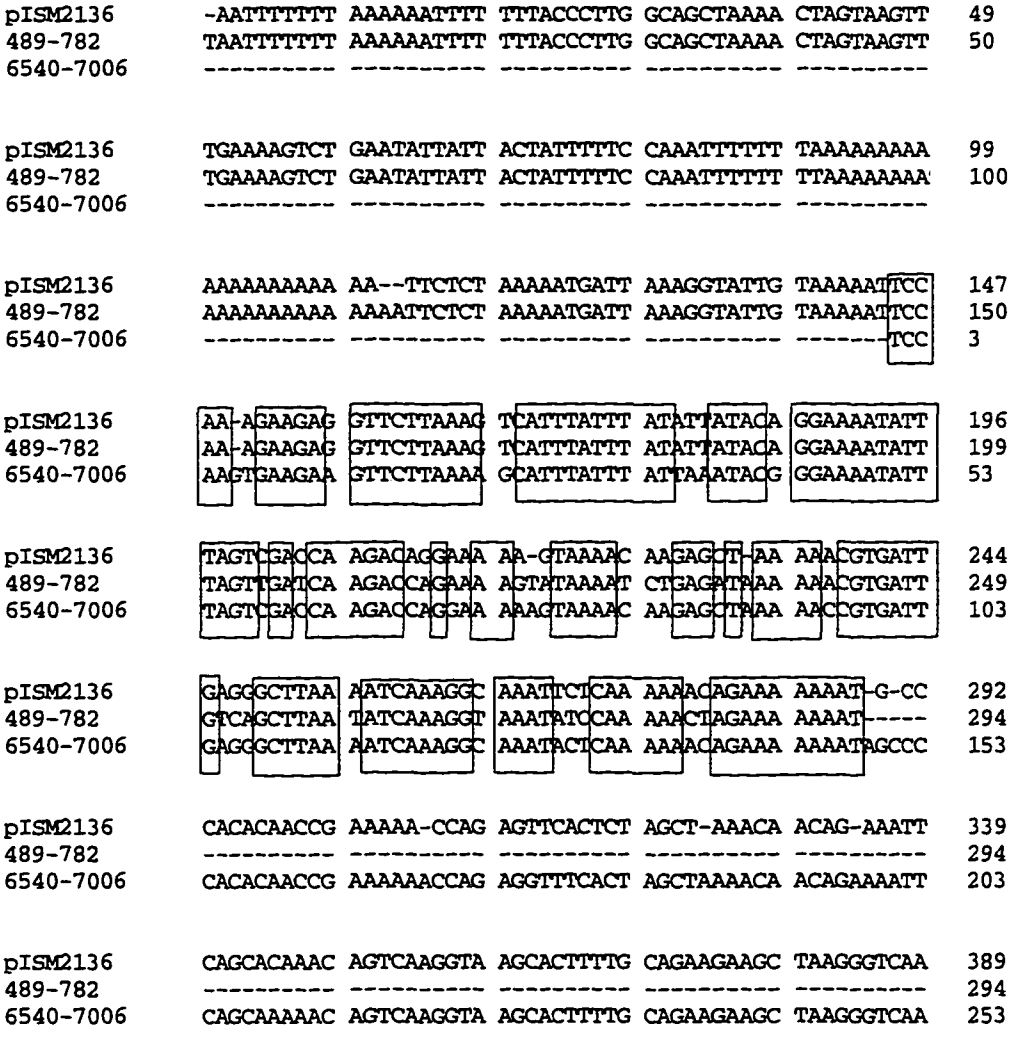

Figure 12. Analysis of the overlapping region between pISM2136 and the P97 contig. The region of overlap in the P97 contig was determined to be the regions consisting of base pairs 489-782 and 6540-7006 in the P97 contig DNA sequence. The regions of identity are shown by the boxes. The numbers on the right indicate the base pair number of the three regions being compared. Dashes indicate mismatched base pairs.

Mapping of P97 to the *M. hyopneumoniae* Genome

As a first step in determining if the P97 gene sequence is found in single or multiple copies in the *M. hyopneumoniae* chromosome, it was decided to map the location of P97 on a physical

genome map. This process was simplified by the studies of Huang and Stemke who had previously constructed a physical map of *M. hyopneumoniae* with the restriction enzymes *Apa*I, *Sno*I, and *Asp*718 (92). Following preparation of *M. hyopneumoniae* chromosomal DNA in SeaPlaque low melting temperature agarose blocks, the DNA was digested with *Apa*I and *Apa*LI, an isoschizomer of *Sno*I. Separation of the fragments was then accomplished by using CHEF pulsed field gel electrophoresis. After electrophoresis, the DNA was stained with ethidium bromide and visualized under UV light. The size of each restriction fragment was determined by using GelReader software (NCSA, Urbana-Champaign, Ill.). *Apa*I digestion gave rise to 6 bands in which the smallest 3 bands appeared to be doublets, resulting in a total of 9 fragments (Figure 13). *Apa*LI restriction digestion also gave rise to 9 restriction fragments in which the largest 2 fragments were doublets. The total calculated genomic size based upon *Apa*LI digests was 1050 kb, which was in good agreement with the published data (92). DNA in the pulsed field agarose gels was denatured and transferred to nylon membranes which were hybridized with probes derived from the P97 contig. Probe A consisted of the 1.75 kb *Eco*RV fragment of pISM2159. Probe B consisted of the 0.42 kb *Eco*RI fragment of pISM2139. Probe A and B both hybridized to the same *Apa*LI and *Apa*I fragments which we calculated to be 186 kDa and 141 kDa in size, respectively (Figure 13). This data indicates that the P97 operon is found within a 120-140 kb region of the chromosome based upon the published physical map (92). It could not be determined by this analysis if there were more than one copy of P97 in this region.

Screening of *M. hyopneumoniae* Library with pISM2136-Specific Probes

One possible explanation for the reactivity of Mab F1B6 with multiple bands on immunoblots (Figure 2, (264)) is the expression of modified copies of the P97 gene sequence or its Mab binding epitope in *M. hyopneumoniae*. This is a second explanation for the 615 bp insert found in plasmid pISM2136 which produces a polypeptide product that reacts with Mab F1B6. The basis for the reactivity of pISM2136 was not obvious once the DNA sequence was known, however. Adhesins or adherence-related genes from several mycoplasmas have been demonstrated to exist as multiple copies in the genome, which include *M. pneumoniae*, *M. genitalium*, *M. hominis* and *M. gallisepticum* (137, 178, 224, 265).

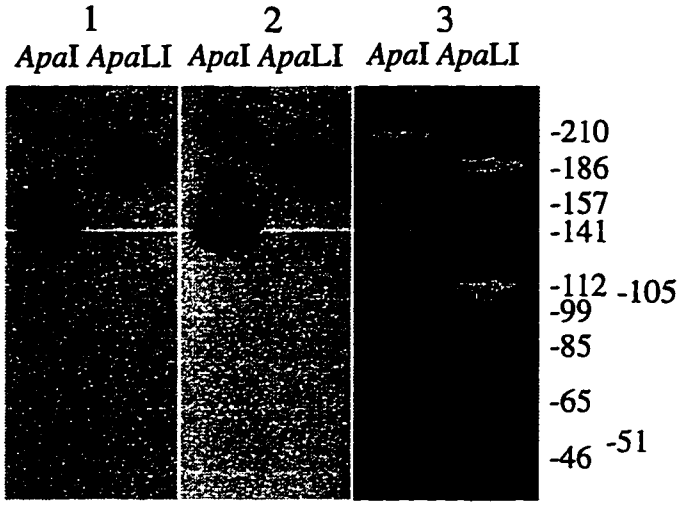

Figure 13. Mapping of the P97 operon sequences to *Apa*I- and *Apa*LI-digested chromosomal DNA of *M. hyopneumoniae*. Following CHEF electrophoresis of *Apa*I- and *Apa*LI-digested chromosomal DNA of *M. hyopneumoniae*, the DNA was transferred to nylon membranes and hybridized to P97 operon-specific probes. The restriction enzymes are indicated above the lanes. Panel 1, probe A: 1.75 kb *Eco*RV fragment of pISM2159; Panel 2, probe B: 0.42 kb *Eco*RI fragment of pISM2139; Panel 3, CHEF gel prior to DNA transfer. The fragment sizes are given in kilobases.

Since pISM2136 contained an internal *Sal*I site which is rare in the *M. hyopneumoniae* chromosome (Minion, unpublished), it was initially placed overlapping the *Sal*I site of the restriction map shown in Figure 1. DNA sequence analysis of both pISM2136 and the region of the P97 contig containing the *Sal*I site failed to support this idea, but there was substantial homology with sequences in this region to a portion of the pISM2136 insert (Figure 11). When the insert of pISM2136 was used as hybridization probe to *Eco*RI-digested *M. hyopneumoniae* chromosomal DNA (designated as pISM2136A in Table 1), three bands of 2.2, 3.3 and 4.2 kb were identified (Figure 14). When the insert was divided into two probes by digestion with *Eco*RV, *Pst*I, and *Sal*I resulting in 200 and 415 bp fragments, the hybridization patterns were distinctly different. The 200 bp probe recognized a single 3.3 kb band; the 415 bp fragment (designated as pISM2136C in Table 1) recognized bands of 2.2 and 4.2 kb strongly and a 3.3 kb fragment weakly (Figure 14). This was the first positive genetic evidence suggesting that the F1B6 Mab epitope might be found in multiple copies in the chromosome.

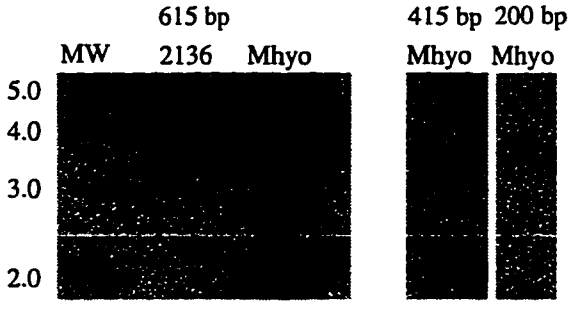

Figure 14. Hybridization analysis of *M. hyopneumoniae* *Eco*RI-digested chromosomal DNA with pISM2136-specific probes. *M. hyopneumoniae* chromosomal DNA was digested with *Eco*RI, separated on 1% agarose gels and blotted to a nylon membrane. The probes used to analyze the digests are indicated at the top of the autoradiograms. The molecular weight standards (MW) are shown on the left in kb.

When pISM2136 fragments were used to screen the *M.* hyopneumoniae genomic library, two groups of clones were obtained following rescue and restriction mapping (Figure 15). One group represented clones from the P97 contig region while the second group represented a distinctly different chromosomal region. None of the group 2 clones were recognized by the F1B6 Mab by immunoblot analysis (data not shown).

The final experiments with pISM2136 sequences to further delineate the origin of pISM2136 was PCR analysis of *M. hyopneumoniae* chromosomal DNA using primers designed to amplify an internal 539 bp fragment (TH127 and TH128). These primers failed to amplify genomic DNA in two different experiments, but did amplify the positive control DNA (pISM2136)(data not shown), suggesting that the genomic structure of the pISM2136 insert does not lie within the genome of *M. hyopneumoniae.*

Hybridization Analysis of *M. hyopneumoniae* 232A with P97 Internal Probes

In order to examine the possibility that multiple copies of P97 might be present in the *M. hyopneumoniae* chromosome, a hybridization study was undertaken using probes from various regions within the P97 operon. Probes 1 through 5 and probe 5.1 were isolated, radiolabeled and used to probe *M. hyopneumoniae* chromosomal DNA digested with restriction enzymes *Bgl*II, *Eco*RI, *Eco*RV, *Hin*cII, and *Hin*dIII (Figure 16). Digested chromosomal DNAs were separated on 0.4% agarose gels, transferred to nylon membranes, and hybridized with the ^{32}P-radiolabeled probes. Probe 1 hybridized to restriction fragments from *Eco*RI, *Eco*RV, and *Hin*dIII digestions as predicted by the restriction map shown in Figure 10. *Hin*cII digestion

gave rise to a 7.6 kb fragment, presumably resulting from the presence of a *Hinc*II site located upstream of P97 gene and outside the cloned region. Fragments hybridizing weakly to probe 1 were also observed. *Bgl*II digestion, however, gave rise to two fragments of equal intensity with apparent sizes of 10.5 kb and 14 kb (Figure 16).

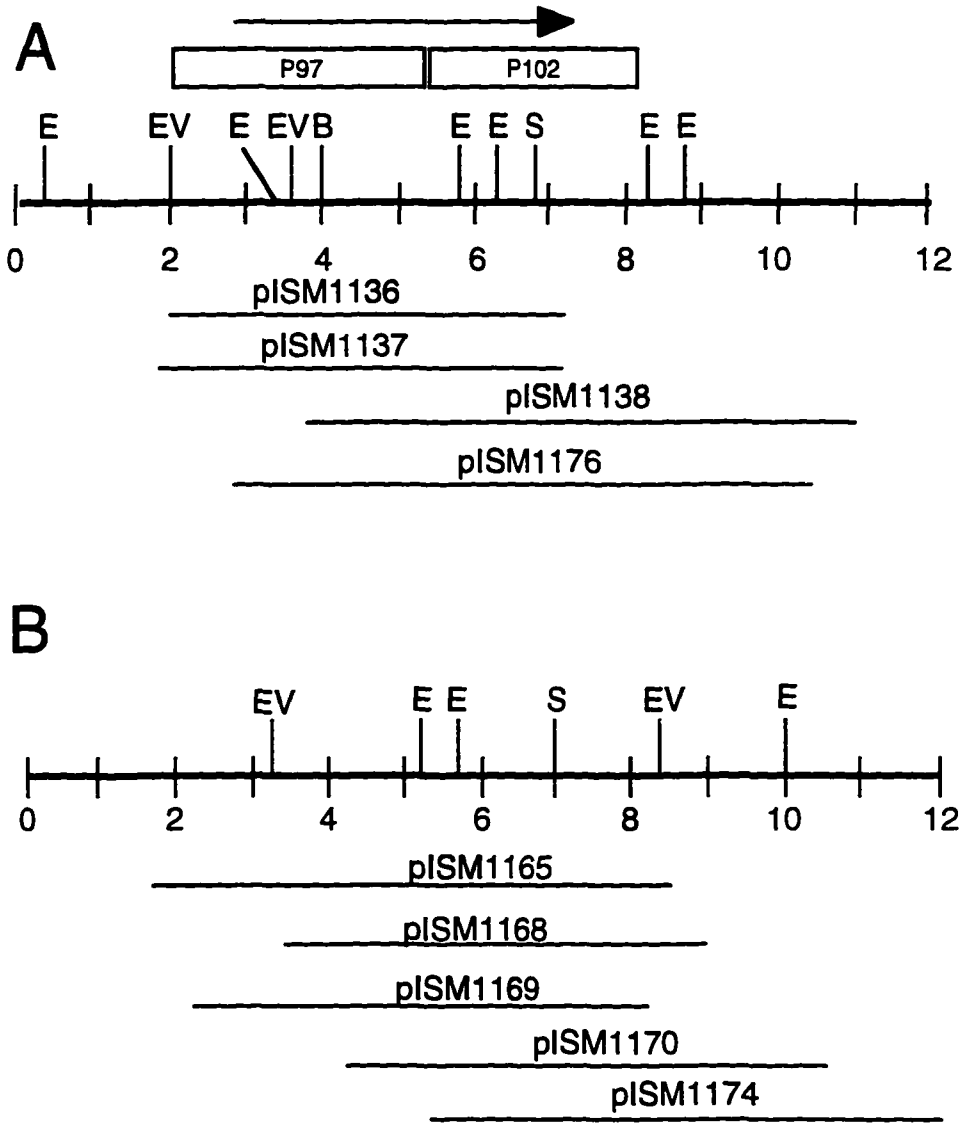

Figure 15. Restriction maps of clones identified with pISM2136-specific probes. A. Clones that overlap the P97 contig region (group 1). B. Clones that failed to overlap the P97 contig region. Plasmid numbers indicate clones that were identified using the 615 bp fragment (pISM1136 - pISM1138) or the 415 bp probe (plasmid numbers ≥ pISM1165). Sizes are given in kilobases.

Figure 16. Hybridization analysis of *M. hyopneumoniae* DNA with P97 operon-specific probes. The physical map of the P97 contig region is shown at the top of the figure. Restriction enzymes: B, *Bam*HI; E, *Eco*RI; EV, *Eco*RV; H, *Hin*dIII; Hc, *Hinc*II; K, *Kpn*I; P, *Pst*I; S, *Sal*I. The probes used in this analysis are shown below the physical map. Each panel represents hybridization with a single probe (shown at the top of the panel). Restricted enzyme digested chromosomal DNA: lane 1, *Hin*dIII; lane 2, *Hinc*II; lane 3, *Eco*RV; lane 4, *Eco*RI; lane 5, *Bgl*II. Lane 6 contains 6 ng of control plasmid DNA digested with the enzymes used to isolate the probe. Probes 1 – 3 were isolated from *Eco*RV – *Hin*dIII – *Nci*I-digested pISM1213 DNA. Probes 4, 5 and 5.1 were isolated from pISM2139 DNA digested with *Hinc*II – *Kpn*I (probe 4), *Hinc*II – *Nci*I – *Kpn*I (probe 5), or *Hinc*II – *Pst*I (probe 5.1). The size of each band was determined using GelReader software, and the sizes are indicated in kilobases.

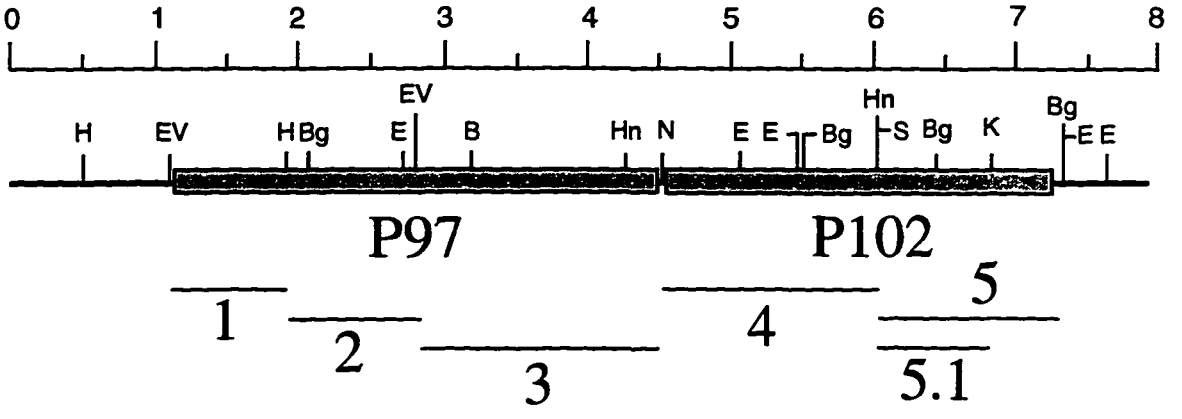
0 1 2 3 4 5 6 7 8
H EV HBg E EV B Hn N E E Bg Hn S Bg K Bg E E
P97
P102
1
2
3
4
5
5.1

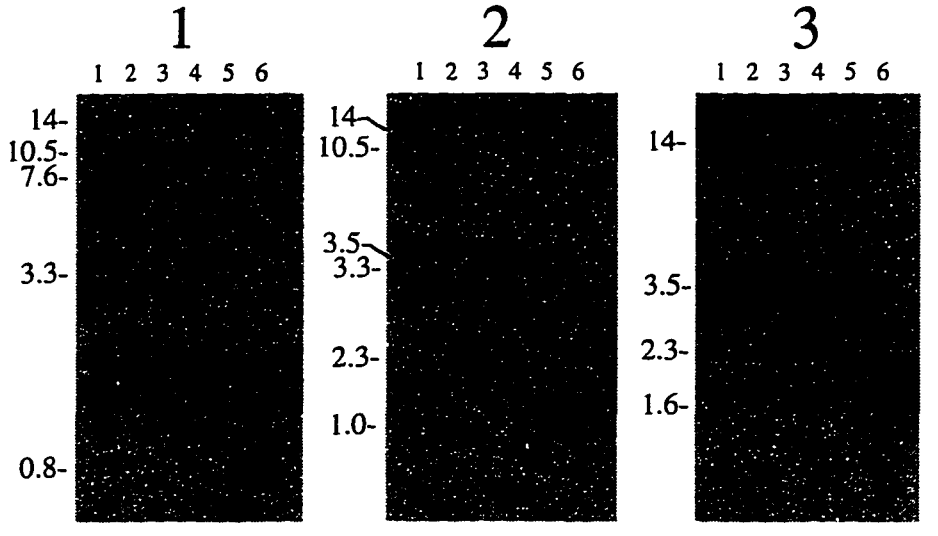
1
1 2 3 4 5 6
14-
10.5-
7.6-
3.3-
0.8-
2
1 2 3 4 5 6
14-
10.5-
3.5-
3.3-
2.3-
1.0-
3
1 2 3 4 5 6
14-
3.5-
2.3-
1.6-

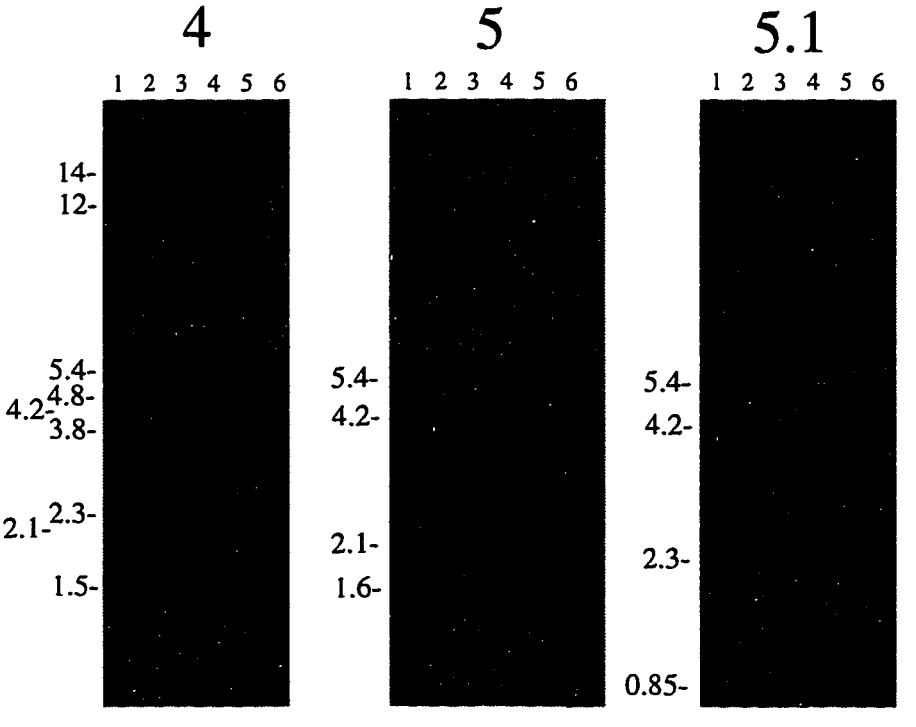
4
1 2 3 4 5 6
14-
12-
5.4-
4.8-
4.2-
3.8-
2.3-
2.1-
1.5-
5
1 2 3 4 5 6
5.4-
4.2-
2.1-
1.6-
5.1
1 2 3 4 5 6
5.4-
4.2-
2.3-
0.85-

Probe 2 also hybridized to fragments of the *Eco*RI-, *Eco*RV-, and *Hinc*II-digested *M. hyopneumoniae* chromosomal DNA as predicted according to the restriction map (Figure 8). *Hin*dIII digestion resulted in a 13.5 kb fragment recognized by probe 2, indicating the presence of a *Hin*dIII downstream of the cloned region. *Bgl*II digestion gave rise to two fragments strongly hybridized by probe 2, one of which (3.5 kb fragment), was predicted by the restriction map. A weakly hybridizing 10.5 kb fragment was also observed in the *Bgl*II lane with probe 2 which, according to the restriction map, should be the fragment containing the 5′ end of P97 gene and its upstream region which overlaps the probe 2 sequence by approximately 200 bp (Figure 16).

Probe 3 hybridized to a 14 kb *Bgl*II fragment, the same size as the larger fragment recognized by probes 1 and 2, in addition to the predicted 3.5 kb *Bgl*II fragment. Since probe 3 did not overlap the 1.75 kb *Eco*RV fragment within the P97 operon, a fragment containing the P102 gene sequences as well as other downstream sequences was observed. This fragment, which was larger than 16 kb, must result from the presence of a downstream *Eco*RV site outside the cloned region (Figure 16).

Probe 4 hybridized to 0.85 and 3.5 kb *Bgl*II fragments as predicted by the restriction map of the P97 operon and to the 14 kb fragment which was also recognized by probes 1, 2, and 3. However, probe 4 also hybridized to two *Bgl*II fragments of 3.0 and 7.5 kb along with several other fragments that were weakly hybridized. In the *Eco*RI digest, probe 4 recognized the 0.5, 2.2, and 2.3 kb fragments expected from the restriction map, but it also recognized three extra fragments of 3.8, 4.2, and 4.8 kb which was not observed with probes 1, 2, and 3. Hybridization of probe 4 to *Eco*RV-, *Hinc*II-, and *Hin*dIII-digested DNA also revealed extra bands that could not be accounted for from the restriction map of the P97 contig (Figure 16).

Interestingly, when probe 5 was hybridized to *Bgl*II -digested DNA, the 14 kb fragment was not recognized. Instead, a 7.7 kb fragment was weakly recognized. According to the restriction map, probe 5 should recognize two *Bgl*II fragments of 0.9 (weak) and 1.3 kb (strong). However, the 0.9 kb fragment hybridized strongly to probe 5, while the 1.3 kb fragment showed a weak hybridization. A 2.2 kb *Eco*RI fragment was hybridized by probe 5 as expected based on the restriction map, but a 4.2 kb *Eco*RI fragment was also recognized. *Eco*RV and *Hin*dIII digests had similar hybridization patterns when using probes 4 and 5. A 5.4 kb *Eco*RV fragment, and 5.2 and 12.1 kb *Hin*dIII fragments could not be accounted for by the restriction map. *Hinc*II digestions gave rise to two fragments (1.8 and 8.2 kb) with probe 5. The P102 internal probe 5.1 had an identical reaction pattern to probe 5.

Hybridization of Chromosomal DNAs of Six *M. hyopneumoniae* Strains With P97 Operon Internal Probes

Zhang et al. demonstrated variation in the ciliary binding activities of different *M. hyopneumoniae* strains (264). To explain this variation, an examination of the P97 operon structure of six *M. hyopneumoniae* strains was performed. These strains included the wild type strain 232A, three 232A clonal isolates that exhibited high (232A.H), medium (232A.M), and low (232A.L) ciliary binding activity, an avirulent strain J and a virulent strain 144L. Strain 144L had previously been shown to express a smaller P97 protein by immunoblot, but it had high ciliary binding activity (264). The *Bgl*II- and *Eco*RI -digested chromosomal DNAs from these strains were hybridized to probes 1 - 5 representing different regions of the P97 contig.

*Bgl*II-digested genomic DNA from the six *M. hyopneumoniae* strains gave almost identical hybridization patterns with probes 1 through 4 (Figure 17). There existed a few differences, however. The 14 kb *Bgl*II fragment in strain 232A hybridized strongly with probes 1 through 4, but weakly in clonal strains 232A.H, 232A.M, 232A.L. Hybridization with DNA from strains J and 144L demonstrated a higher degree of variability as compared to strain 232A. The 10.5 and 14 kb *Bgl*II fragments seen in strain 232A when hybridized with probes 1 and 2 were replaced by two smaller fragments of 8 kb and 11.5 kb in strain 144L. The major 14 kb *Bgl*II band observed in 232A DNA by probes 1–4 was weakly recognized in all of the 232A clonal isolates and was barely detectable in strains J and 144L. Strain J differed from other strains in its hybridization patterns with probes 1 and 2; a 8.2 kb *Bgl*II fragment, rather than one of 10.5 kb, was recognized. With *Bgl*II-digested DNAs, strains J and 144L had similar hybridization patterns with probes 4 and 5, but J lacked the 7.2 kb *Bgl*II fragment observed in other strains with probe 5.

With *Eco*RI-digested DNAs, there was a large similarity between the six strains in their hybridization patterns except for the following differences (Figure 17). A 5.2 kb *Eco*RI fragment from 232A that was barely detectable with probes 1–3, hybridized more strongly with DNA from 232A.H, 232A.M, 232A.L, and was absent in strain J. Probe 4, which contained the 5′ end of P102, recognized two bands of similar size in J and 144L to those of the 232A derivatives, but two other bands were missing and a smaller fragment was present in both strains. For probe 5, the hybridization pattern for both J and 144L were similar to each other, but completely different from 232A and its clonal siblings.

Figure 17. Analysis of six *M. hyopenumoniae* strains for P97 contig–specific sequences. Hybridization was performed on *Bgl*II and *Eco*RI restricted genomic DNAs from six different *M. hyopneumoniae* strains. Each letter represents two blots developed with a specific probe; A, probe 1; B, probe 2; C, probe 3; D, probe 4; E, probe 5; F, R1-specific probe. Each probe was hybridized to *Bgl*II- (left panel) and *Eco*RI- (right panel) digested DNAs: lane 1, 232A (L); lane 2, 232A (M); lane 3, 232A (H); lane 4, 144L; lane 5, J; lane 6, 232A; lane C, control plasmid DNA (see legend to Figure 16 for a description). Sizes of important fragments are given in kilobases.

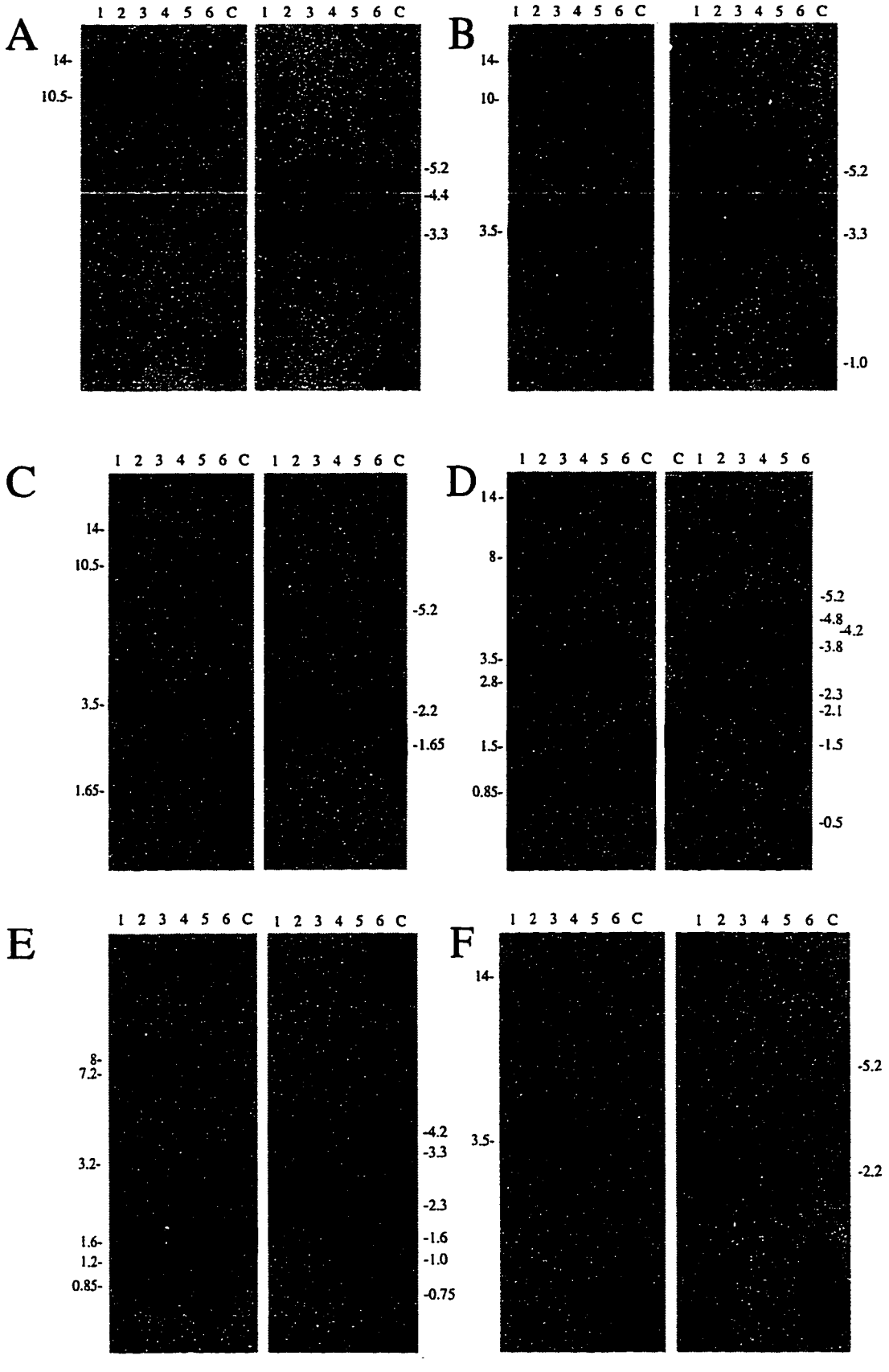
A
1 2 3 4 5 6 C 1 2 3 4 5 6 C
14-
10.5-
-5.2
-4.4
-3.3
B
1 2 3 4 5 6 C 1 2 3 4 5 6 C
14-
10-
3.5-
-5.2
-3.3
-1.0
C
1 2 3 4 5 6 C 1 2 3 4 5 6 C
14-
10.5-
3.5-
1.65-
-5.2
-2.2
-1.65
D
1 2 3 4 5 6 C C 1 2 3 4 5 6
14-
8-
3.5-
2.8-
1.5-
0.85-
-5.2
-4.8
-4.2
-3.8
-2.3
-2.1
-1.5
-0.5
E
1 2 3 4 5 6 C 1 2 3 4 5 6 C
8-
7.2-
3.2-
1.6-
1.2-
0.85-
-4.2
-3.3
-2.3
-1.6
-1.0
-0.75
F
1 2 3 4 5 6 C 1 2 3 4 5 6 C
14-
3.5-
-5.2
-2.2

Mapping of the P97 Mab F1B6 Antigenic and Ciliary Binding Epitopes

Once the P97 gene sequence had been obtained and the role of its product in ciliary binding confirmed, studies were performed to map both the Mab F1B6 binding epitope and the cilium binding site on the gene sequence. Both analyses were begun by insertional mutagenesis of plasmid pISM2159 followed by analysis of the resulting recombinant gene product in *E. coli*. Mutagenized pISM2159 plasmids were isolated, and the Tn*1000* insertions were mapped by restriction digests. The exact location of the Tn*1000* insertion was determined by DNA sequencing using Tn*1000* end-specific primers. Selected plasmids were transformed into *E. coli* ISM612, the transformants were induced, and the lysates were examined for reactivity with Mab F1B6 by immunoblot and for ciliary binding activity.

Immunoblot analysis with lysates from a series of Tn*1000* insertions in pISM2159 showed that transposon insertions at or upstream of pISM2159::Tn*1000.79* (bp 2476 of P97) failed to express Mab F1B6-reactive antigens (Figure 18). Plasmids with Tn*1000* inserts at or downstream of pISM2159::Tn*1000.*133 retained the ability to produce Mab F1B6 reactive proteins. These two inserts are separated by 62 bp, which corresponds to amino acids 830 to 850. Within this amino acid sequence is the AAKP(E/V) (R1) repeated sequence (Figure 19). The Mab epitope appears to be within the R1 repeat and requires at least 2.5 repeating units.

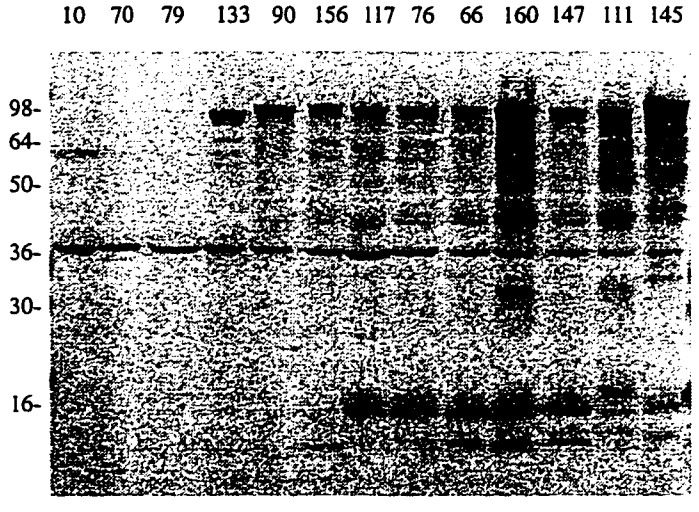

Figure 18. Mapping the P97 F1B6 Mab binding epitope by immunoblot using Tn*1000* insertions in pISM2159. Whole cell antigens were prepared from recombinant *E. coli* as described in Materials and Methods. The proteins were resolved on a 10% polyacrylamide (3 µg per lane), and the resulting blot was developed with Mab F1B6. The lane numbers indicate the number of the Tn*1000* insertion (Figure 18; number 10 location is shown in Figure 3). The molecular weight markers are shown in adjacent lanes and the sizes are indicated in kDa.

Figure 19. Location of Tn*1000* insertions used to identify the Mab epitope and the ciliary binding site of P97. The data is given as translated amino acid sequence. Sequence numbers are from the P97 DNA sequence given in Figure 4. Arrows indicate transposon insertion locations. The transposon insert number is given above each arrow. The underline indicates the first repeat (R1); the hatched underline indicates the second repeat (R2).

```
                 *2340               *2355                *2370               *2385              *2400
S  F  E  A  I    K  K  G  E  T    T  K  E  G  K    R  E  E  V  D    K  K  V  K  E>

                 *2415     70 ↓      *2430                *2445               *2460              *2475
L  D  N  K  I    K  G  I  L  P    Q  P  P  A  A    K  P  E  A  A    K  P  V  A  A>
                                       ___________________________________________

79 ↓             *2490               *2505                *2520               *2535  133 ↓       *2550
K  P  E  T  T    K  P  V  A  A    K  P  E  A  A    K  P  E  A  A    K  P  V  A  A>
_________________________________________________________________________________

                 *2565               *2580                *2595               *2610         90 ↓ *2625
K  P  E  A  A    K  P  V  A  A    K  P  E  A  A    K  P  V  A  A    K  P  E  A  A>
_________________________________________________________________________________

                 *2640 156 ↓         *2655                *2670 ↓66,76 117 ↓160 *2685      147 ↓ *2700
K  P  V  A  A    K  P  E  A  A    K  P  V  A  T    N  T  G  F  S    L  T  N  K  P>
_____________________________________________

   111 ↓         *2715               *2730                *2745               *2760              *2775
K  E  D  Y  F    P  M  A  F  S    Y  K  L  E  Y    T  D  E  N  K    L  S  L  K  T>

                 *2790               *2805                *2820               *2835              *2850
P  E  I  N  V    F  L  E  L  V    H  Q  S  E  Y    E  E  Q  E  I    I  K  E  L  D>

                 *2865               *2880                *2895               *2910              *2925
K  T  V  L  N    L  Q  Y  Q  F    Q  E  V  K  V    T  S  D  Q  Y    Q  K  L  S  H>

                 *2940               *2955                *2970               *2985              *3000
P  M  M  T  E    G  S  S  N  Q    G  K  K  S  E    G  T  P  N  Q    G  K  K  A  E>
                 _ _ _ _ _ _ _ _ _ _ _ _ _ _ _ _ _ _ _ _ _ _ _ _ _ _ _ _ _ _ _ _ _ _

                 *3015               *3030                *3045               *3060              *3075
G  A  P  N  Q    G  K  K  A  E    G  T  P  N  Q    G  K  K  A  E    G  A  P  S  Q>
_ _ _ _ _ _ _ _ _ _ _ _ _ _ _ _ _ _ _ _ _ _ _ _ _ _ _ _ _ _ _ _ _ _

   145 ↓         *3090               *3105                *3120               *3135              *3150
Q  S  P  T  T    E  L  T  N  Y    L  P  D  L  G    K  K  I  D  E    I  I  K  K  Q>
```

Microtiter plate adherence assays were performed with *E. coli* lysates to locate the P97 ciliary binding epitope by using the series of Tn*1000* insertions in pISM2159. Lysates prepared from pISM2159::Tn*1000*.70 and pISM2159::Tn*1000*.133 failed to bind to cilia, whereas lysates prepared from pISM2159::Tn*1000*.90 and those downstream of pISM2159::Tn*1000*.90 showed ciliary binding activity (Figure 20). The two inserts pISM2159::Tn*1000*.133 and pISM2159::Tn*1000*.90 are separated by 75 bp. The corresponding amino acid sequence is within the first repeat between repeats 8 and 12 in the 15 repeat sequence (Figure 19).

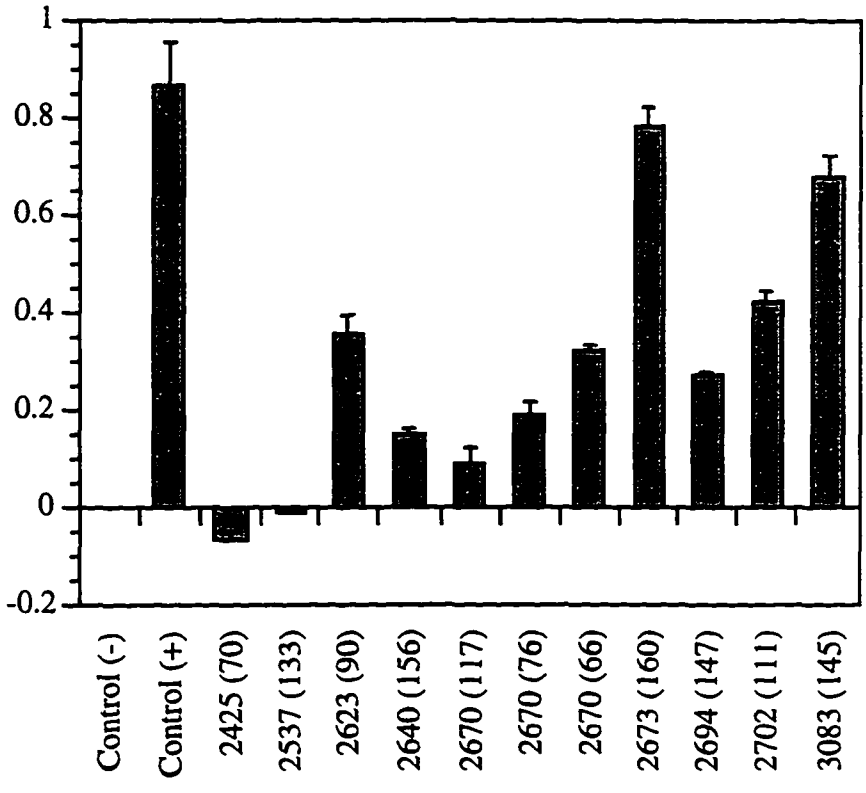

Figure 20. MPAA analysis of Tn*1000* insertions in P97. Lysates were prepared from ISM612 (pISM2159::Tn*1000*) strains and tested in the MPAA assay as described in the Materials and Methods. The data are represented as mean ± standard error of triplicate wells. Numbers refer to the position of the Tn*1000* insertion in the P97 DNA sequence. The transposon number is given in parentheses and corresponds to the number shown in Figure 18.

Analysis of *M. hyopneumoniae* Strains with a R1-Specific Probe

Once the P97 Mab F1B6-reactive epitope was mapped to the first repeat region of P97, it was of interest to test the hypothesis that other proteins in the *M. hyopneumoniae* genome had the same or similar repeat sequence, thus explaining the complex immunoblot banding pattern with Mab F1B6. The two PCR primers TH120 and TH121 were used to prepare a radioactive PCR product using *M. hyopneumoniae* DNA as template, and hybridized to *Bgl*II- and *Eco*RI-digested genomic DNA from *M. hyopneumoniae* strains 232A, J, 144L, and the 232A clonal derivatives 232A.H, 232A.M, and 232A.L.

The R1-specific probe hybridized to the 3.5 kb *Bgl*II fragment from all 6 strains of *M. hyopneumoniae* as expected from the restriction map of the P97 operon contig, although the hybridization was weak for both J and 144L strains (Figure 17). The R1 probe also hybridized to the 14 kb *Bgl*II fragment in all strains except for strain J. The signal strength of strain 232A was strong compared to those of the 232A clonal isolates although equal amounts of DNA was loaded in each lane of the gel. The R1 probe hybridized strongly to the 2.3 kb *Eco*RI fragments from strains 232A and its derivatives, but only weakly with those from strains J and 144L. Weak hybridization was observed with an *Eco*RI fragment of approximate 5.2 kb derived from strains 144L, 232A.H, 232A.M, and 232A.L, but not with strains 232A and J.

Analysis of Size Variation in the P97 Repeat Regions by PCR Analysis

Zhang et al. demonstrated size variation in P97 adhesins among different isolates of *M. hyopneumoniae* (264). The presence of two repeated sequences, R1 and R2, at the carboxy end of P97 suggested that there might be a relationship between the size of these repeat regions in different strains and the resulting size of the P97 product. To study this, two primer pairs (TH120/TH121 for amplification of R1 and TH122/TH123 for amplification of R2, respectively) were used. Chromosomal DNA from *M. hyopneumoniae* 232A, J, and 144L strains were isolated and used in PCR amplification with these two primer pairs. Figure 20 shows the results of this study. *M. hyopneumoniae* 232A gave rise to a product of the R1 region 57 bp larger than that of strain 144L, which in turn was 22 bp larger than that of strain J. On the contrary, amplification of R2 from strain J produced a fragment 23 bp larger than that from strain 144L which was 7 bp larger than that from strain 232A (Figure 21).

DNA Sequence Analysis of the P97 Repeat Sequence R1 in Different Strains

Zhang et al. had previously shown that *M. hyopneumoniae* exhibited variable ciliary binding activity among different strains (264). Analysis of the P97 sequence for the cilia binding epitope by transposon mutagenesis indicated that it was located within the central

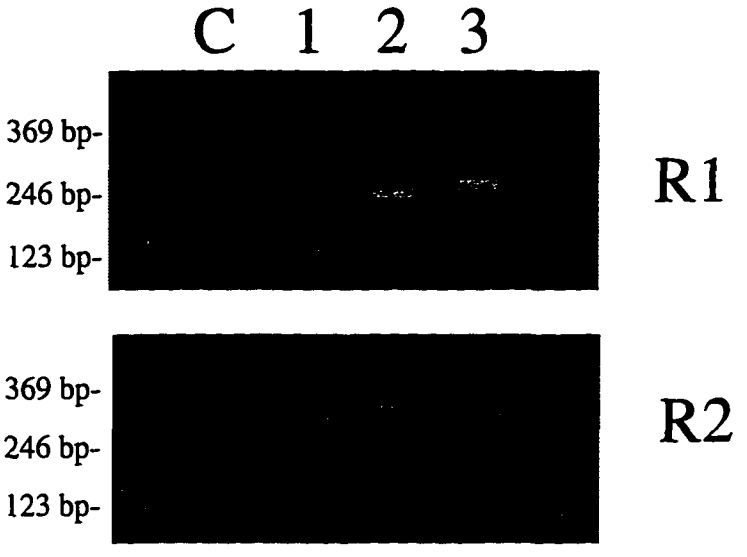

Figure 21. Analysis of size variation in the P97 repeat regions by PCR analysis. The bands represent PCR products produced from template DNA from different *M. hyopneumoniae* strains. Lane 1, strain 232A; lane 2, strain J; lane 3, strain 144L, lane C, no template DNA control. R1, repeat region 1 amplified with primer set TH120/TH121; R2, repeat region 2 amplified with PCR primer set TH122/TH123.

portion of the first repeat region. None of the strains analyzed above by PCR lacked the R1 repeat region and all of the strains seemed to have sufficiently large regions to code for the epitope. Another hypothesis was that the repeat sequence was modified to create a missense or loss of function mutation. This was addressed by amplifying the region of P97 containing both repeat regions of different strain chromosomal DNAs and analyzing the PCR products by DNA sequencing. The primers TH120 (upper primer for R1) and TH123 (lower primer for R2) were used for these studies. Following gel purification, the PCR products were sequenced using the TH120 primer and the sequences analyzed. The R1 sequences exhibited a high degree of sequence homology among the six strains analyzed some of which lacked cilia binding activity (J and 232 (L)). All 6 strains retained the AAKP(V/E) R1 repeat sequences. Only 10 and 11 repeats were observed in strain J and 144L, respectively, while strain 232A and its derivatives had 15 repeats (Figure 22).

```
232A P97 AA     KGILPQPPAA KPEAAKPVAA KPETTKPVAA KPEAAKPEAA KPVAAKPEAA   50

232A            KGILPQPPAA KPEAAKPVAA KPETTKPVAA KPEAAKPEAA KPVAAKPEAA   50
232A.H          KSILPQPPAA KPEAAKPVAA KPETTKPVAA KPEAAKPEAA KPVAAKPEAA   50
232A.M          KGILPQPPAA KPEAAKPVAA KPETTKPVAA KPEAAKPEAA KPVAAKPEAA   50
232A.L          KSILPQPPAA KPEAAKPVAA KPETTKPVAA KPEAAKPEAA KPVAAKPEAA   50
J               KSILPQPP-- ---------- --------AA KPEAAKPVAA KPEAAKPETT   30
144L            KGILPQPP-- ---------- --------AA KPEAAKPVAA KPVAAKPEAA   30


232A P97 AA     KPVAAKPEAA KPVAAKPEAA KPVAAKPEAA KP-VATNTGF SLTNKPKEDY   99

232A            KPVAAKPEAA KPVAAKPEAA KPVAAKPEAA KP-VATNTGF SLTNKPKEDY   99
232A.H          KPVAAKPEAA KPVAAKPEAA KPVAAKPEAA KP-VATNTGF SLTNKPKEDY   99
232A.M          KPVAAKPEAA KPVAAKPEAA KPVAAKPEAA KP-VATNTGF SLTNKPKEDY   99
232A.L          KPVAAKPEAA KPVAAKPEAA KPVAAKPEAA KP-VATNTGF SLTNKPKEDY   99
J               KPVAAKPEAA KPVAAKPVAA KPVATN---- ---TNTNTGF SLTNKPKEDY   73
144L            KPVAAKPEAA KPVAAKPEAA KPVAAKPVAT NTNTNTNTGF SLTNKPKEDY   80


232A P97 AA     FPMAFSYKLE YTDENKLSLK TPEINVFLEL VHQSEYEEQE IIKELDKTVL   149

232A            FPMAFSYKLE YTDENKLSLK TPEINVFLEL VHQSEYEEQE IIKELDKTVL   149
232A.H          FPMAFSYKLE YTDENKLSLK TPEINVFLEL VHQSEYEEQE IIKELDKTVL   149
232A.M          FPMAFSYKLE YTDENKLSLK TPEINVFLEL VHQSEYEEQE IIKELDKTVL   149
232A.L          FPMAFSYKLE YTDENKLSLK TPEINVFLEL VHQSEYEEQE IIKELDDTVL   149
J               FPMAFSYKLE YTDENKLSLK TPEINVFLEL VHQSEYEEQK IIKELDKTVL   123
144L            FPMAFSYKLE YTDENKLSLK TPEINVFLEL VHQSEYEDQK IIKELDKTVL   130


232A P97 AA     NLQYQFQ  156

232A            NLQYQFQ  156
232A.H          NLQYQFQ  156
232A.M          NLQYQFQ  156
232A.L          NLQYQFQ  156
J               NLQYQFQ  130
144L            NLQYQFQ  137
```

Figure 22. Sequence comparison between the P97 R1–R2 region of six *M. hyopneumoniae* strains. Amino acid sequence alignment between the original strain 232A P97 sequence (Figure 4) and the PCR products of 232A, its single colony isolates 232A.L, 232A.M, and 232A.H, strains J and 144L. The alignment was generated using DNA sequence information obtained from PCR products with primers flanking the R1/R2 region of P97.

Analysis of Clones Overlapping the Second Chromosomal Copy of P102

Since the hybridization data indicated that *M. hyopneumoniae* contained at least one additional copy of the P102 gene sequence (Figure 16), the cloning of this region was undertaken. *Eco*RI digests of *M. hyopneumoniae* chromosomal DNA were resolved on agarose gels, the regions of the gel representing the 3.8 and 4.2 kb fragments were excised, and the DNA was isolated. These fragments were then cloned into pSK- as described in the Materials and Methods. Probe number 4, which contained the 5′ half of P102 (Figure 16), was then used in colony hybridization (195) to identify the appropriate recombinant plasmids containing the P102 sequence. Two plasmids, pISM1232 and pISM1233, were identified, restriction mapped, and the ends of the cloned fragments were subjected to DNA sequencing. A sequencing primer was used to obtain additional sequence information of the 3′ end of pISM1232. The sequence obtained was then aligned to the P97 contig sequence using MacVector software. Figure 22 shows the results of this study. Restriction site mapping of the two cloned fragments, 3.8 and 4.2 kb, suggested that these two clones are from the same chromosomal region as the five clones identified with the pISM2136 probe (Figure 15). The DNA sequence of the 3′ end of pISM1232 and the 5′ end of pISM1233 aligned perfectly with the P102 sequence, but ended abruptly at the 3′ end of the P97 gene sequence. The 5′ end of pISM1232 showed no homology with the P97 gene or any other known sequence. The 3′ end of pISM1233 had homology with the heat shock protein Clp.

Figure 23. Analysis of clones overlapping the second chromosomal copy of P102. The *M. hyopneumoniae* 3.8 and 4.2 kb *Eco*RI fragments identified by probe 4 (Figure 16) were cloned, restriction mapped, and the ends of each fragment were sequenced. The physical map of the P97 contig is shown as a reference along with the direction of transcription (large arrow), and the P97 and P102 gene boundaries. The physical maps of clones pISM1232 and pISM1233 are shown below the P97 contig map. The 5′ and 3′ ends of the plasmids are relative to the orientation of P102. The sequence information derived from these two plasmids are indicated by the smaller arrows. The boxes above the second P102 copy indicate alignment results of the DNA sequence information. The open boxes indicate almost perfect alignment with P102 sequences, the black boxes indicate no sequence homology with known sequences, and the hatched boxes indicate no sequence information available. The actual sequence alignment is shown at the bottom of the figure. The end of the P97 sequence is indicated as well as *Eco*RI sites (E) used for cloning, the *NciI* site (N) which lies between P97 and P102 in the P97 operon, and the *SalI* site (S) that has been modified in the second copy of P102. Also shown are the *Eco*RV sites (EV). The upper sequence is from the P97 operon. The sequence alignment is indicated in the lower sequence as follows: capital letters indicate agreement and small letters indicate no match in the 3′ end of P97, periods indicate perfect alignment with P97 operon sequences. No sequence information is available for the small 422 bp region between the two *Eco*RI sites within the second P102 copy.

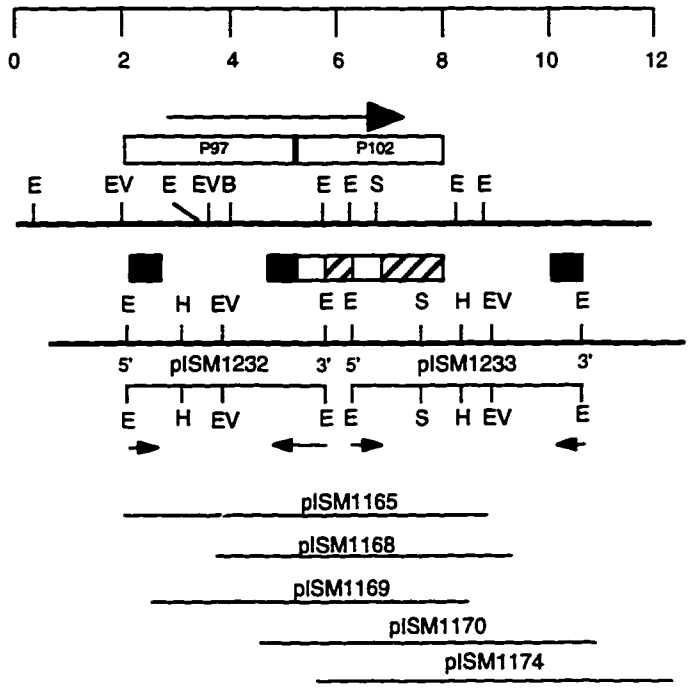


```
          *         *         *         *         *         *         *         *
GATGCTAAATTGCTATACTTTATCCTAAGGGATGATTCAAAATCCGGTGATCCTAAAAAATCAAGTCTAAAAGTTAAAAT   5040
agTaCaAAAaaaacAaAaaaaAggtTAtaattTGAaTatAtAagacaaGcaaaTttccccctttgCagttcaaTAAAAa
                                  end of P97      NciI
AACAGTAAAACAAAGTAATAATAATCAGGAACCAGAATCTAAATAAAACCCGCAGGTATTTATCCTATGAAGTTAGCAAA   5120
ActttTtAcAgtAAaTtgccAccAT-AatccCCtc.....................................................>

ATTACTTAAAAAACCTTTTTGATTAATAAC......<450 bp of identical sequence>.....................   5200
.......-.....................................................................................>
                                                                          EcoRI
TTTTAGTCAAATTGATTCAAGCAAGTCTTTTGTTGATCTTTCAAGAGCAAATCTAACTTTGATGGAATTCCAAATTTTGC   5680
......c.....................................g.............c.......__________

TTGCCCAAAATTTTGAAAATGAAAGAGGAAGTAATTGATTTTCACGACTTGAAAGAGCTTTGGTTGCATCAAAAGCGAGT   5760

CTTTCACTTTATAATTCCTTAGGAGAACCCGTATTTTTAGGCCCAGATTATCAATTAGACCCAGTTTTGGACCGAAAAAA   5840

ATTATTAACTTTGTTAAATAAAGATGGAAAATTAGTTCTTGGACTTAATTTAGTGCAAATTTCAACTAAAAAAACTATGA   5920

ATTTAAATCTTGAAGTTCGCGGCGCGATTTCAAATCAGGAAATTTCTAAAATTCTAAAATCCTGACTTGAAACAAATCTT   6000

CAAGGCAAATTAAAAACCAAAGATGATTTGCAAATGGCACTAGTAAAAGATAAAATTAGCCTCTCTGATTATTGATATGG   6080
      EcoRI
ATCTCCGAATTCAAAAGTAAATACATCCCAAA...<450 bp of identical sequence>.....................   6160
_____.....................................................................................>
                                        SalI*
AAGCATTTATTTATTAAATACGGGAAAATATTTAGTCGACCAAGACCAGGAAAAAGTAAAACAAGAGCTAAAAACCGTGA   6640
.....................................t.....................................................>
```

DISCUSSION

General Discussion

M. hyopneumoniae colonization of the swine trachea occurs by attachment directly to the cilia of the tracheal epithelial cells (144, 268). The attachment is mediated by specific *M. hyopneumoniae* surface proteins, adhesins (264). The adhesins appear to bind specifically to receptor molecules on the swine cilia and not to the epithelial cell bodies. Non-adherent strains of *M. hyopneumoniae* are avirulent (Ross, R. F., and T. F. Young, unpublished). Therefore, the ciliary adhesin(s) appear to be a crucial virulence factor for *M. hyopneumoniae* pathogenesis. Previous studies have suggested that the *M. hyopneumoniae* surface protein P97 functions as the cilium adhesin (264, 267). To examine this hypothesis more thoroughly, this study was undertaken.

In the study reported here, a molecular and functional analysis of the P97 protein was performed to further characterize its adhesive properties and potential role in ciliary adherence in vivo. To accomplish this, the P97 gene was cloned and expressed in *E. coli*. The recombinant protein (rP97) was then examined for its ability to bind to purified swine cilia. The results of this study show that P97 can bind to swine cilia, and its binding mimics the binding characteristics of intact *M. hyopneumoniae* in the MPAA. The latter was established by inhibition assays showing that rP97 binding to cilia was inhibited by the sulfated polysaccharides heparin, fucoidan, and mucin in a similar manner to that observed with whole cells of *M. hyopneumoniae*. This is the first reported functional analysis of a cloned mycoplasmal gene in *E. coli* and represents a significant advance in mycoplasmal research.

These results do not directly link P97 with ciliary adherence of *M. hyopneumoniae* in vivo, however. For instance, it was not possible to explain the discrepancy between the lack of ciliary adherence in strains J and 232A.L with either the expression of P97 in these strains or with changes in the ciliary binding site as defined by these studies. Further analysis will be required to either introduce mutations in P97 in *M. hyopneumoniae* or link other proteins to the ciliary adherence phenotype. These results, however, do support the hypothesis that P97 is involved in ciliary adherence, possibly as the major adhesin, since rP97 has ciliary adhesive properties.

The expression of P97 in ISM612 resulted in production of multiple proteins recognized by Mab F1B6 in immunoblot analysis. The largest protein had an apparent molecular weight of 124.9 kDa which correlated well with the predicted size of P97 (Figure 2). Other smaller F1B6-reactive proteins are either prematurely truncated P97

proteins because of the presence of UGA codons in P97 gene, or are the result of aberrant initiation of translation at sites other than the ATG start codon of P97. This could be due to the high AT content of mycoplasmal genomic DNA that could serve as ribosome binding sites. Tn*1000* mutagenesis proved to be the essential genetic tool in the molecular characterization of rP97. The minimum coding sequence of P97 in cloned fragments was determined, DNA sequencing was facilitated, and the antigenic and cilia binding epitopes of P97 were mapped all by the use of Tn*1000* mutagenesis.

Sequence analysis of the P97 gene contig region also suggests that P97 belongs to a two gene operon, designated the P97 operon. The second gene which lies downstream of P97 codes for a putative surface protein with a predicted molecular weight of 102 kDa. Screening of a *M. hyopneumoniae* genomic Lambda ZAP® II library with P97 operon-specific internal DNA probes revealed that P97 operon sequences are present in no more than two copies in the *M. hyopneumoniae* chromosome. Mutation of P97 gene sequences with Tn*1000* followed by immunoblot and MPAA analysis of the mutagenized plasmids was used to identify the Mab F1B6 antigenic and cilia binding epitopes in the rP97 protein.

Sequence and Functional Analysis of the P97 Adhesin

Immunoblot analysis of Tn*1000* mutagenized pISM2121 plasmids under IPTG induction in *E. coli* ISM612 revealed that transposon insertions in a 2.2 kb region resulted in the loss of expression of Mab F1B6-reactive proteins, or as in the case of insert 16.13, resulted in the production of a protein with reduced size. Therefore, this 2.2 kb region in pISM2121 represents the minimum coding sequence of the P97 structural gene. This study also suggested that the F1B6 antigenic epitope is located in the region between inserts 16.13 and 1.14 (Figure 2). DNA sequencing of this region using Tn*1000*-specific primers revealed a 3.3 kb ORF with a protein coding capacity for a 124.9-kDa protein. This study indicated that P97 underwent post-translational processing because the amino terminal amino acid sequence of the native P97 protein was mapped to position 195 of the P97 amino acid sequence. The cleavage of P97 protein at the putative processing site results in a protein with a predicted molecular weight of 102 kDa which is in good agreement with the size of the native P97 protein by SDS-PAGE. A protein kinase ATP binding domain was also identified in an amino terminal transmembrane domain. It is still unknown whether this processing event is required for the translocation of the protein to the mycoplasmal surface and if it is dependent on the binding of ATP.

Analysis of the predicted amino acid sequence of P97 demonstrated that the protein is highly hydrophilic, which confirmed the findings by Ross and Young. They found that native

P97 partitioned in the aqueous (hydrophilic) phase in Triton X-114 extracts of *M. hyopneumoniae* proteins or was found in the insoluble portion (Ross, R.F., and T. F. Young, personal communication). Immunoelectron microscopic studies of *M. hyopneumoniae* with anti-P97 Mabs revealed a translucent space between the gold beads and the mycoplasma membrane, suggesting that P97 was not directly associated with the membrane surface, but was possibly linked to the membrane by an electron translucent structure such as a glycocalyx. This could not occur through cysteine linkages since P97 lacks cysteine residues. P97 would function as the bridge between *M. hyopneumoniae* and the host epithelial cells by binding to receptors on cilia. Since *M. hyopneumoniae* lacks the tip organelle observed in other mycoplasmas including *M. pneumoniae*, *M. gallisepticum*, *M. pulmonis*, and *M. genitalium*, polarized attachment to cilia would not occur.

Mapping of the P97 Mab F1B6 Antigenic Epitope and Cilia Binding Site

The use of repeat sequences to mediate the interaction between adhesins and receptors in eucaryotes has been well documented, especially when the interaction involves protein-protein interaction such as extracellular matrix proteins which mediate cell-cell recognition. The repeat sequences in *S. pyogenes* F protein and Sfb were proposed to mediate bacterial adherence to fibronectin (230, 240). In this study, amino acid sequence analysis of P97 has revealed two repeat sequences, R1 and R2, at the carboxy terminus of the protein. The R1 sequence consists of 15 repeats of AAKP(V/E) and has been demonstrated in this study to mediate the binding of rP97 to cilia (Figures 19 and 20). Insertion of Tn*1000* in the seventh repeat of R1 (insert number 133) yielded a protein with negative cilia binding activity when expressed in *E. coli* ISM612, whereas an insertion 5 repeats further downstream (insert number 90) yielded a protein with cilia binding activity. It is concluded that the cilia binding activity requires a minimum of at least seven repeats of the AAKP(V/E) sequence.

Sequence analysis of 5 other *M. hyopneumoniae* strains that exhibit different degrees of cilia binding activity was performed. These studies failed to show a significant difference in the number of R1 repeats n these strains, and thus, it was not possible to make a correlation of cilia binding with number of R1 repeats. The low adherent strain J had ten R1 repeat sequences, and the high adherent strain 144L had eleven R1 repeat sequences. To examine this issue further, clonal isolates of 232A exhibiting high, medium and low adherence to swine cilia were also studied. These isolates retained the identical sequence and structure in R1 region. Therefore, it is concluded that cilia binding activity in *M. hyopneumoniae* is subject to regulation from mechanisms other than changes in the R1 region of P97. There is evidence that protein conformation may play an important role; a Tn*1000* insert at location 160 seems to have

significantly higher cilia binding activity than those of neighboring locations (Figures 19 and 20). This suggests that cilia binding activity may require proper folding of the cilia binding domain. Alternatively, cilia binding assays with recombinant proteins may vary significantly due to differences in protein expression (Figure 18). Nonetheless, it is clear from these studies that transposon insertions in the R1 region result in abolition of cilia binding activity in P97.

The R2 repeat sequence, four repeats of NQGKK(S/A)EG(A/T)P, revealed a strikingly high homology (> 88% identity) to a 180-kDa canine ribosome receptor. Sequencing analysis of the cloned ribosome receptor gene revealed that the receptor contains an NQGKKAEGAP sequence that is repeated 54 times without interruption in the N-terminal end of the protein. The ribosome receptor protein is an integral membrane protein of the endoplasmic reticulum; the repeat sequence functions as a ribosome binding domain mediating the interaction between the ribosome and the endoplasmic reticulum. Since the P97 adhesin is suggested to exist as a secreted protein associated with membrane components outside the mycoplasma, this association may involve interactions with membrane proteins through the R2 repeat sequence in P97. Further studies are needed to confirm this.

The Mab F1B6 antigenic epitope in the P97 protein was mapped to the R1 repeat region and demonstrated a minimum of two and a half repeating units for the formation of the epitope. The region was defined by the loss of immunoreactivity of pISM2159::Tn*1000*.79 *E. coli* lysates and and not with pISM2159::Tn*1000*.133 lysates (Figure 18). Both cilia binding activity and the antigenic epitope have thus been mapped to the R1 region. The observation that Mab binding to P97 requires a smaller R1 region than does cilia binding may explain the fact that binding of P97 to cilia does not completely block the ability of the Mab to recognize the protein, as shown by the ability to use Mab F1B6 in the MPAA assay. Short synthetic peptides comprising the amino acid sequence from this junction region could be used in MPAA inhibition assays to determine more precisely the Mab F1B6 antigenic epitope. This may have important consequences in designing subunit vaccines.

Because of the nature of Tn*1000* mutagenesis which results in the fusion of transposon sequences with structural gene sequences, one could argue that changes in the cilia binding activity observed in the MPAA may be influenced by extra amino acid sequences derived from Tn*1000* prior to the first stop codon. This could vary depending upon the reading frame of the transposon insertion site. The extra amino acid sequence from Tn*1000* may help to explain a reduction in cilia binding activity through steric hindrance effects on cilia binding domain. To test the hypothesis, synthetic peptides consisting of the AAKP(V/E) repeat sequences could be examined for the ability to block cilia binding activity of either rP97 or *M. hyopneumoniae* whole cells. A second approach would be to construct a fusion protein consisting of the

putative cilia binding domain and an enzymatic domain, i.e. β-galactosidase, the binding of which could be easily followed in the MPAA. The sequence and structural analysis of the cilia binding domain could then proceed at the molecular level.

Sequence analysis of the repeat regions R1 and R2 among different strains of *M. hyopneumoniae* indicated a high conservation of DNA sequence (Figure 22). In the six strains analyzed, a stretch of 70 amino acids immediately downstream of the R1 sequence were identical. This suggests that this domain may be critical in maintaining the structure and function of the two repeat sequences. It may be helpful to sequence additional *M. hyopneumoniae* strains to examine this issue more closely.

Analysis of the P97 Operon Contig Sequence

Sequence analysis of the P97 contig has revealed several interesting features. Other mycoplasmas encode tissue adhesins within operons, i. e. *M. pneumoniae* and *M. genitalium*. Thus, it is not surprising to find P97 within an operon as well. The P97 operon contains only two ORFs, P97 and P102. The P102 gene codes for a protein with a amino terminal transmembrane domain followed by a sequence with high hydrophilicity. Therefore, P102 appears to be a membrane-targeted protein. Future studies should focus on mapping the location of P102 in the cell and determining whether P102 has a function in ciliary adherence. Monospecific, polyclonal antisera could be used in immunoelectron microscopy to determine its location and whether the presence of anti-P102 antibodies has an effect on adherence to swine cilia. Another approach to determine the function of P102 is by nearest-neighbor analysis involving a cross-linking reagent such as 3′,3′ dithiobis (sulfosuccinimidyl propionate) and monospecific antisera. Close association of the P102 protein and P97 would result in a cross-linked product containing both proteins.

Although there is no direct evidence that P97 is part of a two gene operon, this conclusion is based upon the observation that only a single putative promoter sequence has been identified 145 bp upstream of the P97 gene start codon, there is only 20 bp between the P97 stop codon and the P102 start codon, and that an ORF transcribed in reverse orientation was identified downstream of P102. The putative P97 promoter contained a unique feature; the -10 and -35 sequences were separated by a stretch of seventeen adenine residues. This polyadenine stretch was also observed by Wise and co-workers in genes that underwent phase variation in *M. hyorhinis* (256). A change in the number of adenine residues determined expression in that system. It could be speculated that *M. hyopneumoniae* also utilizes the same mechanism to control expression of P97, but in all strains that have been examined, P97 is constitutive. Since our hybridization studies suggest that there may be two copies of the P97 gene sequence in *M.*

hyopneumoniae, there may be random phase switching occurring in each copy, but a bias towards the ON phenotype would prevent identifying a clone lacking P97 completely by immunoblot analysis. *M. hyopneumoniae* may also contain more than a single cellular adhesin, and different stages in *M. hyopneumoniae* pathogenesis may involve the expression of different adhesin molecules. The possibility of phase switching of P97 warrants further investigation.

Open reading frame 2 is 426 bp in length with a coding capacity for a 16.4-kDa protein with a pI of 10.52. It has no homology to any known sequence. It is located between ORF 1 and the P97 structural gene with 534 bp and 411 bp of noncoding sequence, respectively, separating the genes. Two potential stem-loop structures were identified flanking ORF 2 inside these noncoding sequences. It is not uncommon for regulatory proteins to be found located upstream of the target promoter and transcribed separately. A stretch of 21 adenine residues was also found 340 bp upstream of ORF 2 possibly providing a recognition sequence for a recombinational event. This along with the high pI of ORF 2 suggests that ORF 2 may serve as a regulatory protein. To test this hypothesis, one must first establish the DNA binding ability of the protein product of ORF 2 followed by analysis of its sequence specificity.

Copy Number of P97 Operon Sequences

Zhang et al. demonstrated that Mab F1B6 recognized multiple proteins, including P97, in immunoblot analysis of *M. hyopneumoniae* (264). The source of these multiple proteins can be explained as either the result of degradation of 124.9-kDa P97, the existence of multiple copies or partial copies of P97 gene sequences, or a combination of the two possibilities. Hybridization of *M. hyopneumoniae* 232A genomic DNA with probes derived from P97 operon internal sequences showed that a second copy of P97 may be present in the *M. hyopneumoniae* 232A genome (Figure 16). An additional 14 kb *Bgl*II fragment was recognized by probes which spanned the entire P97 gene and the 5′ half of P102. However, when genomic DNA was digested with four other enzymes, *Eco*RI, *Eco*RV, *Hinc*II, and *Hind*III, no additional bands were observed. At least two explanations are possible. First, if P97 exists as two copies in the chromosome, the more frequent cutting enzymes were unable to identify the additional junction site of the duplicated sequence, and the *Bgl*II site within the second copy of P97 was modified. A putative *Bgl*II site exists approximately 10.5 kb upstream of the *Bgl*II site in P97 accounting for the 10.5 kb band in Figure 16; the second copy of P97 would account for the 14 kb band and both would be in equal concentration as suggested by the intensity of the bands in Figure 16.

If P97 exists in only a single copy, however, an alternative explanation would be necessary for the hybridization data. One possibility is a modification of the P97 internal *Bgl*II site in a subset of cells within the population which would result in a 14 kb *Bgl*II fragment recognized by probes 1 - 4, but not by probe 5. This fragment would include sequences from the upstream *Bgl*II site to the first *Bgl*II site downstream of the P97 operon. Modification would have to occur in about half of the cells to give approximately equal concentrations of the two fragments as suggested by the similar intensity of the two bands. Restriction-modification might account for this variability, but it is unclear what type of modification might account for inhibition of *Bgl*II digestion in half of the DNA molecules.

It is not uncommon for mycoplasmal adhesins to be present in multiple copies in the genome (41, 224). To resolve this issue, it might be necessary to clone the 14 kb *Bgl*II fragment and restriction digest the clone. If the P97 internal *Bgl*II site in the single copy model is modified in *M. hyopneumoniae* by an unknown mechanism, this modification would be resolved in *E. coli* resulting in a restriction map identical to the restriction map already determined. This would be the first direct evidence of the presence of a restriction-modification system in *M. hyopneumoniae*, and help to explain the failure to transform *M. hyopneumoniae* 232A with foreign DNA. If there is a second copy and the *Bgl*II site has been permanently modified by mutation, the restriction map will reflect this change. Further analysis of this clone by restriction mapping and DNA sequencing would be necessary to determine the exact nature of this second copy.

When the *Bgl*II-digested genomic DNA was analyzed with probes 4 and 5, the 14 kb fragment was recognized only by probe 4, but not by probe 5. In addition to the expected *Bgl*II fragments recognized by probe 4, two extra fragments of 7.5 kb and 2.8 kb were also recognized, indicating the presence of a second copy of the P102 gene in the genome of *M. hyopneumoniae* (Figure 16). Hybridization of genomic DNA digested with other enzymes by probes 4 and 5 also confirmed the presence of the second copy of the P102 gene. Hybridization of *Eco*RI-digested DNA with probe 4 resulted in three bands of 3.8, 4.2, and 4.8 kb. One fragment, 4.2 kb was also recognized by probe 5. These fragments were cloned into the vector pSK- to derive plasmids pISM1232, pISM1233 and pISM1234 and restriction mapped. Preliminary results of restriction mapping and sequence analysis of the ends of these clones revealed that the 4.8 kb fragment was only partly homologous to the P102 sequence which resulted in the weak hybridization observed in hybridization analysis (Figure 16). The 3.8 and 4.2 kb fragments shared significant homology to P102 sequences with identical sequences spanning up to one third of the P102 gene sequence. Alignment of the sequences of

the 3.8 and 4.2 kb fragments to the P102 gene sequence suggested that the 3.8 kb fragment contains the 5′ sequence of P102, the 4.2 kb fragment contains the 3′ region of P102 and other downstream sequences, and that the two fragments are separated by a 0.5 kb gap (Figure 23). Sequence homology of the 3.8 kb fragment to the P102 sequence was found to terminate abruptly at the junction region between the P102 gene and P97, but it included the *Nci*I site; the remaining sequence displayed no homology to known sequences in the database. Sequence analysis of the 4.2 kb fragment revealed about 500 bp which were almost identical to sequences surrounding the *Sal*I site in P102. Further sequencing of the 4.2 kb fragment downstream of the *Sal*I site is needed to determine if the second copy of P102 includes the entire P102 sequence or only a portion of the sequence. The former possibility is more likely since probe 5 which included the 3′ half of the P102 gene also recognized the 4.2 kb *Eco*RI fragment. When the 3.8 and 4.2 kb fragments were aligned to the corresponding P102 gene sequence and separated by 0.5 kb, the restriction map derived from the alignment revealed a pattern similar to the chromosomal region overlapped with the Lambda ZAP® II clones obtained by hybridization screening of the genomic library with pISM2136-specific probes that did not align with the P97 operon (Figure 23). This restriction map is distinct from the P97 operon contig shown in Figures 10 and 23. The restriction map predicted the 5.4 kb *Hin*dIII and 5.5 kb *Eco*RV fragments which were both confirmed by hybridization with probes 4 and 5 (Figure 16).

CONCLUSIONS

The impact that *M. hyopneumoniae* has had and continues to have on the swine industry is significant. Vaccines have not proven satisfactory for a variety of reasons, but mainly they fail to prevent colonization of the organism. Since colonization of the swine trachea is the first step to infection, studies of the mechanisms utilized by *M. hyopneumoniae* to adhere to tracheal tissues are crucial in dealing with this important disease. Previous studies by Zhang et al. demonstrated that the surface protein P97 seemed to be involved in adherence to swine epithelial cells, specifically to the cilia of those cells (263, 264, 266). We have extended those studies and have shown that rP97 binds to swine cilia in vitro. This was accomplished by the cloning of the P97 gene and functional analysis of the recombinant P97 protein. It was also demonstrated that the p97 gene is part of a two gene operon, which also includes an ORF coding for a 102-kDa protein designated P102. This protein has characteristics of a membrane protein, but its function is not clear. Its DNA sequence has no homology with any known genes, and thus, we are unable to predict a possible function for P102.

These studies represent the first molecular and genetic analysis of any *M. hyopneumoniae* adhesin. Through the use of novel opal suppressor strains of *E. coli*, it was possible to identify P97 expressing epitopes in a lambda genomic library. In the absence of opal suppression, these cloned fragments did not produce F1B6-reactive polypeptides in *E. coli*. Therefore, these strains made a critical contribution to this project; their use resulted in the initial identification of four clones, three of which contained the P97 gene sequence. The fourth clone, pISM2136, has been difficult to explain, but it appears to be derived from another region of the chromosome which contains a second copy of P102. It is not clear why pISM2136 produces a product that is recognized by Mab F1B6 since its DNA or predicted protein sequence has no homology with the Mab binding site region in P97.

Attempts to define the size variation observed in immunoblot analysis of *M. hyopneumoniae* with Mab F1B6 have not been successful. Screening of the genomic library with F1B6 for additional copies of the P97 gene resulted only in clones that matched the restriction map of the P97 operon. Only the hybridization analysis of the *Bgl*II-digested chromosomal DNA suggests that at least two copies of P97 exist in *M. hyopneumoniae* (Figure 16).

The P97 F1B6-reactive antigenic epitope and cilia binding site was localized to the carboxy terminus where two repeat sequences are found. The cilia binding site was localized to the R1 repeat. This may allow the development of a subunit vaccine carrying this repeat sequence which would induce swine cilium adherence blocking antibodies. The Mab F1B6 binding

epitope defined by these studies include the 5′ end of R1 as well as additional upstream sequences. It is not yet clear if the upstream sequences define the epitope or if R1 sequences are also involved. The resolution of the system did not allow further refinement of this problem.

It is clear from these studies that there at least two copies of P102 in the *M. hyopneumoniae* chromosome. The second copy has been partially cloned and analyzed. It has a high homology with the sequence in the P97 operon, but there are no P97 sequences associated with this copy of P102. It is not known why P102 is found in multiple copies in the chromosome since its function is not understood. We can only surmise that it is involved with adherence since one copy is found adjacent to the ciliary adhesin. If examples from other mycoplasmal systems are any indication, P102 will have a direct role in adherence. It is likely that a P102-specific antisera would help to resolve its function.

It has not been possible to directly relate cilia binding activity of different *M. hyopneumoniae* strains with changes in the P97 gene sequence. It was hoped that changes in the R1 repeat region could be correlated with loss of adherence activity, but these results indicate that there is little change in this region of the protein. Nor has it been possible to correlate lack of P97 expression with loss of adherence activity (T. Young, personal communication). Therefore, it is not yet possible to directly link P97 with the ciliary adherence phenotype of *M. hyopneumoniae* in vivo. Undoubtedly there are other proteins and activities associated with ciliary adherence that have not yet been identified. Further analysis of P102 may shed some light on this complicated process.

REFERENCES

1. Abiven, P., B. Blanchard, C. Saillard, M. Kobisch, and J. M. Bove. 1992. A specific DNA probe for detecting *Mycoplasma hyopneumoniae* in experimentally infected piglets. Mol. Cell. Probe 6:423-429.
2. Akkan, M. L., L. Wong, and F. J. Silverblatt. 1986. Change in degree of type 1 piliation of *Escherichia coli* during experimental peritonitis in the mouse. Infect. Immun. 54:549-554.
3. Alting-Mees, M. A., and J. M. Short. 1989. pBluescript II: gene mapping vectors. Nucl. Acids Res. 17:9494.
4. Arico, B., S. Nuti, V. Scarlato, and R. Rappuoli. 1993. Adhesion of *Bordetella pertussis* to eukaryotic cells requires a time-dependent export and maturation of filamentous hemagglutinin. Proc. Natl. Acad. Sci. USA 90:9204-9208.
5. Artiushin, S., M. Duvall, and F. C. Minion. 1995. Phylogenetic analysis of mycoplasma strain ISM1499 and its assignment to the *Acholeplasma oculi* strain cluster. Int. J. Syst. Bacteriol. 45:104-109.
6. Artiushin, S., L. Stipkovits, and F. C. Minion. 1993. Development of polymerase chain reaction primers to detect *Mycoplasma hyopneumoniae*. Mol. Cell. Probes 7:381-385.
7. Asai, T., M. Okada, M. Ono, T. Irisawa, Y. Mori, Y. Yokomizo, and S. Sato. 1993. Increased levels of tumor necrosis factor and interleukin 1 in bronchoalveolar lavage fluids from pigs infected with *Mycoplasma hyopneumoniae*. Vet. Immunol. Immunopathol. 38:253-260.
8. Asai, T., M. Okada, M. Ono, Y. Mori, Y. Yokomizo, and S. Sato. 1994. Detection of interleukin-6 and prostaglandin E2 in bronchoalveolar lavage fluids of pigs experimentally infected with *Mycoplasma hyopneumoniae*. Vet. Immunol. Immunopathol. 44:97-102.
9. Ashworth, L. A., A. B. Dowsett, L. I. Irons, and A. robinson. 1985. The location of surface antigens of *Bordetella pertussis* by immunoelectron microscopy. Dev. Biol. Stand. 61:143-151.
10. Baseman, J. B. 1993. The cytadhesins of *Mycoplasma pneumoniae* and *Mycoplasma genitalium*, p. 243-259. *In* S. Rottem and I. Kahane (ed.), Subcellular biochemistry. vol. 20. Mycoplasma cell membranes. Plenum Press, New York.
11. Baseman, J. B., R. M. Cole, D. C. Krause, and D. K. Leith. 1982. Molecular basis for cytoadsorption of *Mycoplasma pneumoniae*. J. Bacteriol. 151:1514-1522.

12. Baseman, J. B., J. Morrison-Plummer, D. Drouillard, B. Puleo-Scheppke, V. V. Tryon, and S. C. Holt. 1987. Identification of a 32 kilodalton protein of *Mycoplasma pneumoniae* associated with hemadsorption. Isr. J. Med. Sci. 23:474-479.
13. Beachey, E. H., and H. S. Courtney. 1987. Bacterial adherence: the attachment of group A streptococci to mucosal surfaces. Rev Infect Dis 5:s475-81.
14. Beachey, E. H., and H. S. Courtney. 1989. Bacterial adherence of group A streptococci to mucosal surface. Respiration 55:33-40.
15. Beachey, E. H., and I. Ofek. 1976. Epithelial cell binding of group A streptococci by lipoteichoic acid on fimbriae denuded of M protein. J. Exp. Med. 143:759-771.
16. Bereiter, M., T. F. Young, H. S. Joo, and R. F. Ross. 1990. Evaluation of the ELISA, and comparison to the complement fixation test and radial immunodiffusion enzyme assay for detection of antibodies against *Mycoplasma hyopneumoniae* in swine serum. Vet. Microbiol. 25:177-192.
17. Bernhard, W., A. Gbarah, and N. Sharon. 1992. Lectinophagocytosis of type 1 fimbriated (mannose-specific) *Escherichia coli* in the mouse peritoneum. J. Leukoc. Biol. 52:343-348.
18. Birnboim, H. 1983. A rapid alkaline extraction method for the isolation of plasmid DNA. Methods Enzymol. 100:243-255.
19. Blanchard, B., M. M. Vena, A. Cavalier, J. Le Lannic, J. Gouranton, and M. Kobisch. 1992. Electron microscopic observation of the respiratory tract of SPF piglets inoculated with *Mycoplasma hyopneumoniae*. Vet. Microbiol. 30:329-341.
20. Bloch, C. A., and P. E. Orndorff. 1990. Impaired colonization by and full invasiveness of *Escherichia coli* K12 bearing a site-directed mutation in the type 1 pilin gene. Infect. Immun. 58:275-278.
21. Blomfield, I. C., P. J. Calie, K. J. Eberhardt, M. S. Mcclain, and B. I. Eisenstein. 1993. Lpr stimulates phase variation of type 1 fimbriation in *Escherichia coli* K-12. J. Bacteriol. 175:27-36.
22. Blomfield, I. C., M. S. Mcclain, J. A. Princ, P. J. Calie, and B. I. Eisenstein. 1991. Type-1 fimbriation and *fimE* mutants of *Escherichia coli* K-12. J. Bacteriol. 173:5298-5307.
23. Boner, G., A. M. Mhashilkar, M. Rodriguez-Ortega, and N. Sharon. 1989. Lectin-mediated, nonopsonic phagocytosis of type 1 *Escherichia coli* by human peritoneal macrophages of uremic patients treated by peritoneal dialysis. J. Leukoc. Biol. 46:239-245.

24. Bredt, W. 1979. Motility, p. 141-155. *In* M. F. Barile and S. Razin (ed.), The Mycoplasmas. I. Cell biology. Academic Press, New York.
25. Brubaker, R. R. 1985. Mechanisms of bacterial virulence. Annu. Rev. Microbiol. 39:21-50.
26. Brunner, H., J. Feldner, and W. Bredt. 1984. Effect of monoclonal antibodies to the attachment-tip on experimental *Mycoplasma pneumoniae* infection of hamsters, a preliminary report. Is. J. Med. Sci. 20:878-881.
27. Caparon, M. G., and J. R. Scott. 1987. Identification of a gene that regulates expression of M protein, the major virulence determinant of group A streptococci. Proc Natl Acad Sci USA 84:8677-81.
28. Carruthers, M. M., and W. J. Kabat. 1983. Mediation of staphylococcal adherence to mucosal cells by lipoteichoic acid. Infect. Immun. 40:444-446.
29. Caurso, J. P., and R. F. Ross. 1990. Effects of *Mycoplasma hyopneumoniae* and *Actinobacillus* (*Haemophilus*) *pleuropneumoniae* infections on alveolar macrophage functions in swine. Am. J. Vet. Res. 51:227-231.
30. Chou, P. Y., and G. D. Fasman. 1978. Empirical predictions of protein conformations. Ann. Rev. Biochem. 47:251-276.
31. Cole, B. C., and G. H. Cassell. 1979. Mycoplasma infections as models of chronic inflammation. Arth. Rheum. 22:1375-1381.
32. Cooper, A. C., J. R. Fuller, M. K. Fuller, P. Whittlestone, and D. R. Wise. 1993. In vitro activity of danofloxacin, tylosin, and oxytetracycline against mycoplasmas of veterinary importance. Res. Vet. Sci. 54:329-334.
33. Courtney, H. S., M. S. Bronze, J. B. Dale, and D. L. Hasty. 1994. Analysis of the role of M24 protein in group A streptococcal adhesion and colonization by use of omega-interposon mutagenesis. Infect. Immun. 62:4868-4873.
34. Courtney, H. S., Y. Li, J. B. Dale, and D. L. Hasty. 1994. Cloning, sequencing, and expression of a fibronectin/fibronogen-binding protein from group A streptococci. Infect. Immun. 62:3937-3946.
35. Courtney, H. S., C. von Hunolstein, J. B. Dale, M. S. Bronze, E. H. Beachey, and D. L. Hasty. 1992. Lipoteichoic acid and M protein: dual adhesins of group-A streptococci. Microb. Pathog. 12:199-208.
36. Dahlgren, U. I., S. Ahlstedt, and L. A. Hanson. 1987. The localization of the antibody response in milk or bile depends on the nature of the antigen. J. Immunol. 138:1397-1402.

37. Dahlgren, U. I., A. E. Wold, L. A. Hanson, and T. Midtvedt. 1990. The secretory antibody response in milk and bile against fimbriae and LPS in rats monocolonized or immunized in the Peyer's patches with *Escherichia coli*. Immunology 71:295-300.
38. Dal-Nogare, A. R. 1990. Type 1 pili mediate gram-negative bacterial adherence to intact tracheal epithelium. Am. J. Respir. Cell. Biol. 2:433-440.
39. Dale, J. B., R. W. Baird, H. S. Courtney, D. L. Hasty, and M. S. Bronze. 1994. Passive protection of mice against group A streptococcal pharyngeal infection by lipoteichoic acid. J. Infect. Dis. 169:319-323.
40. Dallo, S. F., and J. B. Baseman. 1990. Cross-hybridization between the cytadhesin genes of *Mycoplasma pneumoniae* and *Mycoplasma genitalium* and genomic DNA of *Mycoplasma gallisepticum*. Microb. Pathog. 8:371-375.
41. Dallo, S. F., and J. B. Baseman. 1991. Adhesin gene of *Mycoplasma genitalium* exists as multiple copies. Microb. Pathog. 10:475-480.
42. Dallo, S. F., A. Chavoya, and J. B. Baseman. 1990. Characterization of the gene for a 30-kilodalton adhesin-related protein of *Mycoplasma pneumoniae*. Infect. Immun. 58:4163-4165.
43. Dallo, S. F., J. R. Horton, C. J. Su, and J. B. Baseman. 1990. Restriction fragment length polymorphism in the cytadhesin P1 gene of human clinical isolates of *Mycoplasma pneumoniae*. Infect. Immun. 58:2017-2020.
44. Dallo, S. F., A. L. Lazzell, A. Chavoya, S. P. Reddy, and J. B. Baseman. 1996. Biofunctional domains of the *Mycoplasma pneumoniae* P30 adhesin. Infect Immun 64:2595-2601.
45. DeBey, M. C., and R. F. Ross. 1994. Ciliostasis and loss of cilia induced by *Mycoplasma hyopneumoniae* in porcine tracheal organ cultures. Infect. Immun. 62:5312-5318.
46. DeBey, M. C., J. A. Roth, and R. F. Ross. 1993. Enhancement of the increase in intracelluar calcium concentration in stimulated neutrophils by *Mycoplasma hyopneumoniae*. Vet. Res. Commun. 17:249-257.
47. DiRita, V. J., and J. J. Mekalanos. 1989. Genetic regulation of bacterial virulence. Annu. Rev. Genet. 23:455-482.
48. Dirksen, L. B., T. Proft, H. Hilbert, H. Plagens, R. Herrmann, and D. C. Krause. 1996. Sequence analysis and characterization of the hmw gene cluster of Mycoplasma pneumoniae. Gene 171:19-25.

49. Djordjevic, S. P., G. J. Eamens, L. F. Romalis, and M. M. Saunders. 1994. An improved enzyme linked immunosorbent assay (ELISA) for the detection of porcine serum antibodies against *Mycoplasma hyopneumoniae*. Vet. Microbiol. 39:261-273.
50. Dominick, M. A., M. J. Schmerr, and A. E. Jensen. 1985. Expression of type 1 pili by *Escherichia coli* strains of high and low virulence in the intestinal tract of knotobiotic turkeys. Am. J. Vet. Res. 46:270-275.
51. Dorman, C. J., and C. F. Higgins. 1987. Fimbrial phase variation in Escherichia coli: dependence on integration host factor and homologies with other site-specific recombinases. J. Bacteriol. 169:3840-3843.
52. Doster, A. R., and B. C. Lin. 1988. Identification of Mycoplasma hyopneumoniae in formalin-fixed porcine lung, using an indirect immunoperoxidase method. Am J Vet Res 49:1719-21.
53. Dozois, C. M., N. Chanteloup, M. D. Moulin, A. Bree, C. Desautels, and J. M. Fairbrother. 1994. Bacterial colonization and in vivo expression of F1 (type 1) fimbrial antigens in chickens experimentally infected with pathogenic *Escherichia coli*. Avian Dis. 38:231-239.
54. Dritz, S. S., M. M. Chengappa, J. L. Nelssen, M. D. Tokach, R. D. Goodband, J. C. Nietfeld, and J. J. Staats. 1996. Growth and microbial flora of nonmedicated segregated, early weaned pigs from a commercial swine operation. J. Am. Vet. Med. Assoc. 208:711-715.
55. Duguid, J. P., and R. R. Gillies. 1957. Fimbriae and adhesive properties in dysentery bacilli. J. Pathol. Bacteriol. 74:397-408.
56. Eisenstein, B. I., D. S. Sweet, V. Vaughn, and D. I. Friedman. 1987. Integration host factor is required for the DNA inversion that controls phase variation in Escherichia coli. Proc. Natl. Acad. Sci. USA 84:6506-6510.
57. Emsley, P., I. G. Charles, N. F. Fairweather, and N. W. Isaacs. 1996. Structure of *Bordetella pertussis* virulent factor P.69 pertactin. Nature 381:90-92.
58. Ernst, S., R. Langer, C. L. Cooney, and R. Sasisekharan. 1995. Enzymatic degradation of glycoaminoglycans. Crit. Rev. Biochem. Mol. Biol. 30:387-444.
59. Finlay, B. B., and S. Falkow. 1989. Common themes in microbial pathogenicity. Microbiol. Rev. 53:210-230.
60. Firon, N., S. Ashkenazi, D. Mirelman, I. Ofek, and N. Sharon. 1987. Aromatic alpha-glycosides of mannose are powerful inhibitors of the adherence of type 1 fimbriated *Escherichia coli* to yeast and intestinal epithelial cells. Infect. Immun. 55:472-476.

61. Freeman, M. J., M. Lopez-Osuna, C. H. Armstrong, and L. Sanda-Freeman. 1984. Evaluation of the indirect hemagglutination assay as a practical serodiagnostic test for mycoplasmal pneumonia of swine. Vet. Microbiol. 9:259-270.
62. Frey, J., A. Haldimann, M. Kobisch, and J. Nicolet. 1994. Immune response against the L-lactate dehydrogenase of *Mycoplasma hyopneumoniae* in enzootic pneumonia of swine. Microb. Pathog. 17:313-322.
63. Friis, N. F. 1977. *Mycoplasma suipneumoniae* and *Mycoplasma flocculare* in the growth precipitation test. Acta Vet. Scand. 18:168-175.
64. Fujita, K., T. Yamamoto, and R. Kitagawa. 1991. Binding sites for P and/or type 1-piliated *Escherichia coli* in human ureter. J. Urol. 146:217-222.
65. Funnell, S. G., and A. Robinson. 1993. A novel adherence assay for *Bordetella pertussis* using tracheal organ cultures. FEMS Microbiol. Lett. 110:197-203.
66. Gally, D. L., J. A. Bogan, B. I. Eisenstein, and I. C. Blomfield. 1993. Environmental regulation of the *fim* switch controlling type 1 fimbrial phase variation in *Escherichia coli* K-12: effects of temperature and media. J. Bacteriol. 175:6186-6193.
67. Garnier, J., D. J. Osguthorpe, and B. Robson. 1978. Analysis of the accuracy and implications of simple methods for predicting the secondary structure of globular proteins. J. Mol. Biol. 120:97-120.
68. Gbarah, A., C. G. Gahmberg, G. Boner, and N. Sharon. 1993. The leukocyte surface antigens CD11b and CD18 mediate the oxidative burst activation of human peritoneal macrophages induced by type 1 fimbriated *Escherichia coli*. J. Leukoc. Biol. 54:111-113.
69. Gbarah, A., C. G. Gahmberg, I. Ofek, U. Jacobi, and N. Sharon. 1991. Identification of the leukocyte adhesion molecules CD11 and CD18 as receptor for type 1-fimbriated (mannose-specific) *Escherichia coli*. Infect. Immun. 59:4525-4530.
70. Gbarah, A., A. M. Mhashilkar, G. Boner, and N. Sharon. 1989. Involvement of protein kinase C in activation of human granulocytes and peritoneal macrophage by type 1 fimbriated (mannose-specific) *Escherichia coli*. Biochem. Biophys. Res. Commun. 165:1243-1249.
71. Geary, S. J., and E. M. Walczak. 1983. Cytopathic effect of whole cells and purified membranes of *Mycoplasma hyopneumoniae*. Infect. Immun. 41:132-136.
72. Geuijen, C. A. W., R. J. L. Willems, and F. R. Mooi. 1996. The major fimbrial subunit of *Bordetella pertussis* binds to sulfated sugars. Infect. Immun. 64:2657-2665.

73. Giampapa, C. S., S. N. Abraham, and E. H. Beachey. 1988. Isolation and characterization of a receptor for type 1 fimbriae of *Escherichia coli* from guinea pig erythrocytes. J. Biol. Chem. 263:5362-5367.
74. Goetz, M. B. 1989. Priming of polymorphonuclear neutrophilic leukocyte oxidative activity by type 1 pili from *Escherichia coli*. J. Infect. Dis. 159:533-542.
75. Goetz, M. B., and F. J. Silverblatt. 1987. Stimulation of human polymorphonuclear leukocyte oxidative metabolism by type 1 pili from *Escherichia coli*. Infect. Immun. 55:534-540.
76. Goodwin, R. F. 1984. Apparent reinfection of enzootic-pneumonia-free pig herds: early signs and incubation period. Vet. Res. 115:320-324.
77. Gullberg, D., and P. Ekblom. 1995. Extracellular matrix and its receptors during development. Int. J. Dev. Biol. 39:845-854.
78. Hahn, T.-W., K. A. Krebes, and D. C. Krause. 1996. Expression in *Mycoplasma pneumoniae* of the recombinant gene encoding the cytadherence-associated protein HMW1 and identification of HMW4 as a product. Mol. Microbiol. 19:1085-1093.
79. Haldimann, A., J. Nicolet, and J. Frey. 1993. DNA sequence determination and biochemical analysis of the immunogenic protein P36, the lactate dehydrogenase (LDH) of *Mycoplasma hyopneumoniae*. J. Gen. Microbiol. 139:317-323.
80. Hannan, P. C., and R. F. Goodwin. 1990. Treatment of experimental enzootic pneumonia of the pig by norfloxacin or its 6-chloro analogue. Res. Vet. Sci. 49:203-210.
81. Hannan, P. C., P. J. OHanlon, and N. H. Rogers. 1989. In vitro evaluation of various quinolone antibacterial agents against veterinary mycoplasmas and porcine respiratory bacterial pathogens. Res. Vet. Sci. 46:202-211.
82. Hanski, E., and M. Caparon. 1992. Protein F, a fibronectin-binding protein, is an adhesin of the group A streptococcus *Streptococcus pyogenes*. Proc. Natl. Acad. Sci. USA 89:6172-6176.
83. Hanski, E., P. A. Horwitz, and M. Caparon. 1992. Expression of protein F, the fibronectin-binding protein of *Streptococcus pyogenes* JRS4, in heterologous streptococcal and enterococcal strains promotes their adherence to respiratory epithelial cells. Infect. Immun. 60:5119-5125.
84. Harasawa, R., K. Koshimizu, O. Takeda, T. Uemori, K. Asada, and I. Kato. 1991. Detection of *Mycoplasma hyopneumoniae* DNA by the polymerase chain reaction. Mol. Cell. Probes 5:103-109.
85. Hasty, D. L., I. Ofek, H. S. Courtney, and R. J. Doyle. 1992. Multiple adhesins of streptococci. Infect. Immun. 60:2147-2152.

86. Hazenbos, W. L., C. A. Geuijen, B. M. van den Berg, F. R. Mooi, and R. van Furth. 1995. *Bordetella pertussis* fimbriae bind to human monocytes via the minor fimbrial subunit FimD. J. Infect. Dis. 171:924-929.

87. Hazenbos, W. L., B. M. van den Berg, C. A. Geuijen, F. R. Mooi, and R. van Furth. 1995. Binding of FimD on *Bordetella pertussis* to very late antigen-5 on monocytes activates complement receptor type 3 via protein tyrosine kinases. J. Immunol. 155:3972-3978.

88. Henderson, B., S. Poole, and M. Wilson. 1996. Bacterial modulins: a novel class of virulent factors which cause host tissue pathology by inducing cytokine synthesis. Microbiol. Rev. 60:316-341.

89. Hofman, K., and W. Stoffel. 1993. TMbase - a database of membrane protein spanning segments. Biol. Chem. Hoppe-Seyler 347:166.

90. Hu, P. C., R. M. Cole, Y. S. Huang, J. A. Graham, D. E. Gardner, A. M. Collier, and W. A. J. Clyde. 1982. *Mycoplasma pneumoniae* infection: role of a surface protein in the attachment organelle. Science 216:313-315.

91. Hu, P. C., A. M. Collier, and J. B. Baseman. 1977. Surface parasitism by *Mycoplasma pneumoniae* of respiratory epithelium. J. Exp. Med. 145:1328-1343.

92. Huang, Y., and G. W. Stemke. 1992. Construction of the physical maps of *Mycoplasma hyopneumoniae* and *Mycoplasma flocculare* and the location of rRNA genes on these maps. Can. J. Microbiol. 38:659-663.

93. Hultgren, S. J., W. R. Schwan, A. J. Schaeffer, and J. L. Duncan. 1986. Regulation of production of type 1 pili among urinary tract isolates of *Escherichia soli*. Infect. Immun. 54:613-620.

94. Inamine, J. M., S. Loechel, and P. C. Hu. 1988. Analysis of the nucleotide sequence of the P1 operon of *Mycoplasma pneumoniae*. Gene 73:175-183.

95. Isenberg, H. 1988. Pathogenicity and virulence: Another view. Clin. Microbiol. Rev. 1:40-53.

96. Ishibashi, Y., S. Claus, and D. A. Relman. 1994. *Bordetella pertussis* filamentous hemaggultinin interacts with a leukocyte signal transduction complex and stimulates bacterial adherence to monocyte CR3 (CD11b/CD18). J. Exp. Med. 180:1225-1233.

97. Jacobs, E., M. Drews, A. Stuhlert, C. Buttner, P. J. Klein, M. Kist, and W. Bredt. 1988. Immunological reaction of guinea pigs following intranasal *Mycoplasma pneumoniae* infection and immunization with the 168 kDa adherence protein. J. Gen. Microbiol. 134:473-479.

98. Jacobs, E., A. Stuhlert, M. Drews, K. Pumpe, H. E. Schaefer, M. Kist, and W. Bredt. 1988. Host reactions to *Mycoplasma pneumoniae* infections in guinea-pigs preimmunized systemically with the adhesin of this pathogen. Microb. Pathog. 5:259-265.

99. Jayappa, H. G., R. A. Gooddow, and S. J. Geary. 1985. Role of *Eschirichia coli* type 1 pilus in colonization of porcine ileum and its protective nature as a vaccine antigen in controlling colibacillosis. Infect. Immun. 48:350-354.

100. Johansson, K. E., J. G. Mattsson, K. Jacobsson, C. Fernandez, K. Bergstrom, G. Bolske, P. Wallgren, and U. B. Gobel. 1992. Specificity of oligonucleotide probes complementary to evolutionarily variable regions of 16S rRNA from *Mycoplasma hyopneumoniae* and *Mycoplasma hyorhinis*. Res. Vet. Sci. 52:195-204.

101. Jones, C. H., J. S. Pinkner, A. V. Nicholes, L. N. Slonim, S. N. Abraham, and S. J. Hultgren. 1993. FimC Is a periplasmic PapD-like chaperone that directs assembly of type 1 pili in bacteria. Proc. Natl. Acad. Sci. USA 90:8397-8401.

102. Jones, D. H., B. W. McBride, and G. H. Farrar. 1996. Poly(lactide-co-glycolide) microencapsulation of vaccine antigens. J. Biotechnol. 44:29-36.

103. Kim, M. F., M. B. Heidari, S. J. Stull, M. A. McIntosh, and K. S. Wise. 1990. Identification and mapping of an immunogenic region of *Mycoplasma hyopneumoniae* p65 surface lipoprotein expressed in *Escherichia coli* from a cloned genomic fragment. Infect. Immun. 58:2637-2643.

104. Kishima, M., R. Ross, and C. Kuniyasu. 1985. Cell-mediated and humoral immune response to *Mycoplasma hyopneumoniae* in pigs enhanced by dextran sulfate. Am. J. Vet. Res. 46:456-462.

105. Kishima, M., and R. F. Ross. 1985. Suppressive effect of nonviable *Mycoplasma hyopneumoniae* on phytohemagglutinin-induced transformation of swine lymphocytes. Am. J. Vet. Res. 46:2366-2368.

106. Klemm, P. 1986. Two regulatory *fim* genes, *fimB* and *fimE*, control the phase variation of type 1 fimbriae in *Escherichia coli*. EMBO J. 5:1389-1393.

107. Klemm, P. 1992. FimC, a chaperone-like periplasmic protein of *Escherichia coli* Involved in biogenesis of type-1 fimbriae. Res. Microbiol. 143:831-838.

108. Klemm, P., and G. Christiansen. 1990. The *fimD* gene is required for cell surface location of *Escherichia coli* type 1 fimbriae. Mol. Gen. Genet. 220:334-338.

109. Klemm, P., K. A. Krogfelt, L. Hedegaard, and G. Christiansen. 1990. The major subunit of *Escherichia coli* type 1 fimbriae is not required for D-mannose-specific adhesion. Mol. Microbiol. 4:553-559.

110. Kobisch, M., L. Quillien, J. P. Tillon, and H. Wroblewski. 1987. The *Mycoplasma hyopneumoniae* plasma membrane as a vaccine against porcine enzootic pneumonia. Ann. Inst. Pasteur Immunol. 138:693-705.

111. Krause, D. C. 1996. *Mycoplasma pneumoniae* cytadherence: unravelling the tie that binds. Mol. Microbiol. 20:247-253.

112. Krause, D. C., and K. K. Lee. 1991. Juxtaposition of the genes encoding *Mycoplasma pneumoniae* cytadherence-accessory proteins HMW1 and HMW3. Gene 107:83-89.

113. Krause, D. C., D. K. Leith, R. M. Wilson, and J. B. Baseman. 1982. Identification of *Mycoplasma pneumoniae* proteins associated with hemadsorption and virulence. Infect. Immun. 35:809-817.

114. Kristensen, B., P. Paroz, J. Nicolet, M. Wanner, and A. L. de Weck. 1981. Cell-mediated and humoral immune response in swine after vaccination and natural infection with *Mycoplasma hyopneumoniae*. Am. J. Vet. Res. 42:784-788.

115. Krivan, H. C., L. D. Olson, M. F. Barile, V. Ginsburg, and D. D. Roberts. 1989. Adhesion of *Mycoplasma pneumoniae* to sulfated glycolipids and inhibition by dextran sulfate. J. Biol. Chem. 264:9283-9288.

116. Krivan, H. C., D. D. Roberts, and V. Ginsburg. 1988. Many pulmonary pathogenic bacteria bind specifically to the carbohydrate sequence GalNAc beta 1,4 Gal found in some glycolipids. Proc. Natl. Acad. Sci. USA 85:6157-6161.

117. Krogfelt, K. A., H. Bergmans, and P. Klemm. 1990. Direct evidence that the FimH protein is the mannose-specific adhesin of *Escherichia coli* type 1 fimbriae. Infect. Immun. 58:1995-1998.

118. Krogfelt, K. A., and P. Klemm. 1988. Investigation of minor components of *Escherichia coli* type 1 fimbriae: protein chemical and immunological aspects. Microb. pathog. 4:231-238.

119. Krogfelt, K. A., B. A. McCormick, R. L. Burghoff, D. C. Laux, and P. S. Cohen. 1991. Expression of *Eschirichia coli* F-18 type 1 fimbriae in the streptomycin-treated mouse large intestine. Infect. Immun. 59:1567-1568.

120. Kukkonen, M., T. Raunio, R. Virkola, K. Lahteenmaki, P. H. Makela, P. Klemm, S. Clegg, and T. K. Korhonen. 1993. Basement membrane carbohydrate as a target for bacterial adhesion binding of type-I fimbriae of *Salmonella enterica* and *Escherichia coli* to laminin. Mol. Microbiol. 7:229-237.

121. Kurono, Y., T. Fujiyoshi, and G. Mogi. 1989. Secretory IgA and bacterial adherence to nasal mucosal cells. Ann. Otol. Rhinol. Laryngol. 98:273-277.

122. Layh-Schmitt, G. 1993. The ORF6 gene product of the P1 operon of *Mycoplasma pneumoniae*. Int. J. Med. Microbiol. Virol. Parasitol. Infect. Dis. 278:287-295.

123. Layh-Schmitt, G., and R. Herrmann. 1994. Spatial arragnement of gene product of the P1 operon in the membrane of *Mycoplasma pneumoniae*. Infect. Immun. 62:974-979.

124. Le Potier, M. F., P. Abiven, M. Kobisch, D. Crevat, and P. Desmettre. 1994. A blocking ELISA using a monoclonal antibody for the serological detection of *Mycoplasma hyopneumoniae*. Res. Vet. Sci. 56:338-345.

125. Leininger, E., C. A. Ewanowich, A. Bhargava, M. S. Peppler, J. G. Kenimer, and M. J. Brennan. 1992. Comparative roles of the Arg-Gly-Asp sequence present in the *Bordetella pertussis* adhesins pertactin and filamentous hemagglutinin. Infect. Immun. 60:2380-2385.

126. Leininger, E., M. Roberts, J. G. Kenimer, I. G. Charles, N. Fairweather, P. Novotny, and M. J. Brennan. 1991. Pertactin, an Arg-Gly-Asp-containing *Bordetella pertussis* surface protein that promotes adherence of mammalian cells. Proc. Natl. Acad. Sci. USA 88:345-349.

127. Livey, I., C. J. Duggleby, and A. Robinson. 1987. Cloning and nucleotide sequence analysis of the serotype 2 fimbrial subunit gene of *Bordetella pertussis*. Mol. Microbiol. 1:203-209.

128. Lloyd, L. C., G. S. Cottew, and D. A. Anderson. 1989. Protection against enzootic pneumonia of pigs: intraperitoneal inoculation with live LKR strain of *Mycoplasma hyopneumoniae*. Aust. Vet. J. 66:9-12.

129. Locht, C., P. Bertin, F. D. Menozzi, and G. Renauld. 1993. The filamentous haemagglutinin, a multifaceted adhesin produced by virulent *Bordetella* spp. Mol. Microbiol. 9:653-660.

130. Loosmore, S. M., R. K. Yacoob, G. R. Zealey, G. E. Jackson, Y. P. Yang, P. S. Chong, J. M. Shortreed, D. C. Coleman, J. D. Cunningham, L. Gisonni, and et al. 1995. Hybrid genes over-express pertactin from *Bordetella pertussis*. Vaccine 13:571-80.

131. Low, B., B. Braaten, and M. Van der Woude. 1996. Fimbriae, p. 146-157. *In* F. C. Neidhardt, R. Curtiss, J. L. Ingraham, E. C. C. Lin, K. B. Low, B. Magasanik, W. S. Reznikoff, M. Riley, M. Schaechter and H. E. Umbarger (ed.), *Escherichia coli* and *Salmonella* cellular and molecular biology. AMerican Society for Microbiology, Washington, D.C.

132. Mahairas, G. G., and F. C. Minion. 1989. Random insertion of the gentamicin resistance transposon Tn*4001* in *Mycoplasma pulmonis*. Plasmid 21:43-47 (Author's correction 30:177-178, 1993).

133. Makhov, P. T., J. H. Hannah, M. J. Brennan, B. L. Trus, E. Kocsis, J. F. Conway, P. T. Wingdield, M. N. Simon, and A. C. Steven. 1994. Filamentous hemagglutinin of *Bordetella pertussis*. A bacterial adhesin formed as a 50 nm monomer rigid rod based on a 19-residual repeat motif rich in beta strands and turns. J. Mol. Biol. 241:110-24.

134. Malaviya, R., T. Ikeda, E. A. Ross, and S. N. Abraham. 1996. Mast cell modulation of neutrophil influx and bacterial clearance at sites of infection through TNF-alpha. Nature 381:77-80.

135. Malaviya, R., E. A. Ross, B. A. Jakschik, and S. N. Abraham. 1994. Mast cell degranulation induced by type1 fimbriated *Escherichia coli* in mice. J. Clin. Invest. 93:1645-1653.

136. Malaviya, R., E. A. Ross, J. I. Macgregor, T. Ikeda, J. R. Little, B. A. Jakschik, and S. N. Abraham. 1994. Mast cell phagocytosis of FimH-expressing enterobacteria. J. Immunol. 152:1907-1914.

137. Markham, P. F., M. D. Glew, J. E. Sykes, T. R. Bowden, T. D. Pollacks, G. F. Browning, K. G. Whithear, and I. D. Walker. 1994. The organisation of the multigene family which encodes the major cell surface protein, pMGA, of *Mycoplasma gallisepticum*. FEBS Lett 352:347-352.

138. Mattingly, S. J., and B. P. Johnston. 1987. Comparative analysis of the localization of lipoteichoic acid in streptoccus agalactiae and *Streptococcus pyogenes*. Infect. Immun. 55:2383-2386.

139. Mattsson, J. G., K. Bergstrom, P. Wallgren, and K. E. Johansson. 1995. Detection of *Mycoplasma hyopneumoniae* in nose swabs from pigs by in vitro amplification of the 16S rRNA gene. J. Clin. Microbiol. 33:893-897.

140. Mcclain, M. S., I. C. Blomfield, and B. I. Eisenstein. 1991. Roles of *fimB* and *fimE* in site specific DNA inversion associated with phase variation of type 1 fimbriae in *Escherichia coli*. J. Bacteriol. 173:5308-5314.

141. McCormick, B. A., D. P. Franklin, D. C. Laux, and P. S. Cohen. 1989. Type 1 pili are not necessary for colonization of the streptomycin-treated mouse large intestine by type 1-piliated *Escherichia coli* F-18 and *E. coli* K-12. Infect. Immun. 57:3022-3029.

142. McCormick, B. A., P. Klemm, K. A. Krogfelt, R. L. Burghoff, L. Pallesen, and D. C. Laux. 1993. *Eschirichia coli* F-18 phase locked "on" for expression of type 1 fimbriae is

a poor colonizer of the streptomycin-treated mouse large intestinae. Microb. Pathog. 14:33-43.

143. Mebus, C. A., and N. R. Underdahl. 1977. Scanning electron microscopy of trachea and bronchi from gnotobiotic pigs inoculated with *Mycoplasma hyopneumoniae*. Am. J. Vet. Res. 51:1249-1254.
144. Mebus, C. A., and N. R. Underdahl. 1977. Scanning electron microscopy of trachea and bronchi from gnotobiotic pigs inoculated with *Mycoplasma hyopneumoniae*. Am. J. Vet. Res. 43:1249-1254.
145. Menozzi, F. D., R. Mutombo, G. Renauld, C. Gantiez, J. H. Hannah, E. Leininger, M. J. Brennan, and C. Locht. 1994. Heparin-inhibitable lectin activity of the filamentous hemagglutinin adhesin of *Bordetella pertussis*. Infect. Immun. 62:769-778.
146. Messier, S., and R. F. Ross. 1991. Interactions of *Mycoplasma hyopneumoniae* membranes with porcine lymphocytes. Am. J. Vet. Res. 52:1497-502.
147. Messier, S., R. F. Ross, and P. S. Paul. 1990. Humoral and cellular immune responses of pigs inoculated with *Mycoplasma hyopneumoniae*. Am. J. Vet. Res. 51:52-58.
148. Minion, F. C., C. VanDyk, and B. K. Smiley. 1995. Use of an *Escherichia coli* enhanced opal suppressor strain to screen a *Mycoplasma hyopneumoniae* library. FEMS Microbiol. Lett. 131:81-85.
149. Monga, M., and J. A. Robert. 1994. Spermagglutination by bacteria: receptor-specific interaction. J. Androl. 15:151-156.
150. Mooi, F. R., W. H. Jansen, H. Brunings, H. Gielen, H. G. J. van der Heide, H. C. Walvoort, and P. A. Guinee. 1992. Construction and analysis of *Bordetella pertussis* mutants defective in the production of fimbriae. Microb. Pathog. 12:127-135.
151. Mooi, F. R., A. ter Avest, and H. G. van der Heide. 1990. Structure of the *Bordetella pertussis* gene coding for the serotype 3 fimbrial subunit. FEMS Microbiol. Lett. 54:327-331.
152. Mori, Y., Y. Yoshida, C. Kuniyasu, and K. Hashimoto. 1983. Improvement of complement fixation test antigen for the diagnosis of *Mycoplasma hyopneumoniae* infection. Natl. Inst. Anim. Health Q. Tokyo 23:111-116.
153. Morrison-Plummer, J., A. Laxxell, and J. B. Baseman. 1987. Shared epitope between *Mycoplasma pneumoniae* major adhesin protein P1 and a 140 kilodalton protein of *Mycoplasma genitalium*. Infect. Immun. 55:49-56.
154. Murphy, D., W. G. Van Alstine, L. K. Clark, S. Albregts, and K. Knox. 1993. Aerosol vaccination of pigs against *Mycoplasma hyopneumoniae* infection. Am. J. Vet. Res. 54:1874-1880.

155. Nilsson, K., U. I. Dahlgren, and L. A. Hanson. 1988. Different origins of IgA antibodies with various antigen specificities appearing in rat bile. Scand. J. Immunol. 28:547-551.

156. Ofek, I., W. A. Simpson, and E. H. Beachey. 1982. Formation of molecular complexes between a structurally defined M-protein and acylated or deacylated lipoteichoic acid of *Streptococcus pyogenes*. J. Bacteriol. 149:426-433.

157. Ogle, K. F., K. K. Lee, and D. C. Krause. 1991. Cloning and analysis of the gene encoding the cytadherence phase-variable protein HMW3 from *Mycoplasma pneumoniae*. Gene 97:69-75.

158. Ogle, K. F., K. K. Lee, and D. C. Krause. 1992. Nucleotide sequence analysis reveals novel features of the phase-variable cytadherence accessory protein HMW3 of *Mycoplasma pneumoniae*. Infect. Immun. 60:1633-1641.

159. Okada, M., A. P. Pentland, P. Falk, and M. G. Caparon. 1994. M protein and protein F act as important determinants of cell-specific tropism of *Streptococcus pyogenes* in skin tissue. J. Clin. Invest. 94:965-977.

160. Okada, N., M. K. Liszewski, J. P. Atkinson, and M. Caparon. 1995. Membrane cofactor protein (CD46) is a keratinocyte receptor for the M protein of the group A streptococcus. Proc. Natl. Acad. Sci. USA 92:2489-2493.

161. Olsen, P. B., and P. Klemm. 1994. Localization of promoters in the *fim* gene cluster and the effect of H-NS on the transcription of *fimB* and *fimE*. FEMS Microbiol. Lett. 116:95-100.

162. Orskov, I., and F. Orskov. 1990. Serologic classification of fimbriae. Curr. Top. Microbiol. Immunol. 151:71-90.

163. Oswald, E., J. de Rycke, P. Lintermans, K. van Muylem, J. Mainil, G. Daube, and P. Pohl. 1991. Virulent factors associated with cytotoxic necrotizing factor type two in bovine diarrheic and septicemic strains of *Eschirichia coli*. J. Clin. Microbiol. 29:2522-2527.

164. Ozeri, V., A. Tovi, I. Burstein, S. Natanson-Yaron, M. G. Caparon, K. M. Yamada, S. K. Akiyama, I. Vlodavsky, and E. Hanski. 1996. A two-domain mechanism for group A streptococcal adherence through protein F to the extracellular matrix. EMBO J. 15:989-998.

165. Pakainathan, D. R. 1995. Extracellular matrix proteins and leukocyte function. J. Leuk. Biol. 57:699-702.

166. Paton, J. C., P. W. Andrew, G. J. Boulnois, and T. J. Mitchell. 1993. Molecular analysis of the pathogenicity of *Streptococcus pneumoniae*: the role of pneumococcal proteins. Annu. Rev. Microbiol. 47:89-115.

167. Patti, J. M., B. L. Allen, M. J. McGavin, and M. Hook. 1994. MSCRAMM-mediated adherence of microorganisms to host tissue. Annu. Rev. Microbiol. 48:585-617.

168. Pedroni, P., B. Riboli, F. de Ferra, G. Grandi, S. Toma, B. Arico, and R. Rappuoli. 1988. Cloning of a novel pilin-like gene from *Bordetella pertussis*: homology to the fim2 gene. Mol. Microbiol. 2:539-543.

169. Perez-Casal, J., N. Okada, M. G. Caparon, and J. R. Scott. 1995. Role of the conserved C-repeat region of the M protein of *Streptococcus pyogenes*. Mol. Microbiol. 15:907-916.

170. Perry, A., I. Ofek, and F. J. Silverblatt. 1983. Enhancement of mannose-mediated stimulation of human granulocytes by fimbriae aggregated with antibodies on *Escherichia coli* surfaces. Infect. Immun. 39:1334-1345.

171. Plos, K., H. Lomberg, S. Hull, I. Johansson, and C. Svanborg. 1991. *Escherichia coli* in patients with renal scarring genotype and phenotype of Gal alpha1-4 Gal beta-, Forssman- and mannose-specific adhesins. Pediatr. Infect. Dis. J. 10:15-19.

172. Pointon, A. M., W. D. Hueston, and G. D. Dial. 1990. Disease surveillance: reducing the uncertainty of decision making. Minnesota Swine Conference for Veterinarians. 38-57.

173. Powell, D. A., P. C. Hu, M. Wilson, A. M. Collier, and J. B. Baseman. 1976. Attachment of *Mycoplasma pneumoniae* to respiratory epithelium. Infect. Immun. 13:956-966.

174. Prasad, S. M., Y. B. Yin, E. Rodzinski, E. I. Tuomanen, and H. R. Masure. 1993. Identification of a carbohydrate recognition domain in filamentous hemagglutinin from *Bordetella pertussis*. Infect. Immun. 61:2780-2785.

175. Razin, S., M. Banai, H. Gamliel, A. Pollack, and W. Bredt. 1980. Scanning electron microscopy of mycoplasmas adhering to erythrocytes. Infect. Immun. 30:538-546.

176. Razin, S., and E. Jacobs. 1992. Mycoplasma adhesion. J. Gen. Microbiol. 138:407-422.

177. Razin, S., I. Kahane, M. Banai, and W. Bredt. 1981. Adhesion of mycoplasma to eukaryotic cells. Ciba Found symp. 80:98-118.

178. Reddy, S. P., W. G. Rasmussen, and J. B. Baseman. 1995. Molecular cloning and characterisation of an adherence-related operon of *Mycoplasma genitalium*. J. Bacteriol 177:5943-5951.

179. Relman, D., E. Tuomanen, S. Falkow, D. T. Golenbock, K. Saukkonen, and S. D. Wright. 1990. Recognition of a bacterial adhesion by an integrin: macrophage CR3 (alpha M beta 2, CD11b/CD18) binds filamentous hemagglutinin of *Bordetella pertussis*. Cell 61:1375-1382.

180. Relman, D. A., M. Domenighini, E. Tuomanen, R. Rappuoli, and S. Falkow. 1989. Filamentous hemagglutinin of *Bordetella pertussis*: nucleotide sequence and crucial role in adherence. Proc. Natl. Acad. Sci. USA 86:2637-2641.

181. Reynolds, H. Y. 1987. Bacterial adherence to respiratory tract mucosa: a dynamic interaction leading to colonization. Semin. Respir. Infect. 2:8-19.

182. Roberts, D. D., L. D. Olson, M. F. Barile, V. Ginsburg, and H. C. Krivan. 1989. Sialic acid-dependent adhesion of *Mycoplasma pneumoniae* to purified glycoproteins. J. Biol. Chem. 264:9289-9293.

183. Roberts, M., N. F. Fairweather, E. Leininger, D. Pickard, E. L. Hewlett, A. Robinson, C. Hayward, G. Dougan, and I. G. Charles. 1991. Construction and characterization of *Bordetella pertussis* mutants lacking the *vir*-regulated P.69 outer membrane protein. Mol. Microbiol. 5:1393-1404.

184. Rodriguez-Ortega, M., I. Ofek, and N. Sharon. 1987. Membrane glycoproteins of human polymorphonuclear leukocytes that act as receptors for mannose-specific *Escherichia coli*. Infect. Immun. 55:968-973.

185. Ross, R. F. 1992. Mycoplasmal disease, p. 537-551. *In* A. D. Leman, B. E. Straw, W. L. Mengeling, S. D'Allaire and D. J. Taylor (ed.), Diseases of Swine. Iowa State University Press, Ames.

186. Ross, R. F. 1993. Mycoplasma - animal pathogens, p. 69-109. *In* I. Kahane and A. Adoni (ed.), Rapid diagnosis of mycoplasmas. Plenum Press, New York.

187. Ross, R. F., and D. F. Cox. 1988. Evaluation of tiamulin for treatment of mycoplasmal pneumonia in swine. J. Am. Vet. Med. Assoc. 193:441-446.

188. Ross, R. F., and T. F. Young. 1993. The nature and detection of mycoplasmal immunogens. Vet. Microbiol. 37:369-380.

189. Ross, R. F., B. J. Zimmerman-Erickson, and T. F. Young. 1984. Characteristics of protective activity of *Mycoplasma hyopneumoniae* vaccine. Am. J. Vet. Med. 45:1899-1905.

190. Ruland, K., R. Himmelreich, and R. Herrmann. 1994. Sequence divergence in the ORF6 gene of *Mycoplasma pneumoniae*. J. Bacteriol. 176:5202-5209.

191. Russell, P. W., and P. E. Orndorff. 1992. Lesions in two *Escherichia coli* type 1 pilus genes alter pilus number and length without affecting receptor binding. J. Bacterial. 174:5923-5935.

192. Ryc, M., B. Wagner, M. Wagner, and R. Bicova. 1988. Electron microscopic localization of lipoteichoic acid on group A streptococci. Zentralbl. Bakteriol. Mikrobiol. Hyg. A. 269:168-178.

193. Sajjan, S. U., and J. F. Forstner. 1990. Characteristics of binding of *Escherichia coli* serotype O157:H7 strain CL-49 to purified intestinal mucin. Infect. Immun. 58:860-867.

194. Sajjan, S. U., and J. F. Forstner. 1990. Role of the putative "link" glycopeptide of intestinal mucin in binding of piliated *Escherichia coli* serotype O157:H7 strain CL-49. Infect. Immun. 58:868-873.

195. Sambrook, J., E. F. Fritsch, and T. Maniatis. 1989. Molecular cloning: a laboratory manual, Cold Spring Harbor Laboratory, Cold Spring Harbor, N. Y.

196. Saukkonen, K., W. N. Burnette, V. L. Mar, H. R. Masure, and E. Tuomanen. 1992. Pertussis toxin has eukaryotic-like carbohydrate recognition domains. Proc. Natl. Acad. Sci. USA 89:118-122.

197. Sauter, S. L., S. M. Rutherfurd, C. Wagener, J. E. Shively, and S. A. Hefta. 1991. Binding of nonspecific cross-reacting antigen, a granulocyte membrane glycoprotein, to *Escherichia coli* expressing type 1 fimbriae. Infect. Immun. 59:2485-2493.

198. Sauter, S. L., S. M. Rutherfurd, C. Wagener, J. E. Shively, and S. A. Hefta. 1993. Identification of the specific oligosaccharide sites recognized fimbriae from *Escherichia coli* on nonspecific cross-reacting antigen, a cluster granulocyte glycoprotein. J. Biol. Chem. 268:15510-15516.

199. Schaeffer, A. J., W. R. Schwan, S. J. Hultgren, and J. L. Duncan. 1987. Relationship of type 1 pilus expression in *Escherichia coli* to ascending urinary tract infections in mice. Infect. Immun. 55:373-380.

200. Schuller, W., H. D. Lehmkuhl, and W. P. Switzer. 1976. A fluorescent antibody technique for identification of *Mycoplasma hyopneumoniae* colonies. Am. J. Vet. Res. 37:477-478.

201. Schwan, W. R., H. S. Seifert, and J. L. Duncan. 1992. Growth conditions mediate differential transcription of *fim* genes Involved in phase variation of type 1 pili. J. Bacteriol. 174:2367-2375.

202. Sheldrake, R. F., I. A. Gardner, M. M. Saunders, and L. F. Romalis. 1990. Serum antibody response to *Mycoplasma hyopneumoniae* measured by enzyme-linked

immunosorbent assay after experimental and natural infection of pigs. Aust. Vet. J. 67:39-42.

203. Sheldrake, R. F., I. A. Gardner, M. M. Saunders, and L. F. Romalis. 1991. Intraperitoneal vaccination of pigs to control *Mycoplasma hyopneumoniae*. Res. Vet. Sci. 51:285-291.
204. Sheldrake, R. F., L. F. Romalis, and M. M. Saunders. 1993. Serum and mucosal antibody response against *Mycoplasma hyopneumoniae* following intraperitoneal vaccination and challenge of pigs with *M. hyopneumoniae*. Res. Vet. Sci. 55:371-376.
205. Sherman, P., R. Soni, and E. Boedeker. 1988. Role of type 1 pili (fimbriae) in mucosal attachment of the enteroadherent *Escherichia coli*, strains RDEC-1, in rabbits. J. Pediatr. Gastroenterol. Nutr. 7:594-601.
206. Sherman, P. M., and E. C. Boedeker. 1987. Pilus-mediated interactions of the *Escherichia coli* strain RDEC-1 with mucosal glycoproteins in the small intestine of rabbits. Gastroenterology 93:734-743.
207. Short, J. M., J. M. Fernandez, J. A. Sorge, and W. D. Huse. 1988. Lambda ZAP: a bacteriophage lambda expression vector with in vivo excision properties. Nucleic Acids Res. 16:7583-7600.
208. Simpson, W. A., H. S. Courtney, J. C. Morrison, and E. H. Beachey. 1987. Interactions of fibronectin with streptococci: the role of fibronectin as a recptor for *Streptococcus pyogenes*. Rev. Infect. Dis. 9:S351-S359.
209. Simpson, W. A., H. S. Courtney, and I. Ofek. 1987. Interaction of fibronectin with streptococci: the role of fibronectin as a receptor for *Streptococcus pyogenes*. Rev. Infect. Dis. 9:351-359.
210. Slender, R. K., T. K. Korhonen, V.-R. V., P. H. Williams, P. E. Pattison, and D. A. Caugant. 1986. Genetic relationships and clonal structure of strains of *Escherichia coli* causing neonatal septicemia and meningitis. Infect. Immun. 52:213-222.
211. Smiley, B. K., and F. C. Minion. 1993. Enhanced readthrough of opal (UGA) codons and production of *Mycoplasma pneumoniae* P1 epitopes in *Escherichia coli*. Gene 134:33-40.
212. Smith, H. 1989. The mounting interest in bacterial and viral pathogenicity. Annu. Rev. Microbiol. 43:1-22.
213. Smith, H. 1990. Pathogenicity and the microbe in vivo. J. Gen. Microbiol. 136:377-383.

214. Smith, H. 1995. The state and future of studies on bacterial pathogenicity, p. 335-357. *In* J. A. Roth and e. al (ed.), Virulence mechanisms of bacterial pathogenes, 2nd ed. American society for Microbiology, Washington,D.C.

215. Steadman, R., N. Matthews, M. Lichodziejewska, and J. D. Williams. 1991. Human neutrophil responses to pathogenic *Escherichia coli* are receptor-specific and selectively augmented by recombinant human tumor necrosis factor-alpha. J. Infect. Dis. 163:1033-1039.

216. Steadman, R., N. Topley, D. E. Jenner, M. Davies, and J. D. Williams. 1988. Type 1 fimbriated *Escherichia coli* stimulates a unique pattern of degranulation by human polymorphonuclear leukocytes. Infect. Immun. 56:815-822.

217. Stemke, G. W. 1989. A gene probe to detect *Mycoplasma hyopneumoniae*, the etiological agent of enzootic pneumonia. Mol. Cell. Probes 3:255-232.

218. Stevens, M. K., and D. C. Krause. 1990. Disulfide-linked protein associated with *Mycoplasma pneumoniae* cytadherence phase variation. Infect. Immun. 58:3430-3433.

219. Stevens, M. K., and D. C. Krause. 1991. Localization of the *Mycoplasma pneumoniae* cytadherence-accessory proteins HMW1 and HMW4 in the cytoskeletonlike triton shell. J. Bacteriol. 173:1041-1050.

220. Stevens, M. K., and D. C. Krause. 1992. *Mycoplasma pneumoniae* cytadherence phase-variable proteins HMW3 is a component of the attachment organelle. J. Bacteriol. 174:4265-4274.

221. Stjernquist-Desatnik, A., D. N. Kurl, and P. Christensen. 1986. Repeated passage of freshly isolated group A streptococci on blood agar. Acta. Pathol. Microbiol. Immunol. Scand. B. 94:405-408.

222. Strasser, M., J. Frey, G. Bestetti, M. Kobisch, and J. Nicolet. 1991. Cloning and expression of a species-specific early immunogenic 36-kilodalton protein of *Mycoplasma hyopneumoniae* in *Escherichia coli*. Infect. Immun. 59:1217-1222.

223. Strathmann, M., B. A. Hamilton, C. A. Mayeda, M. I. Simon, E. M. Meyerowitz, and M. J. Palazzolo. 1991. Transposon-facilitated DNA sequencing. Proc. Natl. Acad. Sci. USA 88:1247-1250.

224. Su, C.-J., A. Chavoya, and J. B. Baseman. 1988. Regions of *Mycoplasma pneumoniae* cytadhesin P1 structural gene exist as multiple copies. Infect. Immun. 56:3157-3161.

225. Su, C. J., A. Chavoya, and J. B. Baseman. 1988. Regions of *Mycoplasma pneumoniae* cytadhesin P1 structural gene exist as multiple copies. Infect. Immun. 56:3157-3161.

226. Su, C. J., S. F. Dallo, and J. B. Baseman. 1990. Molecular distinctions among clinical isolates of *Mycoplasma pneumoniae*. J. Clin. Microbiol. 28:1538-1540.

227. Su, C. J., V. V. Tryon, and J. B. Baseman. 1987. Cloning and sequence analysis of cytadhesin P1 gene from *Mycoplasma pneumoniae*. Infect. Immun. 55:3023-3029.

228. Switzer, W. P., and R. F. Ross. 1975. Mycoplasmal disease, p. *In* H. W. Dunn and A. D. Leman (ed.), Diseases of swine. Iowa Stae University Press, Ames.

229. Tajima, M., and T. Yagihashi. 1982. Interaction of *Mycoplasma hyopneumoniae* with the porcine respiratory epithelium as observed by electron microscopy. Infect. Immun. 37:1162-1169.

230. Talay, S. R., P. Valentin-Weigand, P. G. Jerlstrom, K. N. Timmis, and G. S. Chhatwal. 1992. Fibronectin-binding protein of *Streptococcus pyogenes*: sequence of the binding domain involved in adherence of streptococci to epithelial cells. Infect. Immun. 60:3837-3844.

231. Tewari, R., J. I. Macgregor, T. Ikeda, J. R. Little, S. J. Hultgren, and S. N. Abraham. 1993. Neutrophil activation by nascent FimH subunits of type 1 fimbriae purified from the periplasm of *Escherichia coli*. J. Biol. Chem. 268:3009-3015.

232. Topley, N., R. Steadman, R. Mackenzie, J. M. Knowlden, and J. D. Williams. 1989. Type 1 fimbriae strains of *Eschirichia coli* initiate renal parenchymal scarring. Kidney Int. 36:609-616.

233. Towbin, H., T. Staehelin, and J. Gordon. 1979. Electrophoretic transfer of proteins from polyacrylamide gels to nitrocellulose sheets: procedure and some application. Proc. Natl. Acad. Sci. USA 76:4350-4354.

234. Truszczynski, M., and J. Osek. 1987. Occurence of mannose resistant hemagglutinins in *Escherichia coli* strains isolated from porcine colibacillosis. Comp. Immunol. Microbiol. Infect. Dis. 10:117-124.

235. Tullus, K., I. Kuhn, I. Orskov, and R. Mollby. 1992. The important of P and type 1 fimbriae for the persistence of *Escherichia coli* in the human gut. Epidemiol. Infect. 108:415-421.

236. Tully, J. G., J. M. Bove, F. Laigret, and R. F. Whitcomb. 1993. Revised taxonomy of the class *Mollicutes* - proposed elevation of a monophyletic cluster of arthropod-associated mollicutes to ordinal rank (*Entomoplasmatales* ord-nov), with provision for familial rank to separate species with nonhelical morphology (*Entomoplasmataceae* fam-nov) from helical species (*Spiroplasmataceae*), and emended descriptions of the order *Mycoplasmatales*, family *Mycoplasmataceae*. Int. J. Syst. Bacteriol. 43:378-385.

237. Tuomanen, E., H. Towbin, G. Rosenfelder, D. Braun, G. Larson, G. C. Hanson, and R. Hill. 1988. Receptor analogs and monoclonal antibodies that inhibit adherence of

Bordetella pertussis to human ciliated respiratory epithelial cells. J. Exp. Med. 168:267-277.

238. Tuomanen, E., and A. Weiss. 1985. Characterization of two adhesins of *Bordetella pertussis* for human ciliated respiratory-epithelial cells. J. Infect. Dis. 152:118-125.
239. Tylewska, S. K., V. Fischetti, and R. J. Gibbbons. 1988. Binding selectivity of *Streptococcus pyogenes* and M-protein to epithelial cells differ from that of lipoteichoic acid. Curr. Microbiol. 16:209-216.
240. Valentin-Weogand, P., S. R. Talay, K. N. Timmis, and G. S. Chhatwal. 1993. Identification of a fibronectin-binding protein as adhesin of *Streptococcus pyogenes*. Int. J. Med. Microbiol. Virol. Parasitol. Infect. Dis. 278:238-245.
241. van't Wout, J., W. N. Burnette, V. L. Mar, E. Rozdzinski, S. D. Wright, and E. I. Tuomanen. 1992. Role of carbohydrate recognition domains of pertussis toxin in adherence of *Bordetella pertussis* to human macrophages. Infect. Immun. 60:3303-3308.
242. VanHeyningen, T., G. Fogg, D. Yates, E. Hanski, and M. Caparon. 1993. Adherence and fibronectin binding are environmentally regulated in the group A streptococci. Mol. Microbiol. 9:1213-1222.
243. Wang, J. R., and M. W. Stinson. 1994. M protein mediates streptococcal adhesion to Hep-2 cells. Infect. Immun. 62:442-448.
244. Wang, J. R., and M. W. Stinson. 1994. Streptococcal M6 protein binds to fucose-containing glycoproteins on cultured human epithelial cells. Infect. Immun. 62:1268-1274.
245. Westerlund, B., and T. K. Korhonen. 1993. Bacterial proteins binding to the mammalian extracellular matrix. Mol. Microbiol. 9:687-694.
246. Whittlestone, P. 1979. Porcine mycoplasmas, p. 133-176. *In* J. G. Tully and R. F. Whitcomb (ed.), The mycoplasmas. volume II. Human and animal mycoplasmas. Academic Press, New York.
247. Wiedermann, U., S. Ahlstedt, B. Andersson, and U. I. Dahlgren. 1993. Antibody response in bronchoalveolar lavage and bile in rats after aerosol immunization with an *Escherichia coli* strain producing ovalbumin. Int. Allergy Immunol. 101:254-259.
248. Wieslander, A., M. J. Boyer, and H. Wroblewski. 1992. Membrane protein structure, p. 93-112. *In* J. Maniloff, R. N. McElhaney, L. R. Finch and J. B. Baseman (ed.), Mycoplasmas: molecular biology and pathogenesis. American Society for Microbiology, Washington, D.C.
249. Willems, R. J., C. Geuijen, H. G. van der Heide, M. Matheson, A. Robinson, L. F. Versluis, R. Ebberink, J. Theelen, and F. R. Mooi. 1993. Isolation of a putative fimbrial

adhesin from *Bordetella pertussis* and the identification of its gene. Mol. Microbiol. 9:623-634.

250. Willems, R. J., H. G. van der Heide, and F. R. Mooi. 1992. Characterization of a *Bordetella pertussis* fimbrial gene cluster which is located directly downstream of the filamentous haemagglutinin gene. Mol. Microbiol. 6:2661-2671.
251. Williams, P. P., and J. E. Gallagher. 1978. Cytopathogenicity of *Mycoplasma hyopneumoniae* in porcine tracheal ring and lung explant cultures alone and in combination with monolayers of fetal lung fibroblasts. Infect. Immun. 20:495-502.
252. Wilson, M. H., and A. M. Collier. 1976. Ultrastructural study of *Mycoplasma pneumoniae* in organ culture. J. Bacteriol. 125:332-339.
253. Wise, K. S., G. H. Cassell, and R. T. Acton. 1978. Selective association of murine T lymphoblastoid cell surface alloantigens with *Mycoplasma hyorhinis*. Proc. Nat. Acad. Sci. USA 75:4479-4483.
254. Wise, K. S., and M. F. Kim. 1987. Identification of intrinsic and extrinsic membrane proteins bearing surface epitopes of *Mycoplasma hyopneumoniae*. Isr. J. Med. Sci. 23:469-473.
255. Wise, K. S., and M. F. Kim. 1987. Major membrane surface proteins of *Mycoplasma hyopneumoniae* selectively modified by covalently bound lipid. J. Bacteriol. 169:5546-5555.
256. Wise, K. S., D. Yogev, and R. Rosengarten. 1992. Antigenic variation, p. 473-489. *In* J. Maniloff, R. N. McElhaney, L. R. Finch and J. B. Baseman (ed.), Mycoplasmas: molecular biology and pathogenesis. American Society for Microbiology, Washington, D.C.
257. Wold, A. E., J. Mestecky, M. Tomana, A. Kobata, H. Ohbayashi, T. Endo, and C. S. Eden. 1990 Sep. Secretory immunoglobulin A carries oligosaccharide receptors for *Escherichia coli* type 1 fimbrial lectin. Infect. and Immun. 58:3073-3077.
258. Wold, A. E., M. Thorssen, S. Hull, and C. S. Eden. 1988. Attachment of *Escherichia coli* via mannose- or Gal alpha 1-4 Gal beta-containing receptors to human colonic epithelial cells. Infect. Immun. 56:2531-2537.
259. Yogev, D., R. Watson-McKown, R. Rosengarten, J. Im, and K. S. Wise. 1995. Increased structural and combinatorial diversity in an extended family of genes encoding Vlp surface proteins of *Mycoplasma hyorhinis*. J. Bacteriol. 177:5636-5643.
260. Young, T. F., B. Z. Erickson, R. F. Ross, and Y. Wannemuehler. 1989. Hemagglutination and hemagglutination inhibition of turkey red blood cells with *Mycoplasma hyopneumoniae*. Am. J. Vet. Res. 50:1052-1055.

261. Young, T. F., and R. F. Ross. 1987. Assessment of antibody response of swine infected with *Mycoplasma hyopneumoniae* by immunoblotting. Am. J. Vet. Res. 48:651-656.

262. Young, T. F., R. F. Ross, and J. Drisko. 1983. Prevalence of antibodies to *Mycoplasma hyopneumoniae* in Iowa swine. Am. J. Vet. Res. 44:1946-1948.

263. Zhang, Q., T. F. Young, and R. F. Ross. 1994. Glycolipid receptors for attachment of *Mycoplasma hyopneumoniae* to porcine respiratory ciliated cells. Infect. Immun. 62:4367-4373.

264. Zhang, Q., T. F. Young, and R. F. Ross. 1995. Identification and characterization of a *Mycoplasma hyopneumoniae* adhesin. Infect. Immun. 63:1013-1019.

265. Zhang, Q. J., and K. S. Wise. 1996. Molecular basis of size and antigenic variation of a *Mycoplasma hominis* adhesin encoded by divergent *vaa* genes. Infect. Immun. 64:2737-2744.

266. Zhang, Q. J., T. F. Young, and R. F. Ross. 1994. Microtiter plate adherence assay and receptor analogs for *Mycoplasma hyopneumoniae*. Infect. Immun. 62:1616-1622.

267. Zielinski, G. C., and R. F. Ross. 1993. Adherence of *Mycoplasma hyopneumoniae* to porcine ciliated respiratory tract cells. Am. J. Vet. Res. 54:1262-1269.

268. Zielinski, G. C., T. Young, and R. F. Ross. 1990. Adherence of *Mycoplasma hyopneumoniae* to cell monolayers. Am. J. Vet. Res. 51:339-343.

269. Zielinski, G. C., T. Young, R. F. Ross, and R. F. Rosenbusch. 1990. Adherence of *Mycoplasma hyopneumoniae* to cell monolayers. Am. J. Vet. Res. 51:339-343.

270. Zingler, G., G. Schmidt, I. Orskov, F. Orskov, U. Falkenhagen, and G. Naumann. 1990. K-antigen identification, hemolysin production, and hemagglutination types of *Escherichia coli* O6 strains isolated from patients with urinary tract indections. Int. J. Med. Microbiol. 274:372-381.

ACKNOWLEDGMENTS

I would like to thank Drs. C. F. Ford, S. L. Carpenter, M. Nilsen-Hamilton, J. S. Haynes, and C. O. Thoen for serving on my examining committee. Their suggestions and especially, their patience will always be remembered. I would like to express my special thanks to my major advisor Dr. F. Chris Minion without whom the completion of this dissertation would have been impossible. I thank him for his advice, patience, encouragement, and support throughout this study. I am deeply indebted to his having faith in me and his willingness to let me join his laboratory at a most difficult time. I also like to thank Drs. P. A. Kapke, S. Artiushin, and I. Morozov for helpful discussions and advice.

I thank Mrs. T. F. Young, B. Z. Erickson, N. J. Upchurch, and Dr. R. F. Ross for providing me with the *M. hyopneumoniae* strains, swine cilia, and chemicals as well as their assistance in making Friis media and training in the adherence assay.

I like to thank the following people with whom I have had the honor to work with in this laboratory. They are B. A. Esswein, S. Ambalakkat, and C. T. VanDyk. My special thanks go to C. T. VanDyk for her technical support in constructing and initial screening of the *M. hyopneumoniae* genomic library. I am fortunately enough to be part of VMRI where I have had the opportunity to work with so many intelligent and interesting people. I thank all of them.

Finally, I would like to thank my family in Taiwan who have supported me throughout this degree process. Without that support I would have not been able to complete my studies. I would like to dedicate this dissertation to my father who did not live to see its completion.